A GRAVITY PROFILE ACROSS NEWFOUNDLAND

HARVEY C. WEIR, B.Sc. (Hons.)

16699

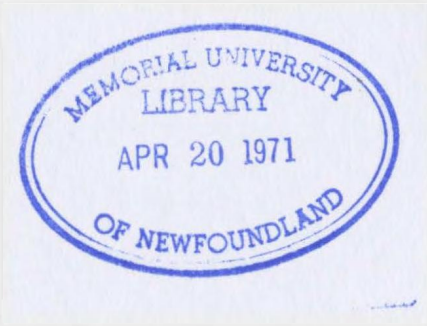
MEMORIAL UNIVERSITY
LIBRARY
APR 20 1971
OF NEWFOUNDLAND

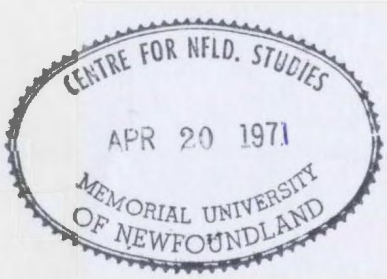
CENTRE FOR NFLD. STUDIES
APR 20 1971
MEMORIAL UNIVERSITY
OF NEWFOUNDLAND

A GRAVITY PROFILE ACROSS NEWFOUNDLAND

by

© Harvey C. Weir, B.Sc. (Hons.)

Submitted in partial fulfilment
of the requirements for the degree of Master of Science
Memorial University of Newfoundland

August 31, 1970.

ABSTRACT

A gravity profile, with 0.8 km station spacing, has been established along the Trans-Canada highway between Port-aux-Basques and Come-by-Chance, Newfoundland. A modified "one-base" barometric method gave improved elevation results, yielding a standard deviation which is less than one-half that associated with the traditional "one-base" method. Techniques have been devised to facilitate the determination of various model representation errors, and for making end corrections. A "winding-route" apparent anomaly effect has been studied.

A qualitative profile interpretation has suggested the presence of unmapped gypsum deposits (south-western Newfoundland) and intrusive bodies (at several locations along the route). A detailed study between Notre Dame Junction and Traytown shows the Ackley batholith to be, in cross-section along the route, a funnel-shaped lopolith and this region to be underlain by an intermediate to basic layer.

ACKNOWLEDGEMENTS

I wish to thank the following people:

Dr. E. R. Deutsch, for initiating and supervising the project, and for considerable patience during the many delays that occurred.

Dr. S. W. Breckon, Head of the Department of Physics, for encouragement during all phases of the study.

Drs. D. Rendell and J. Wright, Department of Physics, for many valuable discussions and suggestions.

Dr. H. Williams, Department of Geology, for assistance in the classification of rock samples, and for several discussions.

Mr. H. Miller, Department of Physics, for many discussions and suggestions.

Mr. W. Drodge, Department of Physics, for assistance in elevation and latitude determinations, and for many worthwhile suggestions in connection with data procurement and processing.

Dr. D. Balsom, for assistance in barometric altimetry data reductions.

Mr. G. Pedersen, for assistance in computer programming, and for many worthwhile discussions.

Messrs. D. Walsh and W. Russell, for gravity field work in 1964 and 1965.

Messrs. F. Doyle, and assistant, for elevation surveying in 1965.

Mr. R. Butler, for gravity surveying assistance in 1966.

Mr. C. Drodge, for barometric altimetry field assistance in 1967, and for determining the majority of rock sample densities.

Messrs. W. Smith and D. Granter, for assistance in preliminary barometric altimetry determinations.

Messrs. R. Tucker and W. Higgins, for drafting and photographic services, respectively.

Mrs. G. Critch and Miss D. Janes, for typing this thesis.

I am also grateful to:

The Newfoundland & Labrador Computer Services, Ltd., for the efficient handling of the many programs submitted.

Messrs. A. Robertson, L. Crumley, and S. Andrews for computer programming advice.

Mrs. J. Moriarity, for keypunching gravity data, and contributing to the smoothness of program handling.

Dr. M. J. S. Innes, Chief of the Gravity Division of the Observatories Branch of the federal department of Energy, Mines, and Resources, for hosting, in 1966, a two-week initiation of the author into gravity work.

Dr. J. Tanner of the Gravity Division, for initially suggesting the project.

Dr. D. Nagy and Mr. R. Buck of the Gravity Division, for computer programming advice and the use of some of their reduction and interpretation programs.

The Provincial Department of Highways for copies of road profile plans.

Mr. J. Greene and other members of the Meteorological Office, Gander Airport, for weather equipment, maps, and valuable advice.

The Government of the Province of Newfoundland & Labrador for a graduate fellowship.

The National Research Council of Canada (research grants to Dr. E. R. Deutsch) and Memorial University for the financial support which made this project possible.

CONTENTS

CHAPTER ONE

INTRODUCTION

1.1 Purpose and scope.

The island of Newfoundland forms the northeastern land terminus of the 3500 km-long Appalachian mountain system. This project has consisted of a gravity survey, with 0.8 km station spacing, along the Trans-Canada highway across the island from Port-aux-Basques on the west coast to Come-by-Chance on the east coast (Figure 1.1.1).

This study was undertaken to make a gravimetric contribution to an understanding of the region's crustal structure. It has included a general examination of the full gravity profile (Chapter 4), as well as a detailed interpretation of the section between Notre-Dame Junction and Traytown (Chapter 5). The data has been presented (Chapter 2 with Appendices 2, 3 and 5) in a manner to facilitate its use in future geophysical interpretation within the region. The profile is also important as a base line for future gravity surveying in Newfoundland, and for deciding the best areas for such work.

1.2 History of geophysical surveying in and near Newfoundland.

Although many geophysical surveys, including gravity, have been conducted in connection with mineral exploration within this region, none of their results have been utilized in this project.

Work by the Gravity Division of the Dominion Observatory, Ottawa, has included a survey, from 1947-51, along the Canadian National railway line across Newfoundland, with station spacing approximately 8 km; a 1964 survey in which a grid of about 1200 regional gravity stations, with spacing 10 to 13 km, was established (Weaver, 1967); and work in the Gulf of St. Lawrence (Goodacre, 1964; Goodacre and Nyland, 1966).

The Physics Department of Memorial University has undertaken two gravity surveying projects since 1964. As part of the one covered by this thesis, approximately 1000 stations have been established along the Trans-Canada highway across Newfoundland. The gravity readings were taken in 1964, 1965, and 1966, and the associated elevation surveying was done during 1965, 1966, and 1967. The processing of this gravity and elevation data was carried on intermittently from May, 1967, to December, 1969.

A second project, begun in 1967, has included the setting up of a grid of more than 300 gravity stations in the eastern Notre-Dame Bay region of the province (Miller, 1970). Station spacing is approximately 2.5 km.

Aeromagnetic maps for Newfoundland (Scales 1:253,440 and 1:63,360), based on a 1953 airborne survey with flight altitude approximately 300 m above ground level, have been published by the Geological Survey of Canada since 1967.

Dalhousie University, the Bedford Institute of Oceanography, and the Lamont Geological Observatory of Columbia University, have all

conducted seismic experiments, concerned with the structure of the crust and upper mantle, in the waters off Newfoundland (Ewing et al., 1966; Sheridan and Drake, 1968).

1.3 Fundamentals of gravity surveying.

In studies of this type, the acceleration due to gravity, g_{obs}, is observed at a large number of positions, called gravity stations, at or just above the earth's surface. The gravity meters used do not measure g_{obs} directly, but are capable of giving differences in this quantity with high precision. Two units of measurement employed are the gal (1 gal = 1 x 10^{-2} m/s^2) and the milligal (1 mgal = 1 x 10^{-3} gal).

It is usually desirable to assign to each station a value of g_{obs} which, although stated with greater numerical significance than is absolutely measureable, would agree with the most accurate absolute determination which could be made there at the time the station is established.

To achieve this aim it is necessary to have a network of control stations which have been carefully "tied" to each other and to some point at which gravity has been absolutely determined with great accuracy. In this survey the network used was established by the Gravity Division of the Dominion Observatory (Weaver, 1967), and these control stations are here referred to as gravity bases. In some areas it was necessary to set up other control stations by "tying-in" to these bases.

These secondary control stations are called gravity sub-bases.

Reduction of the gravity measurements to a common elevation datum, usually the earth's geoid, is accomplished by means of the free-air and Bouguer corrections. The first, $\Delta g_{fc} = +0.3086\ h$ mgal, accounts for the elevation, h, of the station above the datum plane, ignoring the mass between. The second, $\Delta g_{bc} = -0.0419\ \rho\ h$ mgal, accounts for this mass, treating it as a horizontally infinite slab of density ρ and thickness h. In these corrections, derivations of which are found in standard texts (e.g., Garland, 1965), h is given in meters. Usually a value of 2.670 g/cm^3 is assumed for the slab density, giving a Bouguer correction $\Delta g_{bc} = -0.1119\ h$ mgal. Combining these gives

$$\Delta g_{fc} + \Delta g_{bc} = +0.1967\ h \text{ mgal} \qquad (1.3.1)$$

A terrain correction, Δg_t, accounts for the undulations in the top surface of the Bouguer slab, and is always positive. Tables (e.g., Bible, 1962) have been devised to facilitate its computation.

Theoretical gravity, g_{th}, obtained by treating the earth as an oblate spheroid closely fitted to the geoid, and incorporating the effect of the earth's rotation, is given by the international gravity formula of 1930.

$$g_{th} = 978.049\ (1 + 0.0052884 \sin^2\phi - 0.0000059 \sin^2 2\phi) \qquad (1.3.2)$$

where ϕ is the geographic latitude.

A comparison of observed gravity, reduced to the geoid, with the theoretical gravity is contained in the Bouguer anomaly, g_B, defined by

$$g_B = g_{obs} + \Delta g_{fc} + \Delta g_{bc} + \Delta g_t - g_{th}$$

This quantity is a measure, at the physical surface of the earth, of the vertical component of the gravity associated with density variations in the crust and upper mantle. The following data are required for its computation: observed gravity, g_{obs}; station elevation, h, for the free-air and Bouguer corrections; a measure of the topography surrounding the station, for the terrain correction; and the latitude, ϕ, for calculation of theoretical gravity.

An isostatic anomaly, defined in standard texts (e.g., Dobrin, 1960), may be obtained by adding an isostatic correction to the Bouguer anomaly. Although these anomalies have not yet been calculated in this study, the extent of the island's isostatic compensation has been briefly considered (section 4.9).

Regional corrections, described in various references (e.g., Grant and West, 1965), may sometimes be used to separate the effect of smaller scale features in the upper crust from the effects associated with larger features there and with density contrasts deeper in the crust and upper mantle. In this study, quantitative regional considerations have accompanied only the investigation of the "winding-route" effect in the St. George's region of the west coast (section 3.5).

Profile interpretation normally involves the indirect method, in which the interpreter, utilizying all available geophysical and

geological knowledge of the region, assumes the size, shape, and density of the contrasting rock masses and calculates, either analytically or by numerical techniques, the associated gravity. Adjustments to the model are made until an acceptable agreement between the calculated and observed Bouguer anomalies is obtained. The method suffers from the fundamental ambiguity, associated with inverse boundary value problems, common to all potential fields. That is, an infinite number of different mass distributions are capable of fitting any given Bouguer anomaly distribution. More detailed descriptions of this method are found in standard references (e.g., Grant and West, 1965).

1.4 Gravity instrumentation.

The three gravity meters used in the project were of the same model, CG-2, manufactured by Sharpe Instruments of Canada. These astatic-type instruments, similar to the Worden gravity meters (described in various texts, e.g., Garland, 1965), are capable of giving gravity differences with high precision. The specifications quoted for the CG-2 model by the manufacturer are given in Table 1.4.1.

Each gravity meter was assigned a fine-dial constant, S, sometimes called a scale constant, by the manufacturer. A study (Appendix 1) showed that the use of these quoted values in this project's base network

would give profile discontinuities of up to 1 mgal at the meeting points of traverses from different gravity bases. Hence it was necessary, using procedures shown in Appendix 1, to assign new scale constants. Table 1.4.2 lists the old and new constants for the three meters.

Damrel (1960) has discussed the effect of temperature changes, internal pressure, and time, on the scale constant, S, of the Worden gravity meter. He concluded (i) that S changes by approximately 0.013% per ^{o}C change in ambient temperature; (ii) a decrease in S is associated with a pressure increase inside the evacuated element container system (maximum decrease of 0.3% for an internal pressure increase from 15 mm to 60 mm Hg); and (iii) there is no significant change in scale constant with time, other than that due to temperature and pressure changes.

During this survey, the maximum atmospheric temperature change during the working day seldom exceeded 15^{o}C. Assuming that the behavior of the Model CG-2 gravity meters is no worse than that of the Worden instruments, then temperature changes would result in changes in the scale constant of less than ±0.0002 mgal/div.

A check of the internal pressure of the 1966 meter was made at the end of the summer of field work, and the result of 15 mm Hg indicated no change from the value set by the manufacturer. No pressure check data is available for the instruments used in 1964 and 1965.

1.5 Basis of data error determinations.

Error treatment in this project follows procedures described in standard references (e.g., Topping, 1957; Beers, 1958). Unless otherwise noted, the standard deviation represents the error calculated on the basis of repeated measurements, and the limit of error is recorded for the uncertainty in instrumental scale reading.

Table 1.4.1 Sharpe Instruments of Canada specifications for the Model CG-2 gravity meter.

Range:	500 mgal
Fine dial range:	1000 div x scale constant
Coarse dial range:	Reset screw
Fine dial constant:	Varies with instrument, but within range 0.09 to 0.11 mgal/div
Fine dial linearity:	1 in 1000
Accuracy:	0.1 dial division
Drift:	< 0.1 mgal/day
Level sensitivity:	40 sec of arc per mm bubble displacement

Table 1.4.2 Gravity meter scale constants.[1]

Instrument[2] number	Year used	Scale constant, S (mgal/div)		
		Manufacturer's value	Recalibrated value	Recalibration error
	1964	0.10252	0.1015	±0.0003
183	1965	0.10010	0.0991	±0.0003
192	1966	0.10360	0.10260	±0.00009

[1] See Appendix 1.

[2] Model CG-2 'Canadian' gravity meter.

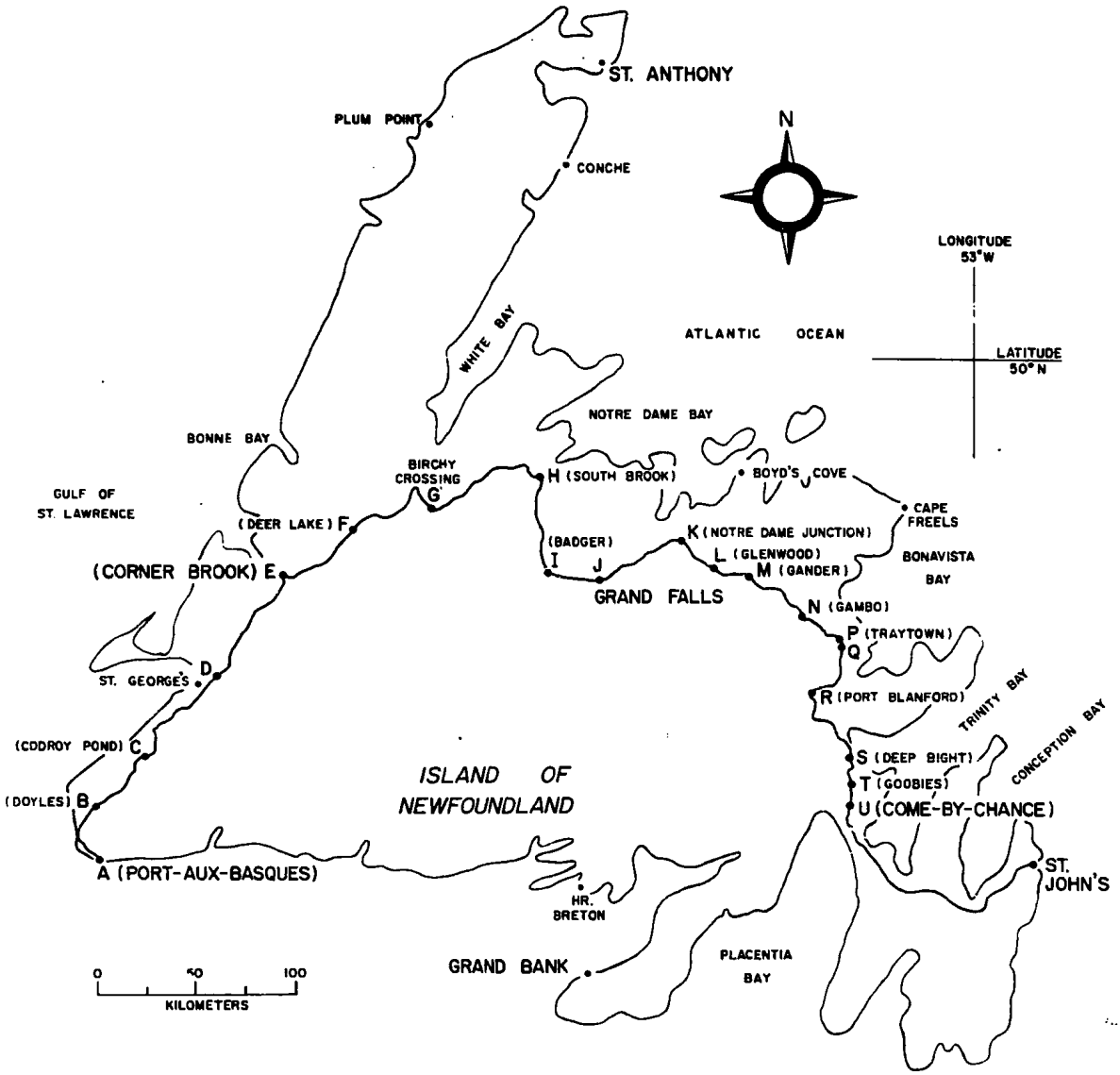

Figure 1.1.1 Map of Newfoundland, showing Trans-Canada Highway. Main reference points are located by symbols A-U.

CHAPTER TWO

DATA PROCUREMENT AND PROCESSING

2.1 The establishment of gravity sub-bases and stations.

Each station gravity value, g_{obs}, may be obtained from a base gravity value, g_{bs}, and from gravity meter readings, R_s and R_{bs}, at the station and base, respectively, by the relation

$$g_{obs} = g_{bs} + S(R_s - R_{bs}) \qquad (2.1.1)$$

where S is the gravity meter scale constant.

Repeated gravity meter readings at the same position show a time dependence. Part of this is due to lunar and solar tidal effects which cause a cyclic variation of up to 0.3 mgal with a period of approximately 12 hours, and the remainder is attributable to a drift within the instrument. This is illustrated by the readings taken during the establishment of sub-base 9101 from base 9001 on August 29, 1966 (Table A2.2 and Figure 2.1.1(A)). Figure 2.1.1(B) based on tidal gravity correction tables,[1] permits the plotting of Figure 2.1(C) in which the readings at 9001 and 9101 have been corrected for lunar and solar tidal effects.

These results suggest that R_s and R_{bs} in equation 2.1.1 have to be compared for the same instant of time. In gravity surveys it is the

---

[1] Tidal Gravity Corrections for 1966, Geophysical Prospecting, Vol. 13, Supp. no. 1, December, 1965.

usual procedure to determine the base reading at the time, t, of the station occupation (when the base is unoccupied) by a linear interpolation between base readings, R'_{bs} and R''_{bs}; these are the readings taken immediately before and after the station visit, at times t' and t", respectively. Thus the base reading, R_{bs}, is given by

$$R_{bs} = R'_{bs} + \frac{R''_{bs} - R'_{bs}}{t'' - t'} \quad (t - t') \quad . \qquad (2.1.2)$$

The establishment of station 10825 is described in Appendix 3 as an illustration of this procedure.

Tidal variations (e.g. Figure 2.1.1(B)) can be considered linear with time only if the traverse from base to the stations and back to base is executed in not more than about two hours. This time limit necessitated the establishment of sub-bases on stretches where adjacent accessible main bases of the Dominion Observatory's Newfoundland network (Appendix 2) were separated by more than approximately 120 km.

Accurate determinations of the observed gravity at each sub-base required reading the gravity meter alternately at it and the nearest main base, normally making four visits to either one and three to the other, travelling as quickly as possible between the two. The base (or sub-base) value at the time of each sub-base (or base) reading was obtained using equation 2.1.2. If R_{sb} represents the reading at the sub-base, obtained either directly or by interpolation, R_{bs} the corresponding reading at the base, and $(R_{sb} - R_{bs})_M$ the mean value of the difference between the two, then the gravity difference, Δg_{obs}, between the base and sub-base is given by

$$\Delta g_{obs} = S(R_{sb} - R_{bs})_M \ . \qquad (2.1.3)$$

The final sub-base gravity value, g_{sb}, is given by

$$g_{sb} = g_{bs} + \Delta g_{obs} \qquad (2.1.4)$$

where g_{bs} is the known value of gravity at the base. The establishment of sub-base 9101, described in Section A2.2, illustrates this procedure.

The standard deviation of the quantity $(R_{sb} - R_{bs})$ about its mean never exceeded ± 0.5 div (≃ 0.05 mgal) in the establishment of this project's sub-bases. The standard error of the mean gravity difference between each sub-base and its base is thus not greater than ± 0.02 mgal. Combining this with the base gravity error, ± 0.07 mgal (Section A2.1), yields an error of just over ± 0.07 mgal for each sub-base gravity value.

Although gravity stations were seldom revisited, an estimate of ± 0.05 mgal, based on data obtained during the establishment of the sub-bases, is perhaps reasonable for the error in gravity difference between a station and its base. Combining this with the base (or sub-base) error of ± 0.07 mgal gives an error of ± 0.09 mgal in observed station gravity.

Appendix 2 contains the principal facts for bases and sub-bases, and Appendix 3 the facts for stations.

2.2 Determination of station elevation.

Gravity station elevations in this project have been determined as follows: 60% by barometric altimetry; 36% by precise (spirit)

levelling; 2½% by placement on benchmarks; and 1½% from highway plans and profiles. An estimate of the cost per station and accuracy for each method is included in Table 2.2.1. Table 2.2.2 gives an error code for use with Figure 2.2.1, which shows the errors for each section surveyed.

2.2.1 Reference bench-marks.

Both precise levelling and barometric altimetry provide elevation differences and thus, for use in this project, require a network of accurately known elevations referred to the geoid.

The primary bench-marks, with elevations quoted in feet to three decimal places, were established, mainly along the Canadian National railway line, by the Geodetic Survey of Canada in 1949.

Secondary bench-marks, precisely levelled from geodetics, have been obtained from road construction surveys. Although elevation accuracies for these are not available, the techniques employed are similar to those used in this project's 1965 elevation surveying, where most of the observed elevation errors were less than ± 0.08 m (Section 2.2.2).

2.2.2 Precise (spirit) levelling.

Precise levelling from geodetic bench-marks in 1965, and from secondary bench-marks in 1966, provided the elevations of 362 gravity stations. A description of the techniques employed may be found in standard textbooks on plane surveying (e.g. Clark, 1958).

For the 1965 precise levelling work, each section of gravity stations was begun and ended at a geodetic, thus permitting a determination of the elevation accuracy. All but one of the end point discrepancies were less than 0.08 m, and that one, on an 80 km section, was less than 0.17 m.

The 1966 stations were seldom separated from their reference bench-mark by more than 0.5 km, and hence the error in the levelling probably does not exceed ± 0.08 m. Assuming an error of not more than ± 0.17 m in the bench-mark value, the limit of error obtained for these stations is ± 0.25 m.

2.2.3 Highway plans and profiles.

Profile plans of several sections of the Trans-Canada highway were made available by the provincial Department of Highways. Errors in gravity station elevations obtained from these plans stem from three sources: (i) an error of approximately ± 0.2 m in reading the profile elevation scale; (ii) elevation uncertainties, between ± 1 m and ± 4 m (depending on the section), due to difficulty in positioning the stations properly on the profile sheets; and (iii) the departure of the real highway from the planned profile. A check of a four-mile section at West Bottom, Halls' Bay, indicated a maximum elevation difference of approximately 1 m between the real and planned highways.

Because of these sources of error, this method was employed only between Goobies and Come-by-Chance, where insufficient funds and poor weather conditions ruled out precise levelling and barometric altimetry, respectively. For this section the three sources combine to give an error of approximately ± 2 m.

2.2.4 Barometric altimetry.

Barometric altimetry was employed in 1967 to obtain the elevations of 607 gravity stations. The "one-base" method was modified to improve elevation accuracy. Standard deviations associated with these elevations varied between ±0.8 m and ±2.0 m, and are shown for the various traverse sections in Figure 2.2.1. Appendix 4 contains a detailed description of the techniques used and the results obtained.

2.3 Latitude measurement.

Station positions were plotted on maps (scale 1:50,000) published by the Surveys and Mapping Branch of the federal Department of Energy, Mines and Resources, and the latitudes (and longitudes) were then read from these. The map scale is readable to approximately ±0.04 min. of arc. The error in positioning a station on these maps depends on the existence of recognizable land-marks, and on the distances and means of measuring distances from them. For all of the 1964 and about 30% of the 1965 gravity stations, the positioning was done on the basis of chainage measurements along the road, for which the accuracy was better than ±0.5% of the distance measured. The remainder of the stations were positioned from measurements by automobile odometers with scale readabilities of ±0.2 km and ±0.05 km for the odometers used in 1965 and 1966, respectively. The error in latitude measurements also depends on the traverse direction, being least for sections that are on the average parallel to lines of latitude, and maximum for sections perpendicular to these lines. Table 2.3.1 gives an error code for use with figure 2.3.1,

in which the latitude accuracy is given for each section surveyed. It is roughly estimated that more than 70% of the stations in each section fall within the uncertainty stated.

Station longitudes, which do not enter into the calculations, are accurate to approximately ±0.15 min. of arc.

2.4 Terrain corrections.

Terrain corrections were carefully determined at 45 stations spread along the route, making use of topographic maps (scale 1:50,000) printed by the federal Department of Energy, Mines and Resources, Ottawa, in conjunction with tables prepared by Bible (1962). More than 75% of these corrections were smaller than 0.5 mgal, and approximately 90% were less than 1.0 mgal. For the remaining stations, the corrections were estimated by a comparison (of terrain features) with the carefully determined ones. To obtain an idea of the errors inherent in this estimating, the careful determinations were first done at 26 stations, and these were used in the estimation of corrections for 19. Then the corrections at these 19 were carefully determined using the tables. Taking $\Delta g_t''$ to be the careful determination at a station, and $\Delta g_t'$ to be the rough estimate, the difference

$$z_t = \Delta g_t'' - \Delta g_t' \qquad (2.4.1)$$

gives an estimate of the error involved. For these observations z_t has a mean of 0 mgal, and a standard deviation of ±0.23 mgal. The value of z_t is dependent on the size of $\Delta g_t''$, being greater for larger terrain

corrections. These have been divided into three broad categories: (i) $\Delta g_t'' < 0.30$ mgal, with error ±0.06 mgal; (ii) 0.30 mgal $\leq \Delta g_t'' < 1.0$ mgal, with error ±0.22 mgal; (iii) $\Delta g_t'' \geq 1.0$ mgal, with error ±0.6 mgal. Terrain corrections and associated errors are given in Tables A3.1 and 2.5.1, respectively, for the gravity stations in this survey.

2.5 Bouguer anomaly calculation.

The Bouguer anomaly at each station was calculated from equation 1.3.3 utilizying a reduction program written in Fortran II for use on the IBM 1620 computer and later modified for use on the IBM 360 machine. The determination of this anomaly at station 10825 is given in section A3.1 as an illustration of the steps involved. Table A3.1 contains the Bouguer anomalies from this survey; the anomaly profile is drawn in Figures A5.2.1 to A5.2.6, inclusive. Anomaly values range from -18 - +44 mgal.

The acceptability and usefulness of the geologic interpretation of the gravity anomaly profile across a region depends to a large extent on the accuracy of the anomaly values obtained. The error in an individual Bouguer anomaly calculation results from the composite effect of the errors in the quantities on the right-hand side of equation 1.3.3. The errors in g_{obs} and Δg_t have already been discussed in sections 2.1 and 2.4, respectively, and are listed in Table 2.5.1.

The error, E_{fbc}, in the combined free-air and Bouguer correction may be obtained from equation 1.3.3 and the discussion in section 1.3,

$$E_{fbc} = 0.1967\ \Delta h \text{ mgal} - 0.0419\ h\ \Delta\rho \text{ mgal} \qquad (2.5.1)$$

where h is the station elevation in meters, Δh the elevation uncertainty, and $\Delta\rho$ the Bouguer slab density error associated with the assumed value of 2.67 g/cm^3. Although density contrasts of 0.1 g/cm^3 between formations are not uncommon (Chapter 4; Table A5.1; Figures A5.2.1 to A5.2.6, inclusive), these are not classed as errors. Instead these departures from the assumed mean density of 2.67 g/cm^3 will be discussed as part of the profile interpretation. Equation 2.5.1 may then be simplified to

$$E_{fbc} = 0.1967\ \Delta h \text{ mgal} \qquad (2.5.2)$$

and the union of this equation with Figure 2.2.1 and Table 2.2.2 permits the calculation of the combined free-air and Bouguer correction error, and these are given in Table 2.5.1.

Random errors in values of g_{th} stem from the latitude determinations (section 2.3), which contribute approximately 1.50 mgal per minute of latitude uncertainty (i.e., about 0.15 mgal for the estimated uncertainty of 0.10 min). These errors in theoretical gravity are listed in Table 2.5.1. A comparison of the international gravity formulae of 1930 and 1967 suggests that errors in g_{th} inherent in them are systematic. For example, the 1930 formula yields, at North latitude 47^o oo', a value which is larger by more than 10 mgal than that obtained from the 1967 formula. The difference between the two decreases uniformly at 0.23 mgal/deg latitude from south to north over the region included in this survey.

On the basis of these considerations the Bouguer anomaly errors have been calculated for each section surveyed, and these are given in

Table 2.5.1. Overall, there is a standard deviation of ± 0.30 mgal associated with individual Bouguer anomaly determinations.

2.6 Rock sampling and density determinations.

A total of 144 rock samples, with average mass approximately 150 gm, were collected at 106 sites along or near the Trans-Canada highway across the island. Table A6.1 gives the location, geologic type, and dry density of these rocks. The samples were given a water-proof plastic coating and their dry densities determined using the "loss of weight" method, as described in standard references (e.g., Garland, 1965). A sample density calculation, with error analysis, is given in section A6.1.

The average density of these rocks, giving unit weight to each site, is 2.73 gm/cm^3, with an r.m.s. deviation of ±0.11 gm/cm^3 about the mean. The rock sample data has been presented in a manner (Table A6.1 with Figures A5.2.1 to A5.2.6 and Table A5.1) to facilitate the grouping of rocks for use in interpretation. This is illustrated in Chapter 5.

2.7 Correlation with Gravity Division surveys.

Over 20 of this project's stations coincided (separation of less than about 100 m) with stations of the Gravity Division's (Dominion Observatory) surveys. In all cases the Bouguer anomalies obtained agreed to within the experimental errors associated with them.

Table 2.2.1 Synopsis of elevation work.

Method or source of elevation	Location (Figure 2.2.1)	Number of stations	Error[1] ±(m)	Approximate cost per station
(i) Station at geodetic bench mark		4	0.01	
(ii) Station at secondary bench mark		20	0.17	
(iii) Precise levelling from geodetics[2]	B-C,D-F,J-K	297	0.17	$12.50
(iv) Precise levelling from secondary bench-marks[3]	Q-R,S-T	65	0.25	$ 7.00
(v) Barometric altimetry[4]	A-B,C-D,F-J, K-Q,R-S	607	1.1	$ 6.50
(vi) Highway profile plans	T-U	15	2.0	$ 0.50

[1]The error is given as a limit for Methods (or Sources) (i) to (iv), inclusive, and as a standard deviation for the remainder.

Elevations determined in: [2]1965; [3]1966; [4]1967.

Table 2.2.2 Elevation code.

Error ± (m)		Symbol	Associated with
Limit	Standard deviation		
0.10		a	good precise levelling from geodetics
0.25		b	good precise levelling from secondary bench marks; poor precise levelling from geodetics
	0.80	c	excellent barometric altimetry
	1.10	d	good barometric altimetry
	1.50	e	fair barometric altimetry
	2.00	f	highways plans and profiles and poor barometric altimetry

Table 2.3.1 Latitude error code for use with figure 2.3.1.

Symbol	Standard deviation (min)	Associated with
g	±0.05	(i) Measurements obtained by chaining along road, (ii) measurements with automobile odometer in 1966 on sections approximately parallel to lines of latitude.
h	±0.07	Measurements with automobile odometer: (i) in 1965 on sections approximately parallel to lines of latitude, (ii) in 1966 on sections not parallel to lines of latitude.
j	±0.10	Measurements with automobile odometer in 1965 on sections not parallel to lines of latitude.

Table 2.5.1 Standard deviations in Bouguer anomaly determinations.[1]

Section	E_{gobs} ±(mgal)	E_{fbc} ±(mgal)	$E_{\Delta gt}$ ±(mgal)	E_{gth} ±(mgal)	E_{gB} ±(mgal)
A - B	0.09	0.30	0.22	0.15	0.40
B - C	0.09	0.02	0.22	0.08	0.25
C - D	0.09	0.30	0.06	0.15	0.35
D - E	0.09	0.05	0.06	0.08	0.15
E - F[2]	0.09	0.02	0.22	0.08	0.25
F - G	0.09	0.16	0.06	0.11	0.20
G - H	0.09	0.22	0.06	0.11	0.25
H - I	0.09	0.30	0.06	0.11	0.35
I - J	0.09	0.22	0.06	0.08	0.25
J - K	0.09	0.02	0.06	0.08	0.15
K - L	0.09	0.22	0.06	0.15	0.30
L - M	0.09	0.22	0.06	0.11	0.25
M - N	0.09	0.30	0.06	0.15	0.35
N - P	0.09	0.39	0.06	0.15	0.45
P - Q	0.09	0.30	0.06	0.11	0.35
Q - R	0.09	0.05	0.06	0.11	0.15
R - S	0.09	0.22	0.06	0.11	0.25
S - T	0.09	0.05	0.06	0.11	0.15
T - U	0.09	0.39	0.06	0.11	0.40

[1]Symbols

Section — Letters (A to U) refer to Table A3.1 and Figures 1.1.1, A5.2.1 to A5.2.6.

E_{gobs} — Error in observed gravity.

E_{fbc} — Error in combined Bouguer and Free-air correction.

$E_{\Delta gt}$ — Error in terrain correction, using broad classifications given in Section 2.4. Except for Sections E - F, G - H, and S - T, more than 70% of stations fall within these categories. For simplicity this error is here treated as a standard deviation.

E_{gth} — Random error in theoretical gravity determination.

E_{gB} — Random error in Bouguer anomaly, given to nearest 0.05 mgal.

[2]Several terrain corrections here are larger than 2 mgal, with correction error approaching 1 mgal.

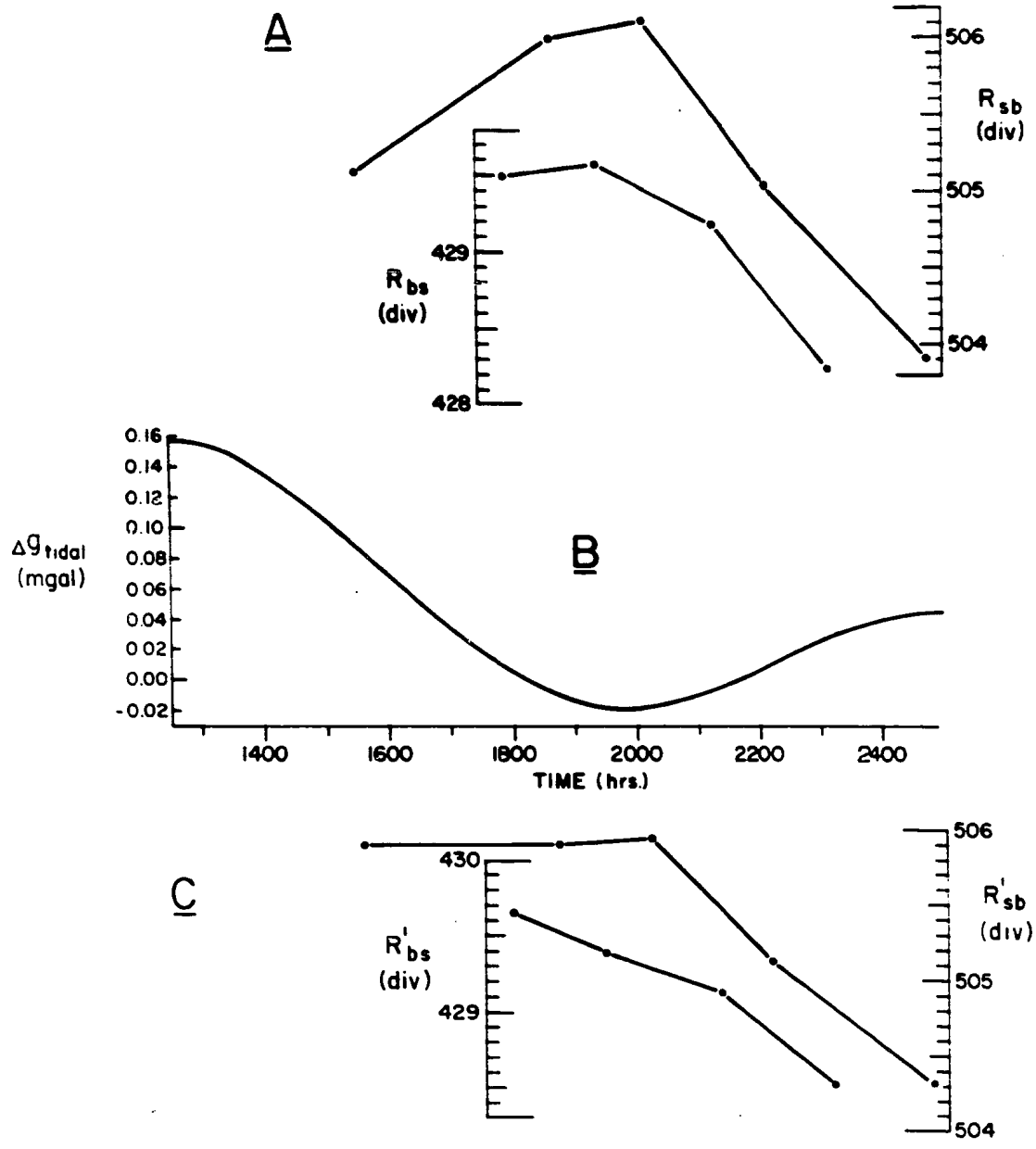

Figure 2.1.1 Gravity meter readings and tidal gravity corrections for August 29, 1966. (A) R_{bs} and R_{sb} are gravity meter readings at Base 9001 and Subbase 9101, respectively. (B) Lunar and solar tidal correction chart. (C) Gravity meter readings at 9001 and 9101 corrected using Figure 2.1.1 (B). Time scales for (A) and (C) are shown with (B).

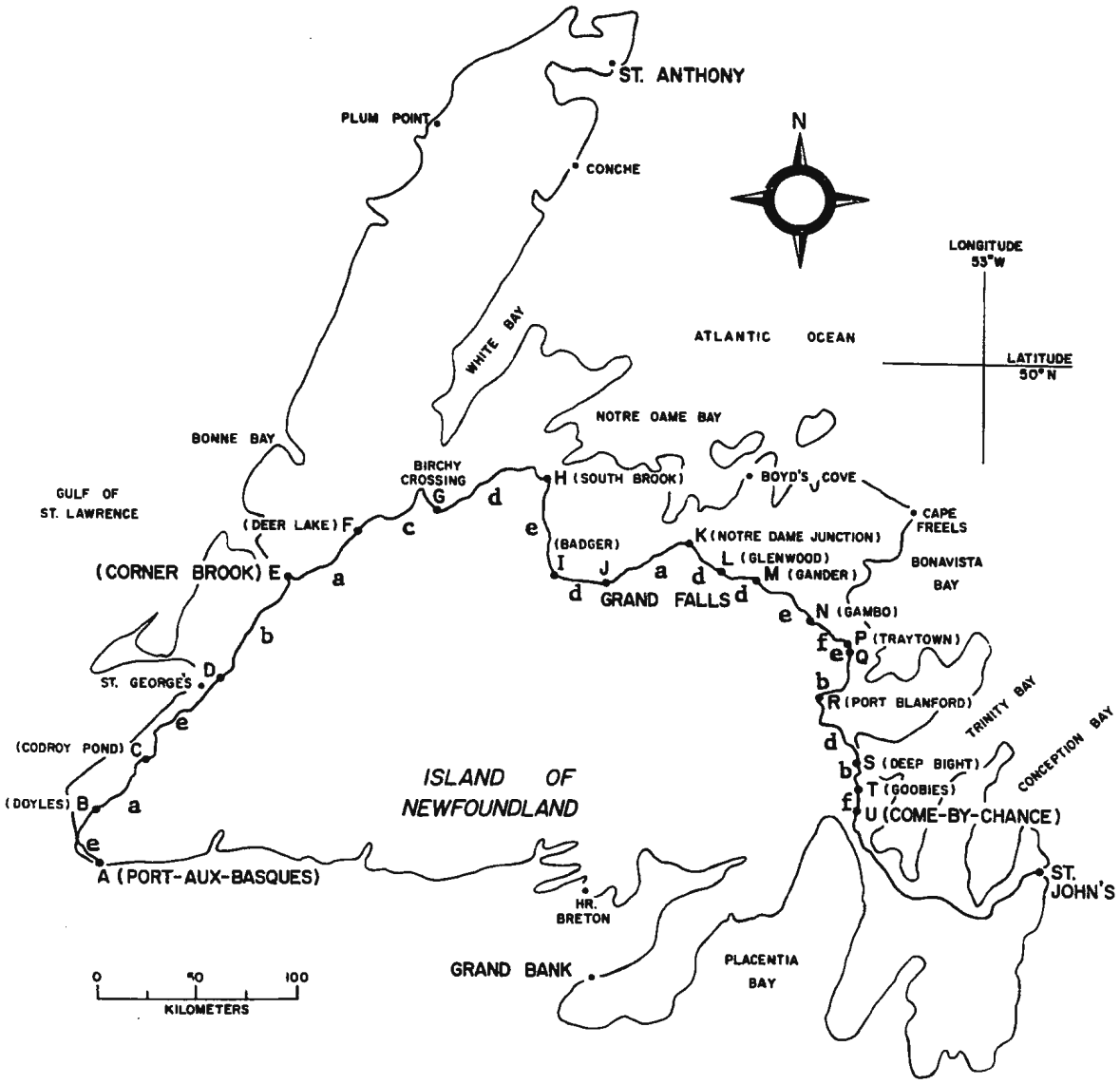

Figure 2.2.1 Map of Newfoundland with Trans-Canada Highway. Symbols a-f refer to elevation accuracy (Table 2.2.2), and A-U are explained in Figure 1.1.1.

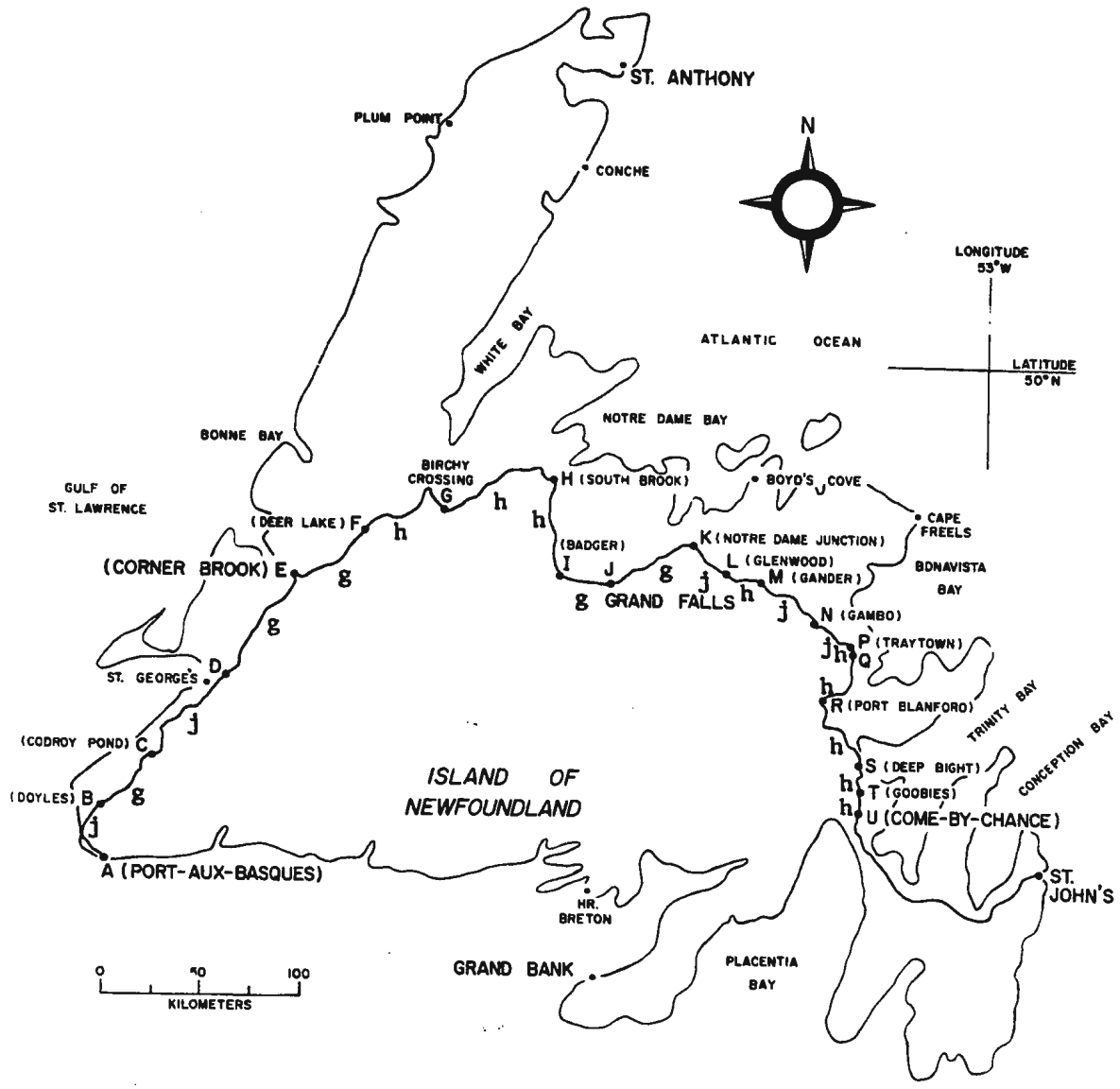

Figure 2.3.1 Map of Newfoundland with Trans-Canada Highway. Symbols g-j give the accuracy of station latitude determinations (Table 2.3.1), and A-U are explained in Figure 1.1.1.

CHAPTER THREE

ASPECTS OF INTERPRETATION

3.1 Introduction.

This chapter forms a basis for the detailed interpretation of the traverse between Notre-Dame Junction and Traytown (Sections 3.2 and 3.3, with chapter 5); for future detailed interpretation of other profiles in this survey (Sections 3.4 and 3.5); and for a general (qualitative) interpretation (Chapter 4).

The general method normally used in gravity profile interpretation was briefly described in section 1.3. In this method, the geologic structure is represented by a model whose gravitational effect corresponds to the measured profile anomalies, and is consistent with all other available geophysical and geological evidence. Often many models are designed and tested before a satisfactory one is obtained, a process facilitated by high-speed computers.

Because anomalous mass contributions diminish rapidly with distance from the gravity profile (Section 3.3 and figure 3.3.1), these models are usually two-dimensional and give a vertical section of the structure along the direction of the traverse. A "two-dimensional" model or body is here defined as one with uniform infinite rectilinear elongation, and thus whose structure is completely shown in cross-section normal to this direction. Where such models are obviously inadequate, three-dimensional ones may be used, although this is usually more expensive. The method of

selecting and testing models is determined by considerations of both the cost (mainly computing) and the agreement desired between model and measured anomalies. Often three-dimensional modifications can be made to the two-dimensional models in the form of "end-corrections".

Model studies are more straightforward along rectilinear than along winding sections of the traverse. Along the meandering route of this gravity survey, however, straight sections are rarely longer than five kilometers. The traverse given in figures A5.2.1 to A5.2.6, showing many relatively straight sections longer than 10 km, is obtained by ignoring small departures of the route from rectilinearity. Much of the traverse can be broken into segments, 30 km to 120 km long, which fall within rectangles of length at least 10 times width. Those crossing two-dimensional geologic structures can be interpreted along the mean direction of the route. These segments fall into three categories - those parallel, or approximately so, to the northeasterly direction of the main geologic trend; those oblique to this direction; and those perpendicular, or roughly so, to it.

3.2 Available models and their gravitational effect.

The gravitational effect of some simple geometric forms, such as spheres and infinite horizontal cylinders, can be easily computed using exact simple expressions, as given in standard references (e.g. Nettleton, 1940). In most regions, however, an acceptable fit cannot be obtained using such simple models.

The vertical component of gravity associated with a two-dimensional mass of arbitrary shape can be calculated using an exact expression derived by Talwani, Worzel and Landisman (1959), in which the vertical cross-section is approximated by an N-sided polygon. This expression, stated in Appendix 7 in the form given by Grant and West (1965), is the basis of the model studies described in chapter 5. A computer program was written for a model made up of these polygons, giving the gravity effect along a straight traverse perpendicular to the direction of model elongation.

Among the techniques available for making end corrections is one illustrated in Appendix 8, in which use is made of an exact expression for the gravitational attraction of a right rectangular prism, derived by Nagy (1966), and stated in Appendix 7. Calculations were facilitated by a Fortran IV computer program kindly provided by Dr. Nagy. These prisms may also be used to construct three-dimensional models.

The gravity anomaly associated with a three-dimensional body of arbitrary shape is given by an expression developed by Talwani and Ewing (1960). The solution, which is approximate because of the inherent numerical integration, approaches exactness only if a large number of steps are built into the model, and this is sometimes prohibitively expensive.

3.3 Traverses perpendicular to the geologic trend.

The ease of constructing and testing two-dimensional models for traverses perpendicular to the geologic trend often justifies the

neglect of departures of the geologic structure both from perpendicularity and two-dimensionality. It is, however, necessary to establish criteria for determining the adequacy of such models.

To facilitate end-effect considerations, several working graphs have been prepared giving a comparison of the gravitational effect of two-dimensional rectangular prisms with finite prisms of identical cross-sections. Two examples are shown in figure 3.3.1.

On the basis of expressions derived in Sections A7.4 and A7.5, graphs have been plotted to facilitate the determination of errors, for two orientations of line masses, associated with departures from perpendicularity. In both cases the gravity effect of a perpendicular infinite line mass is compared with that of a line mass oblique to it and intersecting it in the vertical plane of the traverse; the comparison is for various angles of obliqueness, γ, and for various angles, β, between the vertical and the normal drawn from the computation point to the perpendicular line mass. For the case given in figure A7.2 the angle γ is in a horizontal plane, while in figure A7.4 γ is in a vertical plane perpendicular to the vertical plane of the traverse.

A body with uniform infinite rectilinear elongation perpendicular to the vertical plane of the traverse and divided by that plane into two semi-infinite parts of different density, each of which is homogeneous, may be represented by a two-dimensional model of identical cross-sectional shape, and having the mean of the two contrasting densities.

3.4 Traverses oblique to the geologic trend.

The computer program for the two-dimensional model studies along traverses normal to the trend (Sections 3.2 and 3.3) can also be used for oblique profile interpretation, provided again, of course, that structural departures from two-dimensionality have a negligible effect on traverse measurements. One way of using the program is to project the profile onto a straight line perpendicular to the geologic trend. Because this line is oblique to the traverse, it is necessary to project the accepted model back to the mean traverse direction. End effect and other three-dimensional considerations, discussed in sections 3.2 and 3.3, may be applied here as well.

3.5 Traverses parallel to the geologic trend.

Where the mean traverse direction is parallel, or nearly so, to the trend of the primary geologic structures, the Bouguer anomaly profile pattern may be significantly affected by the way in which the route meanders. In the regions surveyed there is, as yet, insufficient geologic and gravity information to completely isolate this winding route effect from the total anomaly variation. A partial evaluation may, however, be based on existing geology maps (Section 4.2) and on the Bouguer anomaly values obtained by the Gravity Division of the Dominion Observatory (Section 1.2).

As an example, consider the section between distances 69 km and 142 km from Port-aux-Basques (Figure A5.2.1). Figure 3.5.1(B) gives a plot of this traverse as a function of latitude and longitude, and shows as well some off-route gravity values from the Dominion Observatory's surveys. Straight-line gravity contours have been drawn parallel to each other and nearly parallel to the geologic trend, and were obtained from a visual fit to the actual Bouguer anomaly values both inside and just outside the region illustrated. Figure 3.5.1(A) gives plots along the route for: g_B, the measured Bouguer anomalies; g_C, the values obtained from the contour plot in figure 3.5.1(B); and g_R, the residual gravity obtained by subtracting g_C from g_B. With respect to anomaly variations along the mean traverse direction, g_C represents a "regional" gravity, associated with the primary structures.

Because considerable changes in the residual gravity pattern can accompany even rather small contour shifts, the visual method of contouring is not dependable. An alternate approach is to fit, using multiple regression techniques, a polynomial expression to the region's anomaly values (refer section A7.1). As an illustration, this has been done for polynomials of orders one and two, using a program prepared by Miller (1970) and utilizing the Multiple Regression program in the IBM Scientific Programming Package. Figure 3.5.2(A) gives the measured, regional, and residual profiles when the polynomial of order one is

used to define the regional, and figure 3.5.2(B) gives the corresponding profiles for order two.

A comparison of each residual profile with the measured one shows that, although none of the original features have been completely lost, there are some significant differences in emphasis between the residual and measured plots. This illustrates the danger inherent in the direct interpretation of the measured anomalies. The differences among the residual profiles indicate the need for additional "regional" gravity analysis before detailed interpretation can be confidently done.

It is also necessary to isolate the effect of the route's meandering with respect to such non-regional structures as anomalous ore bodies. Some assistance may be obtained here from detailed geology maps, although quantative analysis may be subject to considerable error. This is further discussed in the interpretation of this region given in section 4.3.

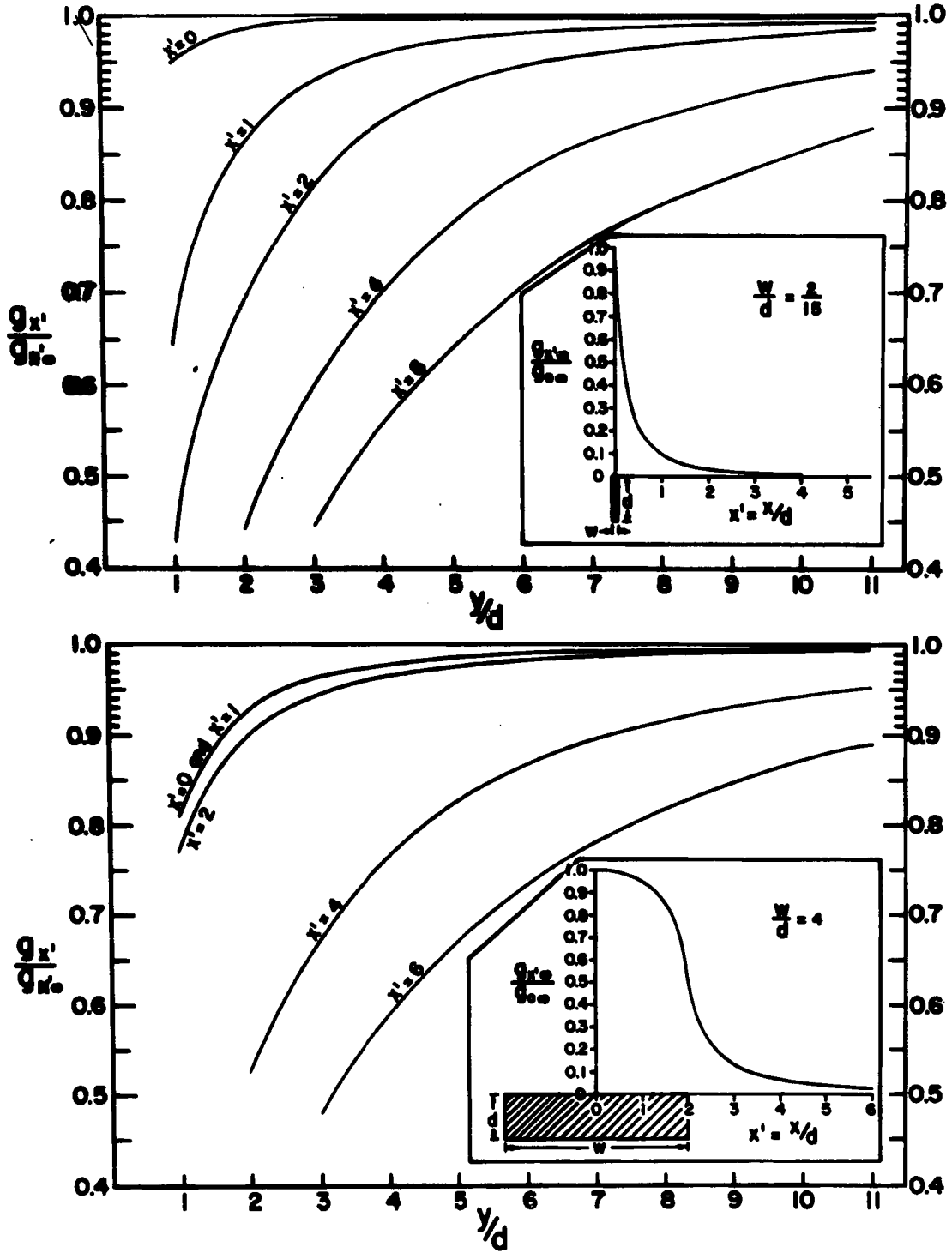

Figure 3.3.1 A comparison of the gravitational effects of finite and infinite bodies of identical cross-section and density.

Symbols: d, depth of body; w, width of body; x, axis along traverse; y, axis perpendicular to vertical plane of traverse; $g_{0\infty}$, maximum gravitational effect of infinite body; $g_{x'\infty}$, gravitational effect at x of infinite body; $g_{x'}$, gravitational effect at x of finite body of length 2y and bisected by traverse.

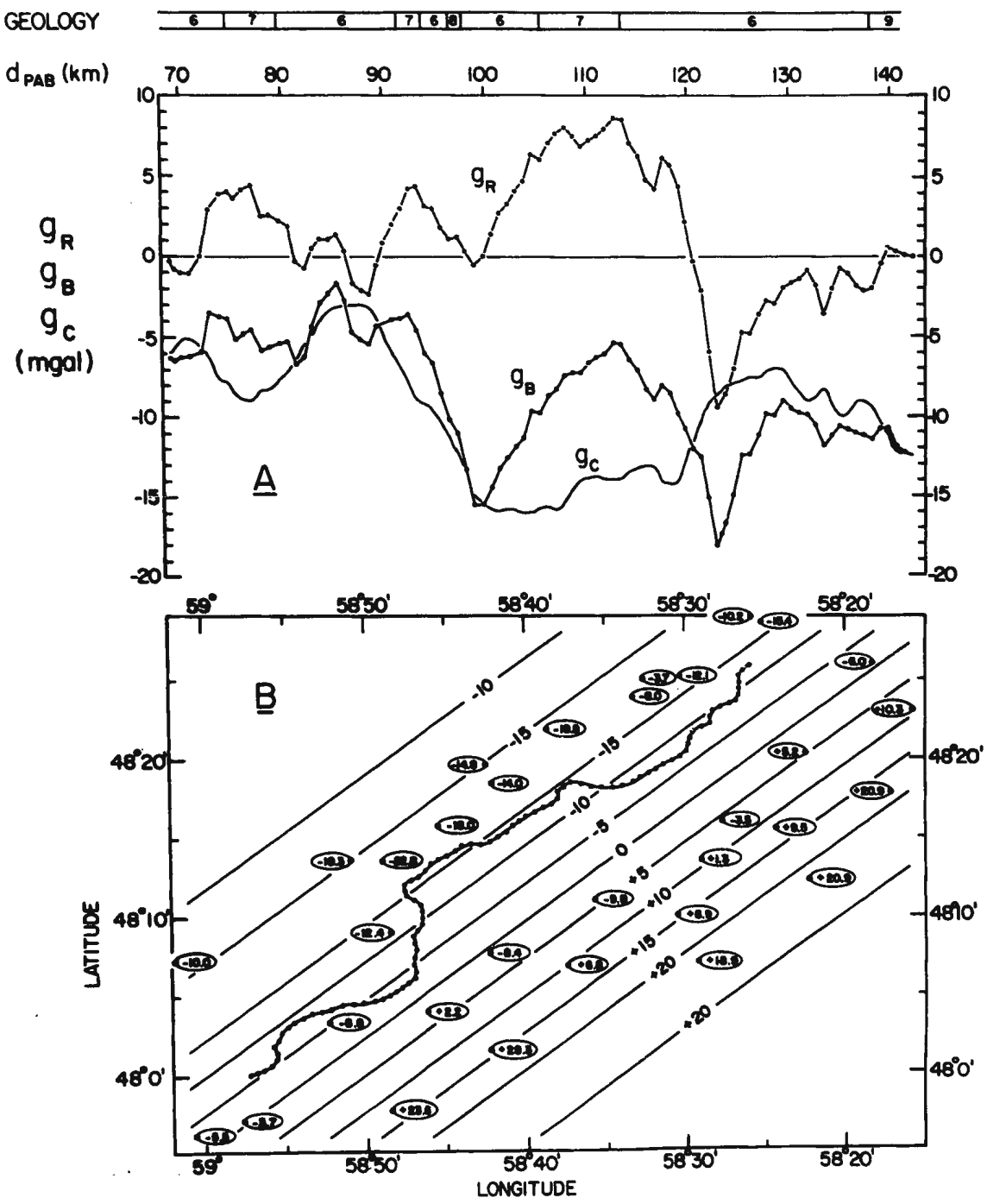

Figure 3.5.1 (B) Plot of traverse between distances 69 km and 142 km from Port-aux-Basques. Heavy dots with ovals show Dominion Observatory stations with Bouguer anomalies. Anomaly contours, with 5 mgal spacing, have been drawn on the basis of these and other Dominion Observatory values.

(A) g_B, observed anomaly profile; g_C, regional gravity pattern obtained from contours (Figure 3.5.1(B); g_R, residual gravity profile.

Geologic symbols are explained in Table A5.1. A further description of the above diagrams is given in Section 3.5.

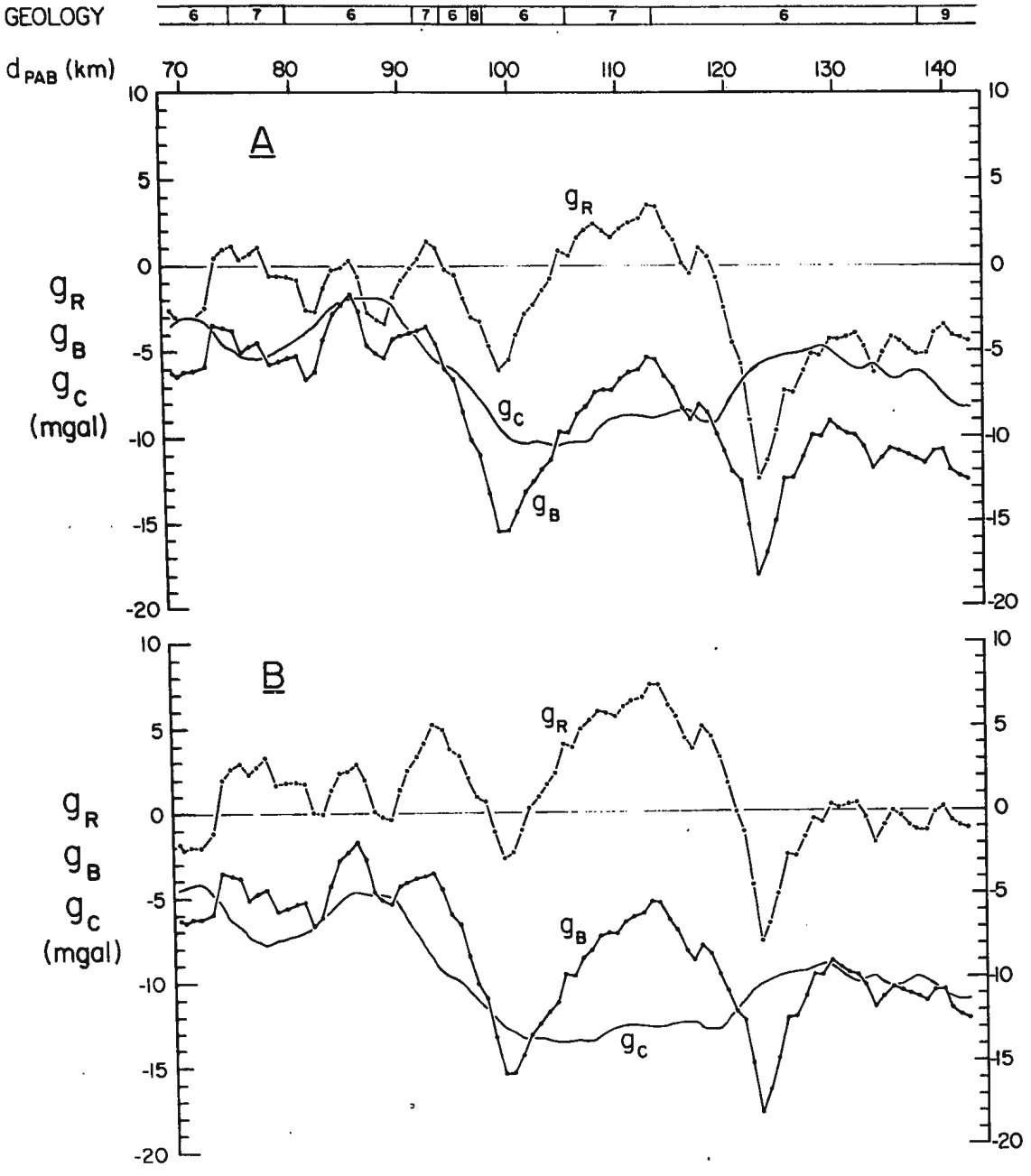

Figure 3.5.2 Observed, regional, and residual anomaly profiles (Figure 3.5.1 and Section 3.5) for regional gravity fits, in region shown in Figure 3.5.1, by polynomials of (A) order 1 and (B) order 2.

CHAPTER FOUR

GENERAL PROFILE INTERPRETATION

4.1 Scope.

In this chapter the Bouguer anomaly profile along the Trans-Canada Highway across Newfoundland is examined and an attempt is made to relate profile features to the mapped geology of the region. The chapter is intended as a prelude to a more thorough interpretation, as is illustrated in Chapter 5 for the section between Notre Dame Junction and Traytown, to be carried out in the "post thesis" phase of this project.

Extrapolation downwards of surface geologic features on the basis of gravity readings alone is always somewhat speculative; to do so qualitatively is even more so. Nevertheless, some possible explanations will be offered for most of the prominent features observed and a number of tentative conclusions will be drawn.

Position along the traverse is given in terms of d_{PAB}, the distance along the route from Port-aux-Basques. Subdivision numbers (to be quoted Sd. followed by the number) refer to Tables A5.1 and Figures A5.2.1 to A5.2.6.

4.2 Geologic setting.

The Appalachian mountain system extends from the southeastern

United States northeastward to the island of Newfoundland, and presumably beyond it to the edge of the continental shelf. In Newfoundland this system is bounded to the southeast by the Atlantic Ocean and to the northwest by the Gulf of St. Lawrence and the Strait of Belle Isle. The geologic synopsis which follows is based primarily on the excellent review of the pre-Carboniferous development of this region given by Williams (1969).

Broadly speaking, three distinct geologic provinces are recognized, with the system exhibiting a two-sided symmetry (Williams, 1964_a), and with the major structures showing a northeasterly trend. These provinces are, from east to west: the Avalon platform, the central Paleozoic mobile belt, and the Western platform. Both platforms are underlain by Precambrian rocks, although no correlation between them has yet been found. Both contain Lower Paleozoic shelf deposits, thought to be primarily of shallow water origin, as well as Paleozoic intrusives. The Precambrian rocks of the Western platform, some of which are more than 940 million years old, are believed to belong to the Grenville province of the Canadian Shield. Those of the Avalon platform, which show less metamorphism, are considered to be younger. The central Paleozoic mobile belt contains Cambrian, Ordovician and Silurian sedimentary and volcanic rocks, which were laid down in a broad geosyncline. These rocks show considerable deformations, and, in a few places, some metamorphism. Major orogenies have affected almost all of the central mobile belt and parts of the platforms areas. Massive intrusions, mainly granitic, are associated with the Acadian orogeny (Devonian), and wide-scale

deformations are associated both with it and with the earlier Taconic orogeny (Ordovician). A narrow Carboniferous belt extends intermittently from Port-aux-Basques northeastward to the Grey Islands, off the Great Northern Peninsula. Folding and faulting in that belt occurred during the Appalachian orogeny of the late Paleozoic. The Barachois Group, of Pennsylvanian age, are the youngest rocks of any significance in Newfoundland.

This survey traverses sections of all three geologic provinces. The boundaries, as estimated from William's (1969) maps, are crossed at roughly the following points:

d_{PAB} = 160 km central Paleozoic mobile belt to Western platform

d_{PAB} = 322 km Western platform to central Paleozoic mobile belt

d_{PAB} = 650 km central Paleozoic mobile belt to Avalon platform

Some geologic information about the regions traversed is given in Table A5.1 and Figures A5.2.1 to A5.2.6, inclusive. Much of this was obtained from maps of the Geological Survey of Canada; these include Map 1231A of the whole island (Williams, 1967) as well as more local maps (scale 1:253,440) for regions near the route.

4.3 Central Paleozoic mobile belt - southwestern Newfoundland.

The traverse along this section extends from d_{PAB} = 0 to 160 km. A major fault at d_{PAB} = 31 km separates the Carboniferous sediments to the west and north from the Long Range complex to the east. The effect of this fault is not clearly seen on the Bouguer anomaly profile because

of the small angle which the route makes with it near the boundary. A small peak superimposed on the anomaly low in the region of d_{PAB} = 31 km is not correlated with the mapped geology. A possible explanation is that it is due to a basic or ultrabasic intrusive body since these are exposed within a few kilometers to the east and northeast.

The author has examined the overall anomaly decrease between Port-aux-Basques and d_{PAB} = 28 km from two viewpoints. The first, assumes that a uniform decrease is associated with the Devonian granite (Sd. 3) and suggests that fluctuations are due to the superposed positive gravity effect from small-scale intermediate to basic intrusives (such as exposed in Sd. 4). This view affixes no special importance to the fault at d_{PAB} = 9 km. A second view, which attaches considerable significance to this fault, divides the anomaly decrease into two parts: (i) from Port-aux-Basques to d_{PAB} = 9 km, and (ii) d_{PAB} = 14 km to 28 km. The lateral displacement of slope (ii) from slope (i) may then be associated, in part, with the fault.

Between d_{PAB} = 31 km and 60 km the traverse stays within a couple of kilometers of the faulted boundary of the Carboniferous belt, and as far as d_{PAB} = 50 km is in close proximity with the Devonian granite of the Long Range complex. The low along this section is thus partly attributable to this granite.

The winding route effect, as discussed in section 3.5, has to be considered when studying this region. For example, it may be noted that, although the low at d_{PAB} = 99 km is de-emphasized in the residual plots (Figures 3.5.1 and 3.5.2), the anomaly pattern may still be

affected by the manner in which the route curves with respect to the body causing the feature. As well, the anomaly plot near d_{PAB} = 123 km, a sharp low which is most likely related to the sodium chloride deposits currently being investigated commercially in the Fischell's Brook area, may be affected by the manner in which the road winds.

Many of the anomaly profile features in this region seem to be closely related to mapped deposits of gypsum and sodium chloride. For example, Map 1117A (Riley, 1962) shows the following deposits near the route; (i) at d_{PAB} = 70 km, gypsum approximately 1 km off route; (ii) at d_{PAB} = 96 km, gypsum within 300 m of route; (iii) at d_{PAB} = 106 km, gypsum 1 km from route on east side and just over 2 km from route on west side; (iv) at d_{PAB} = 116 km, sodium chloride less than 1 km from route; (v) at d_{PAB} = 134 km, gypsum less than 2 km from route; and (vi) at d_{PAB} = 137 km, gypsum less than 2 km from route. Except for (ii) and (iii), where the effects are slight, these deposits correspond to distinct profile troughs. It is perhaps not unreasonable to postulate that deposits of low density minerals are also associated with troughs at some of the following positions: d_{PAB} = 82 km, 88 km, 99 km, and 146 km, where some of these features are best seen on the residual plots.

The possibility that the features of interest are the peaks between the troughs, with a corresponding explanation suggesting intermediate to basic intrusions into the Carboniferous sediments, has been considered. However, no such intrusions are shown on the geologic maps for this area, nor do they seem to be suggested by the aeromagnetic maps of the region.

A density of 2.59 gm/cm^3 is suggested for the Carboniferous sandstone, siltstone, and conglomerate. This value is the weighted arithmetic mean of 2.52 gm/cm^3, obtained from 5 samples on this survey, and 2.64 gm/cm^3, obtained from 8 samples by the Gravity Division of the Dominion Observatory (Weaver, 1967). Because of a shortage of samples, the differences in mean densities among the Anguille, Codroy, and Barachois groups are not known. Relative anomaly lows seem to be associated with the Codroy group, but this may be, in part, due to the low density ore bodies in that group.

The overall decrease in anomaly values from about -3 mgal at d_{PAB} = 60 km to about -15 mgal at d_{PAB} = 160 km, in spite of the fact that the profile approaches to within 5 km of a large body of anorthosite of density approximately 2.70 gm/cm^3 (Weaver, 1967), suggests the following possibilities: (i) an increase in sediment thickness towards the northeast; (ii) an underlying basement of low density material, such as granite, which thickens towards the northeast. In addition, the long wave length of this feature suggests the possibility that the cause may be deep in the crust.

Riley (1962) quotes thicknesses equivalent to more than 1500 m for the Barachois group and more than 750 m for the Anguille group, but does not state a thickness for the Codroy group. Baird and Cote (1964) give a composite thickness equivalent to about 7000 m for the Carboniferous sediments of this region. Rough calculations from this profile, based on the effects of infinite horizontal slabs of density contrast -0.08 gm/cm^3 with the underlying rocks, suggest vertical thicknesses of more

than 1½ km at d_{PAB} = 70 km and about 5 km at d_{PAB} = 150 km.

4.4 The Western platform.

At d_{PAB} = 179 km (Figure A5.2.2) the traverse crosses the boundary, as estimated from Map 1231A (Williams, 1967), between the Carboniferous sediments of southwestern Newfoundland and the St. George's group (Lower Ordovician). The St. George's group is composed principally of limestone (2.76 gm/cm^3) and dolomite with some sandstone and shale, and has an estimated thickness (Riley, 1962) of 745 m. Between d_{PAB} = 170 km and 179 km the route runs quite near the boundary. A major positive anomaly change occurs, as expected, but is centered at about the 170 km mark, rather than 179 km. Since an error in the geologic mapping is unlikely, the anomaly profile in this region might suggest (i) that the thickness of the Carboniferous sediments decreases significantly over the last few kilometers west of the boundary, or (ii) that in this area these sediments are underlain by a low density material, say granite, which meets the basement underlying the St. George's group at about d_{PAB} = 170 km. An intrusion of the granite into this basement might explain the negative anomaly values between d_{PAB} = 179 km and 200 km. A model study by Weaver (1967) for a profile perpendicular to this one shows such a granite body underlying approximately 7 km of Carboniferous sediments. However, the use of a sediment density of 2.59 gm/cm^3 (Section 4.3) would probably eliminate the need for this granite in his model. It should be stressed that the foregoing discussion is largely speculative and that construction

of a reliable subsurface model near this boundary of the Western platform must await further geophysical data.

A Bouguer anomaly increase between d_{PAB} = 192 km and 216 km, a sharp decrease from d_{PAB} = 216 km to 222 km, and an increase between d_{PAB} = 222 km and 268 km do not seem to correlate with the geologic mappings given by Riley (1957, 1962), Baird (1960), or Williams (1967). A winding route effect, already described for a region further south (Sections 3.5 and 4.3), is evident between d_{PAB} = 216 km and 230 km, and accounts in part for the anomaly pattern near d_{PAB} = 222 km. The anomaly profile between d_{PAB} = 165 km and 222 km seems to follow the topography of the route. However, no more than about 1 mgal of this can be explained by the fact that the standard value (2.67 gm/cm^3) instead of the actual mean density of the region (about 2.75 gm/cm^3) was used in the Bouguer correction.

Between d_{PAB} = 179 km and 232 km the profile crosses the St. George's group in four places and the Humber Arm group (Sb. 11; shale, sandstone, conglomerate, and limestone) in three. Recent evidence (by Rodgers and Neale, 1963; Kay, 1969; and others) suggests that rocks of the Humber Arm group are allochthonous, and these authors postulate that they represent klippen formed to the east in the central Paleozoic mobile belt and transported to their present location by a gravity slide during what Kay (1969) calls the "Bonnian disturbance" of the Taconian orogeny. This profile contributes very little to the discussion for two reasons: (i) the route is seldom more than a couple of kilometers from the irregular boundary between the Humber Arm and St. George's groups, and (ii) the density contrast between them is small. In fact, because of a lack of

samples of Humber Arm limestone and St. George's dolomite, shale, and sandstone, the real density contrast is probably less than the value of 0.03 gm/cm^3 obtained in this survey.

The fluctuations between d_{PAB} = 222 km and 250 km are not correlated with the mapped geology. It may be noted that this is a section of excellent elevation control (Figure 2.2.1), but terrain correction errors (Table 2.5.1) may be as large as 1 mgal for some stations.

The effect of the Carboniferous Codroy group (Sd. 6) is seen between d_{PAB} = 250 km and 261 km superposed on the overall increase in the Bouguer anomalies along this section. The boundary at 268 km between Cambrian schists and gneisses (Sd. 13) and the Codroy group marks the end of this overall increase.

Carboniferous sediments of the Codroy group, the Windsor group (Sd. 14), and the Anguille group (Sd. 7) extend from d_{PAB} = 268 to 322 km (Figure A5.2.3), where they are terminated at a major fault. A series of crests and troughs are superposed on the overall anomaly decrease between d_{PAB} = 268 and 306 km. Interpretation of these short-wavelength features is complicated by the meandering of the route and retarded by the absence of rock samples. There does not seem to be a correlation between these and the subdivisions of the Windsor group shown by Baird (1960). It is perhaps interesting to speculate, as was done for the Carboniferous region in southwestern Newfoundland, that these troughs are due to low density ore deposits. Alternately, one of the peaks seems to correlate with a major fault, shown on the geologic maps, and it is possible that the others may be associated with faults not yet mapped.

The overall anomaly decrease in this section is perhaps due to one of or both the following: (i) a thickening of the low density sediments towards the east; (ii) a low-density basement (possibly corresponding to the coarse-grained porphyritic biotite granite exposed on the opposite side of Sandy Lake), which may thicken towards the east.

The rapid increase in Bouguer anomaly values between d_{PAB} = 306 km and 322 km coincides with a more northerly orientation of the route, and may be due to underlying intermediate to basic intrusive rocks with a northerly increase in thickness. It may be noted from Map 1231A (Williams, 1967) that quartz diorite, diorite, and gabbro are exposed several kilometers to the north of point d_{PAB} = 322 km.

4.5 Central Paleozoic mobile belt - northeastern Newfoundland.

An examination of the manner in which the traverse through this region meanders, with respect to the regional gravity contours shown on Weaver's (1967) numerically smoothed regional gravity map of Newfoundland, suggests that a large winding-route effect (Section 3.5) is associated with some of the long-wavelength anomaly profile features, and that this effect is negligible for the short-wavelength features. For the high in the region of d_{PAB} = 415 km, this effect may be as large as 10 mgal; while for the remaining features, it is less than 5 mgal.

The anomaly profile trough between d_{PAB} = 322 km and 370 km corresponds to a body of coarse-grained porphyritic biotite granite (Sd. 15), between d_{PAB} = 322 km and 338 km, and to Silurian rhyolite, trachyte flow, and pyroclastic rocks (Sd. 16), between d_{PAB} = 340 km and

370 km. It seems probable that this granite intrudes the Silurian volcanics, and is the primary cause of the low in this region.

The peak at d_{PAB} = 336 km is in a region of Carboniferous sediments (Sd. 5). It is most likely due to an ultrabasic intrusive body which outcrops just south of the route. The presence of this body also shows up strongly on the Geological Survey of Canada Aeromagnetic Map 4458G. These results suggest that this ultrabasic intrusion is considerably larger than is indicated by the outcropping surface.

The anomaly trough at d_{PAB} = 382 km appears to be due to the granite (Sd. 17) shown on Map 40-1962 (Neale and Nashe, 1963).

Interpretation of the short-wavelength fluctuations between d_{PAB} = 390 km and 425 km is complicated by the manner in which the route appears to wind with respect to the causative bodies. The overall high in this region does not have a strong correlation with the mapped geology. However, since the peak values correspond to a mapped region (Sd. 22) of diorite, quartz diorite, and gabbro (Neale and Nashe, 1963) near South Brook, it is perhaps reasonable to postulate that this high is due to a large body of these rocks underlying the whole area. It may be noted that a large surface area of these rocks (Sd. 25), mapped between d_{PAB} = 431 km and 451 km, seem to have little effect on the profile, thus suggesting that this layer is quite thin in this region.

The long-wavelength variations between d_{PAB} = 435 km and 515 km do not seem to correlate with the mapped geology. Possibly they may be explained by variations in the depths of Ordovician and Silurian rocks in this region.

Between d_{PAB} = 505 km and 515 km the route approaches a large dioritic body, shown on Map 19-1962 (Williams, 1962), and this probably explains the increase in anomaly values in this section.

The region between d_{PAB} = 541 km and 664 km is discussed in Chapter 5.

4.6 The Avalon platform.

The part of the Avalon platform traversed by this profile consists almost entirely of elongated belts of the Love Cove and Musgravetown groups. Interpretation of profile details is complicated by the considerable meandering of the route. A thorough discussion of the gravity profile for the area must thus await an analysis of the winding-route effect, and this is planned for the post-thesis phase of the project.

The overall anomaly decrease between d_{PAB} = 663 km and 745 km does not correlate with the mapped geology. In fact, only two features seem capable of explanation by the surface geologic picture. The first is the relative low at d_{PAB} = 704 km, which appears to be associated with a large body of coarse grained porphyritic biotite granite to the north of this part of the traverse. The second is a contrast between the Musgravetown (Sd. 36) and Connecting Point (Sd. 37) groups in the region between d_{PAB} = 743 km and 781 km. The pattern here suggests one of or both the following: (i) a faulting of the latter with respect to the former; (ii) that the rocks of the latter have a smaller mean density than those of the former. There has not been sufficient rock sampling

to permit a resolution of (ii), but (i) is in accordance with Geologic Map 1130A (Jenness, 1963).

4.7 Profile symmetry.

One of the most striking features of the anomaly profile between d_{PAB} = 200 km and 770 km is that its pattern is roughly symmetrical about the point d_{PAB} = 485 km. Since geologic studies have established no correlation between the Precambrian rocks of the Avalon and Western platforms, the correspondence between the platform sections is quite possibly concidental and without special significance.

However the symmetry of the traverse across the central Paleozoic mobile belt is worth further investigation. That it is not accounted for by the winding nature of the route may be seen from an examination of Weaver's (1968) gravity maps of the island. In actual fact, these maps show that this meandering tends to deemphasize certain pattern features. For example, the anomaly values in the region of d_{PAB} = 550 km would have been larger if the route had gone across instead of around a large body of diorite in that area. Anomaly profiles (not shown), plotted on the basis of Weaver's (1968) maps, have a somewhat similar symmetry along lines drawn perpendicular to the geologic trend across this region. Although there are significant pattern variations, the symmetry appears to extend as far northeast as lines drawn through White Bay and Burnt Bay, and as far southwest as a line drawn between Corner Brook and Goobies.

The profile anomaly highs in this pattern seem to be mainly associated with known bodies of intermediate to basic rocks, while the lows correspond to mapped bodies of granite. The model for the section between Notre Dame Junction and Traytown (Figure 5.3.2) agrees with this, but shows as well a contribution from the irregular thickness of the underlying "intermediate to basic" layer.

4.8 Geologic faults and their gravity effect.

Less than 50% of the faults mapped along the route have a noticeable effect on the gravity profile, with most of these effects being quite small.

The Cabot fault is crossed at d_{PAB} = 31 km and d_{PAB} = 322 km. In both cases, however, its gravitational effect is masked by the orientations of the route near that feature.

The geologic maps show the Musgravetown group, at d_{PAB} = 652 km to 656 km, to be faulted at both its boundaries, and this feature has a strong effect on the gravity profile in that region.

An article entitled "The Hermitage Flexure, the Cabot Fault, and the Disappearance of the Newfoundland Central Mobile Belt", by Williams et al (1970), has come to the author's attention since the writing of the first parts of this chapter. These authors suggest that the central mobile belt is almost completely removed in southwestern Newfoundland. It may also be noted that in their discussion of the Hermitage Flexure, no mention is made of the fault at d_{PAB} = 9 km.

4.9 Isostatic considerations.

The extent of the island's isostatic compensation has been discussed by Weaver (1967). His approach involved the averaging of Bouguer anomalies for lowest, intermediate, and highest stations, which for the region south of Latitude 50^o have average elevations of 3 m, 175 m, and 280 m, respectively. Relative to the lowest stations he noted that there is a slight amount of compensation for the intermediate stations but none for the highest stations.

The calculation of isostatic anomalies is being left for the post-thesis phase of the project.

CHAPTER FIVE

PROFILE INTERPRETATION BETWEEN NOTRE DAME JUNCTION AND TRAYTOWN

5.1 Geology of the region.

The principal geologic subdivisions of this region as well as the route through it are shown in Figure 5.1.1, where the letters, K to P, refer to positions also shown in Figures 1.1.1 and A5.2.1 to A5.2.6. The legend, given in Figure 5.3.2, contains a cross-reference to Table A5.1, in which the geologic subdivisions are described, and Figures A5.2.1 to A5.2.6, in which their boundaries along the route are defined.

The oldest rocks in the region belong to the Precambrian Love Cove and Musgravetown groups, shown together as part of the Avalon platform in Figure 5.1.1. The Love Cove group, which probably has a minimum thickness of 4800 m, consists of a wide variety of sedimentary and volcanic rocks interbedded with each other. The Musgravetown group, with a thickness estimated as roughly 3200 m, consists of coarse clastic sediments and interbedded volcanic rocks. Rocks of the Love Cove group contain regional metamorphism and are believed to be older than the relatively unmetamorphosed Musgravetown group (Jenness, 1963).

The term "Gander Lake Group" was proposed by Jenness (1958) for a great thickness of shales, slates, and greywhackes, and some interbedded volcanic rocks, that cross Gander Lake in a northeasterly direction. Three units have been recognized and described (Jenness, 1963). The

lower unit, with a thickness of at least 3200 m, consists mainly of fine to medium grained greywackes and argillaceous sandstones. Much of this unit has been metamorphosed to schists and gneisses. The middle unit comprises more than 800 m of intercalated volcanic and sedimentary rocks, with nearly half of it consisting of fine to medium grained pyroclastic rocks. The upper unit consists dominantly of shales, and has an estimated thickness of more than 3200 m. The age of the lower unit is uncertain, but is either Ordovician (Jenness, 1963) or Cambrian (Williams, 1969). The middle and upper units have been dated by fossils as Middle Ordovician. The middle and upper units are shown together in Figure 5.1.1, and are separated from the lower unit to the southeast by a boundary drawn just to the southeast of the elongated belt of gabbro and ultrabasic rocks. This belt, presumably of Ordovician age (Jenness, 1963), stretches from the North shore of Gander Lake in a northeasterly direction towards the coast.

The Botwood group consists of sedimentary and volcanic rocks of Silurian age. Williams (1964_b) suggests that these rocks are largely of shallow-water, continental origin, and that they were deposited under conditions of crustal unrest.

These Silurian strata are intruded by a large body of intermediate to basic rocks, probably of Middle to Late Silurian age (Williams, 1969). This is referred to in Figure 5.1.1 as diorite, but Williams (1962) points out that it also contains varieties more basic than diorite, and that there is as well some associated quartz diorite, pink syenite, and granite. Granite, intruding the diorite, is exposed over a large area.

A large body of granite to the south of point M, an elongated belt of granite passing near point N, and a granitic intrusion into the Love Cove group, belong to the Ackley batholith which has been traced from Fortune Bay northeastward to the north side of Bonavista Bay. It consists mainly of a coarse-grained porphyritic biotite granite. Jenness (1963) gives evidence that this granite was intruded in the molten state. Southwest of point M in Figure 5.1.1, the Gander Lake group has been intruded by medium to coarse-grained leucogranite.

There are also dioritic intrusions exposed on Gooseberry Island, Hunch Island, and Gulch Island in Bonavista Bay. Although their age is not known, these bodies intrude members of the Connecting Point group and are thus no older than late Precambrian.

Jenness (1963) suggests that the Gander Lake and Love Cove groups are separated by a fault or fault zone, even though the contact between them has not been observed. The Love Cove and Musgravetown Groups are separated by faults through the region shown in figure 5.1.1. There is also major off-route faulting in the Gander Lake and Botwood Groups, both to the northeast and southwest of the route between Notre Dame Junction and Gander.

William's (1964_b) map shows the bedding of the Botwood Group dipping steeply southeast in the region near the boundary with the Gander Lake group, while the dip is towards the dioritic intrusion in the region surrounding that body. Folding within the Gander Lake group appears to be mostly monoclinal, dipping steeply west. A structural terrace found in the region around Gander appears to be related to the nearly horizontal

attitude of the underlying bedrock structures. In addition to the above, numerous small folds have been observed in rocks belonging to all the sedimentary groups throughout the region.

5.2 Rock sampling.

Rock sampling sites in this region are shown in Figures A5.2.4 to A5.2.6. In addition, six samples of the Botwood group were obtained along the road between Notre Dame Junction and Lewisporte, and four samples of the Musgravetown group were collected along the Trans-Canada highway between Come-by-Chance and Whitbourne. Descriptions of these samples, with density information, are given in Tables A5.1 and A6.1. Although more samples would have been desirable, these tables do show that rocks collected from the Botwood and Gander Lake groups are representative of these areas.

On the basis of samples collected between Gambo and Whitbourne a density of (2.76 ± 0.02) gm/cm^3 has been assigned to the Love Cove and Musgravetown groups, taken as one unit. Unfortunately most of these samples are from regions to the south of the map area of Figure 5.1.1, and it is not known how representative they are of this area; there does seem to be a shortage of sedimentary rock samples.

The Ackley batholith has been sampled at only one site, where a value of 2.62 gm/cm^3 was obtained. Jenness (1963), however, describes the granites in this region as being of fairly homogeneous composition, except along their eastern flank where mixed rocks occur.

Although the large diorite body intruding the Botwood group was not sampled, 14 sites along the profile in other parts of the island yielded a value of (2.82 ± 0.03) gm/cm^3 for this rock type.

No gabbro or ultrabasic rocks were collected in this survey. However, Dobrin (1960) quotes values ranging from 2.85 to 3.12 gm/cm^3 for gabbro, and from 3.10 to 3.30 gm/cm^3 for ultrabasics (not serpentinized).

5.3 Model study and interpretation.

The techniques described in Sections 3.2 and 3.3 have been employed to produce a geometrically simple model to represent the geologic structure along and near the route between Notre Dame Junction and Traytown. This model (i) agrees with the observed Bouguer anomaly profile, (ii) incorporates the available relevant geological information, and (iii) is reasonably consistent with other geophysical data. The projection of the measured anomaly profile onto the mean traverse direction, the representative model, and the model's anomaly profile are all shown in Figure 5.3.2. This picture is intended to represent cross-sections of the structure in planes parallel to, but somewhat displaced towards the gravity stations from, the vertical plane along the mean traverse direction.

To simplify model construction, the densities of the various bodies in the region were referenced to 2.75 gm/cm^3, which is the mean density of rocks collected from the Gander Lake group. Thus the "density

contrast", $\Delta\rho$, of that group is zero. For simplicity, as well, density contrasts of magnitudes less than or equal to 0.01 gm/cm^3 were neglected.

Figure 5.3.2, viewed in conjunction with Figure 5.1.1 and Sections 5.1 and 5.2, is, for the most part, self explanatory. Some aspects of the study, however, do require further comment.

5.3.1 Error analysis.

This consists of an examination of the following: (i) errors in measured anomaly values; (ii) winding route and profile projection errors; (iii) agreement between model and (mapped) surface geology; (iv) "goodness" of fit between observed and model anomaly profiles; (v) interpretation ambiguity.

The random errors in measured anomalies are given in Figure 2.5.1; these are ±0.3 mgal (K to M) and ±0.4 mgal (M to P). Any systematic error associated with the use of the international gravity formula of 1930 (section 2.5) is normally removed as part of the regional correction. However, because such corrections have not been made in this study, the geologic interpretation of the horizontal slab portion of the "intermediate to basic" layer (Figure 5.3.2), which was introduced to give numerical agreement between model and observed anomaly profiles, is somewhat restricted. There is also a systematic error, for most geologic subdivisions, due to the use of 2.67 gm/cm^3, instead of the mean subdivision density, in the Bouguer corrections. In this region these errors, which may be computed using Equation 2.5.1 with elevations and

densities from Tables A3.1 and A5.1, respectively, are less than ±0.4 mgal for more than 90% of the stations. When and where required, the Bouguer anomalies can be corrected for these density discrepancies. However, in view of other uncertainties inherent in the interpretation, these corrections have not been deemed necessary here.

The "winding route" effect (Section 3.5) has been examined for this region in terms of the road's meandering with respect to gravity anomaly contours shown on (i) Weaver's (1967) numerically smoothed regional gravity map of Newfoundland, and (ii) Weaver's (1968) Map No. 55 (Figure 5.3.1). For the former this effect appears to be negligible, while for the latter it may amount to as much as 0.5 mgal (roughly estimated). Some of this distortion is eliminated by a projection of the profile onto the mean traverse direction. The anomaly pattern changes arising from this projection, as seen from a comparison of Figures 5.3.2 and A5.2.5, are mainly reductions in wavelength and changes in anomaly profile slopes. The former is observed for the belt of gabbro and ultrabasic rocks northwest of Gander and for a section of the Gander Lake group northwest of Gambo. The change in profile slope is especially significant along the 4 km section northwest of Traytown, and for which a fit hasn't yet been achieved.

The model shown in Figure 5.3.2 conforms, except for representations of a dioritic body southeast of Notre Dame Junction and a granitic body near the southeastern end of Gander Lake, to the "two-dimensional" definition given in Section 3.1. As well, its elongation axis is perpendicular to the vertical plane of the mean traverse direction.

That the surface of this model only approximates the mapped surface geology can be seen from an inspection of Figures 5.1.1 and 5.3.2. The geologic maps of the region show that most of the bodies have departures of less than 15^{o} from perpendicularity. Figures A7.2 and A7.4 suggest that the error associated with such a small obliqueness does not exceed about 2% of the maximum gravity effect of the model representation of the oblique body. For this study the total contribution from this factor is less than 0.4 mgal for the majority of stations. The errors associated with uncorrected departures from two-dimensionality have been roughly estimated, using graphs of the type illustrated in figure 3.3.1, as not exceeding about ±1½ mgal. A more accurate estimation is difficult because these graphs have been constructed for bodies ending in planes parallel to the vertical plane of the traverse. Furthermore, the sub-surface extensions of the surface boundaries are unknown. It is shown in Appendix 8 that error in making end effect corrections for the bodies of granite and diorite amounts to about ±0.4 mgal.

For this study the mean of $(g_M - g_B)$, the difference between an observed and model anomaly, is -0.2 mgal, and the r.m.s. deviation about this mean is ±1.7 mgal. If the poorly fitted 4 km section near Traytown is neglected, the mean becomes zero, and the deviation ±0.9 mgal. In terms of the preceding error discussion, this fit seems adequate.

There is, as has been mentioned in Section 1.3, a fundamental ambiguity inherent in gravity interpretation. An excellent discussion of the ambiguity in geophysical interpretation, including gravity, has

been given by Roy (1962). What it means is that an infinite number of different models can be constructed to agree with the observed anomaly profile. Fortunately, whole classes of these can be eliminated by other geophysical and geological requirements. For this region, these include: matching model and observed surface geologic features; keeping within the narrow density range associated with crustal rocks; conforming to established geological principles; being reasonably consistent with the aeromagnetic survey of this area, and with the seismic profiles in adjacent regions. The ambiguity could be reduced even further by means of (i) a detailed interpretation of the magnetic anomalies within the region, (ii) seismic studies, (iii) application of some of the wide variety of electrical techniques; (iv) drill-hole data, and (v) more gravity information. A more dependable picture of this region's crustal structure thus awaits further geophysical and geological evidence.

5.3.2 Use of magnetic and seismic information.

One of the features shown in Figure 5.3.2 is an underlaying "intermediate to basic" layer. Its existence is also suggested by seismic refraction profiles run from Newfoundland's northeast coast onto the continental shelf. Ewing et al. (1966) show the top surface of this layer at a depth of about 12 km for the region near Cape Freels, while Dainty et al. (1966) give this depth as about 7.5 km for the Burnt Pond region, west of Grand Falls. The latter have quoted a value of 2.83 gm/cm^3 for its density. A similar seismic profile from Fogo Island northeastward to the edge of the continental shelf has been described by

Sheridan and Drake (1968), and shows a layer of basic and ultrabasic rocks extending downwards from a minimum depth of about 4 km near the Funk Island, with this value increasing towards the northeast and southwest. Weaver (1967), in a correlation of his gravity results with the seismic results of Ewing et al.(1966), treats this as a dioritic layer of density 2.8 gm/cm^3. From these considerations, a density contrast of +0.07 gm/cm^3 has been assigned to the "intermediate to basic" layer required in the model study of this region.

Belts of closely spaced magnetic contours, trending northeastward through this region, correlate with the gravity anomaly profile in two places. The first, northwest of Gander, also coincides with a geologic mapping of gabbro and ultrabasic rocks. A crude estimate, using the "half-width" technique (described in standard references; e.g., Dobrin, 1960), places the source of one of these magnetic anomalies at a depth of approximately 1½ km. Figure 5.3.2 shows that the placement of these rocks at a maximum depth of 1 km and assigning them a density contrast of +0.18 gm/cm^3 gives a satisfactory gravity fit. The other belt, near Traytown, does not have a mapped geologic explanation, and hasn't yet been incorporated into the gravity model. The introduction of a basic to ultrabasic layer, underlying the sedimentary and volcanic rocks, near Traytown would certainly improve the profile fit in that region.

5.3.3 End effects.

Figures 5.1.1 and 5.3.1 (the geology and gravity maps of this region, respectively) suggest that semi-infinite model structures be used

to represent (i) the granite at the southeastern end of Gander Lake, and abutting the Gander Lake group close to the profile, and (ii) the body of diorite southeast of Notre Dame Junction, which meets the Botwood group near the profile. Rather than making conventional end corrections to the plotted profile, it was decided to replace the density of each of these bodies by a weighted mean of that value and the density of its neighbour; this made it possible to continue using the two-dimensional model study computer program. It is assumed that each body and its abutting neighbour extend in opposite directions to infinity from near the profile. The method used to obtain these weighted densities, and the errors involved, are discussed in Appendix 8.

5.3.4 Gravity surveys in adjacent regions.

A concurrent and independent gravity study by Miller (1970) has placed a rock layer of density 2.77 gm/cm^3 between depths of 5 and 10 km beneath the Bay of Exploits area, and a similar layer of density 2.82 gm/cm^3 beneath the Fogo-Change Islands region.

Weaver (1967) has done a model study along a profile, parallel to this one, across the large body of diorite shown in Figure 5.1.1. Because the present survey only skirts the edge of this dioritic body, no valid comparison of its model representations can be made. Weaver underlies the whole region with granodiorite, places the maximum depth of the Botwood group at 6 km, and gives a significantly different representation of the top surface of the large mass of granite underlying the region.

5.3.5 Geologic significance.

The maximum depth shown for the Gander Lake group is roughly equivalent to its original thickness. Because the underlying granite was intruded in a molten state, no geologic restriction has been placed on the shape of its interface with the Gander Lake group. This large mass of granite is a major feature of the model. Most of it is a sub-surface extension of what geologists have mapped as the Ackley batholith. It may be noted that the cross-sectional shape obtained for this body is not batholithic, but is instead somewhat "funnel-shaped". Perhaps the terms "lopolith" or "phacolith" would be more appropriate, although the latter appears to be applied to smaller features (Badgley, 1965).

The vertical interface between the Botwood and Gander Lake groups is in keeping with the geology of the area. The vertical face for this part of the underlying granite does not seem to be geologically realistic; however, this feature can probably be satisfactorily altered without significantly disrupting the profile fit.

The model shows the underlying "intermediate to basic" layer approaching to within 0.5 km of the surface near Traytown. The density assumed for this layer corresponds to that of diorite, and this rock type constitutes several islands to the northeast in Bonavista Bay. The introduction of a near surface basic to ultrabasic body, as suggested in Section 5.3.1, would, however, reduce the necessity of bringing this "dioritic" layer so near the surface in the model.

Very little significance can be attached to the 4 km thickness of the horizontal slab portion of the underlying "intermediate to basic"

layer. This is mainly because an increase in the slab's thickness can be offset by a decrease in its density contrast to yield the same gravitational effect. Systematic errors in the Bouguer anomaly (Section 5.3.1) and in the density contrasts (due to the referencing of densities to 2.75 gm/cm^3 instead of the mean crustal density) have been compensated for by the thickness and density chosen for this slab.

The structural terrace near Gander coincides with the nearly horizontal attitude of the upper surface of the underlying granite, and may be worth further investigation.

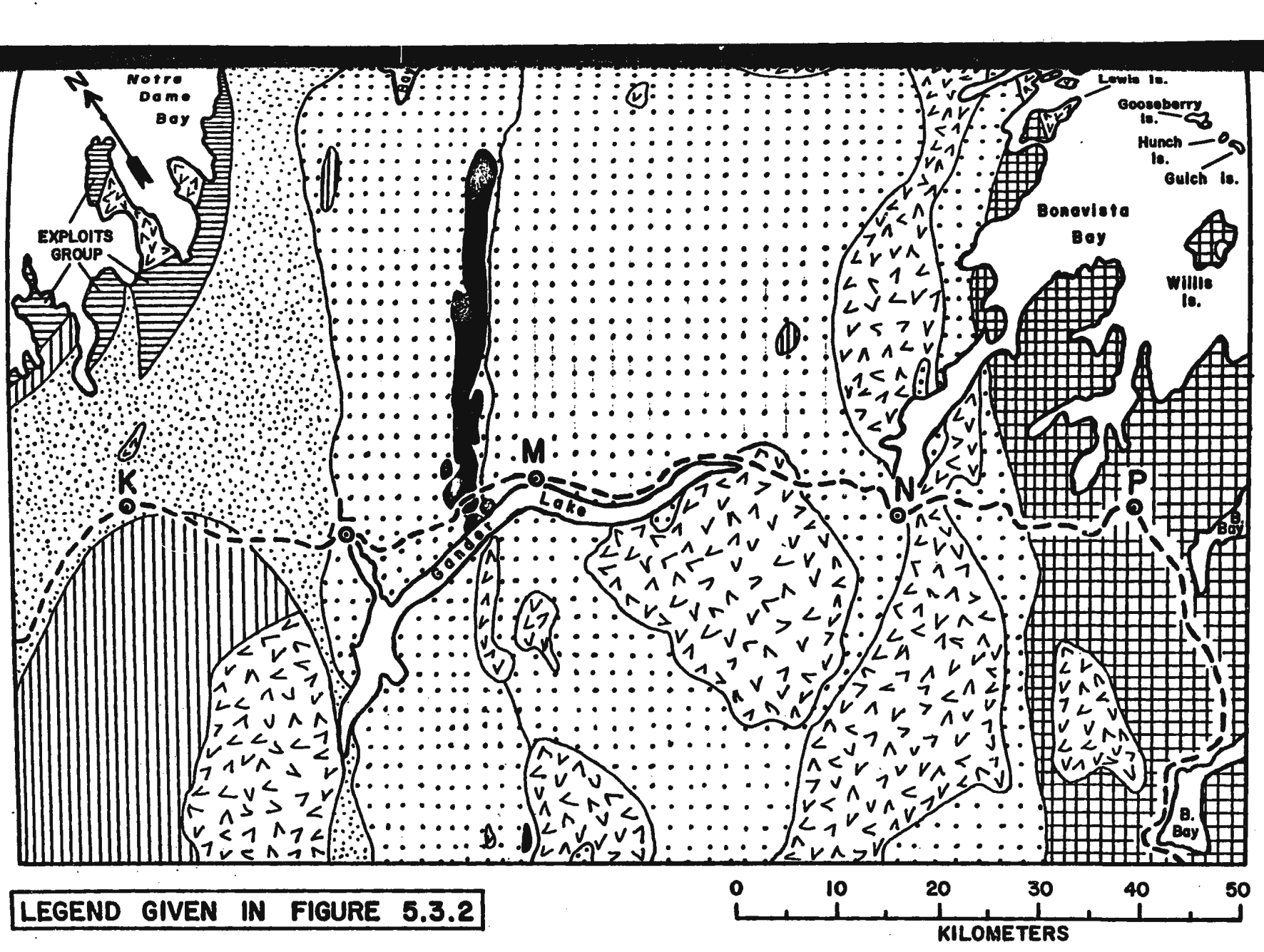

FIGURE 5.1.1 GEOLOGIC MAP OF REGION BETWEEN NOTRE DAME JUNCTION (K) & TRAYTOWN (P). — COMPILED FROM MAPS 60-1963 (WILLIAMS, 1964) & 1129A-1130A (JENNESS, 1963)

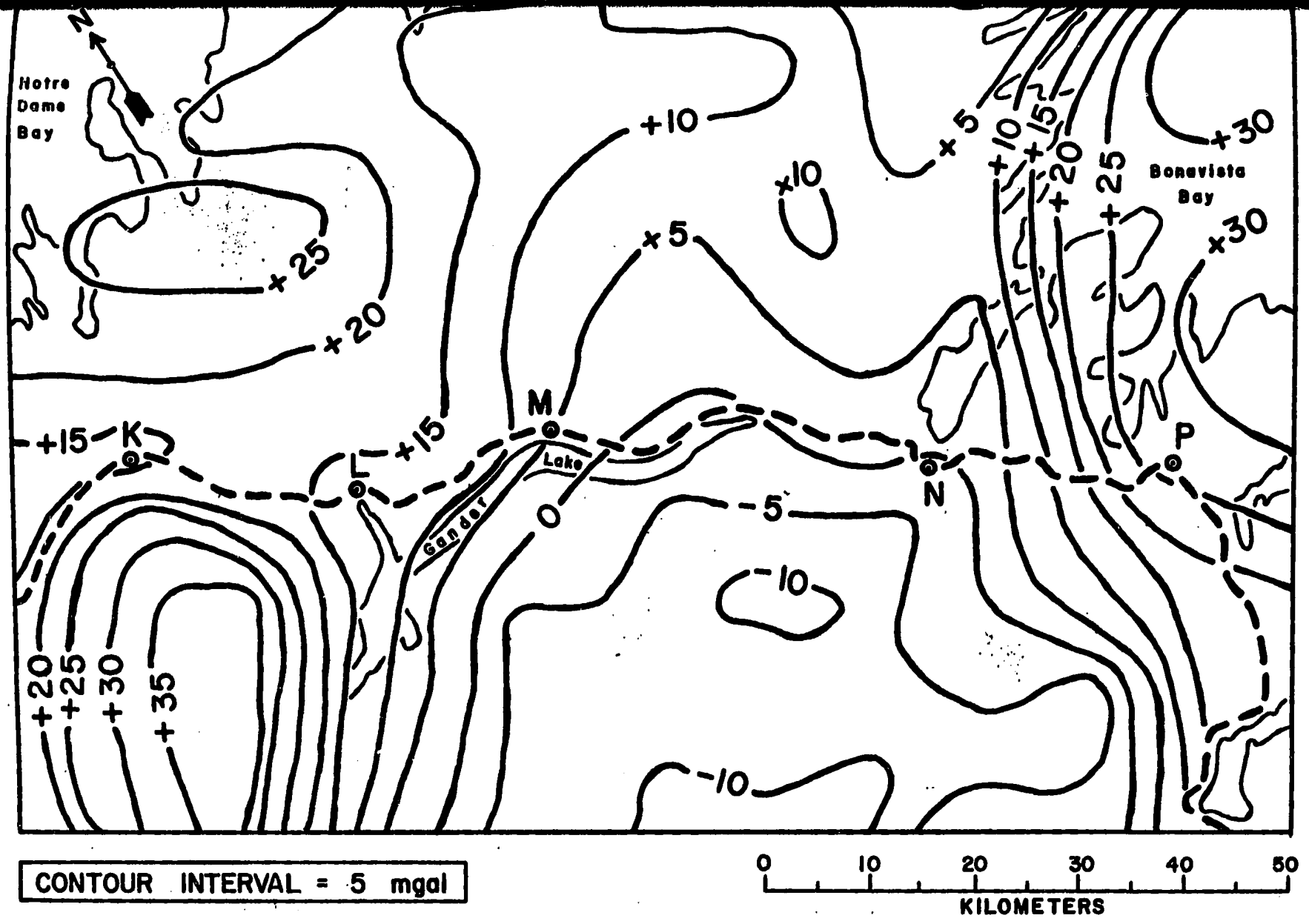

FIGURE 5.3.1 GRAVITY MAP OF REGION BETWEEN NOTRE DAME JUNCTION (K) & TRAYTOWN (P). — FROM GRAVITY MAP SERIES NO. 55 (WEAVER, 1968).

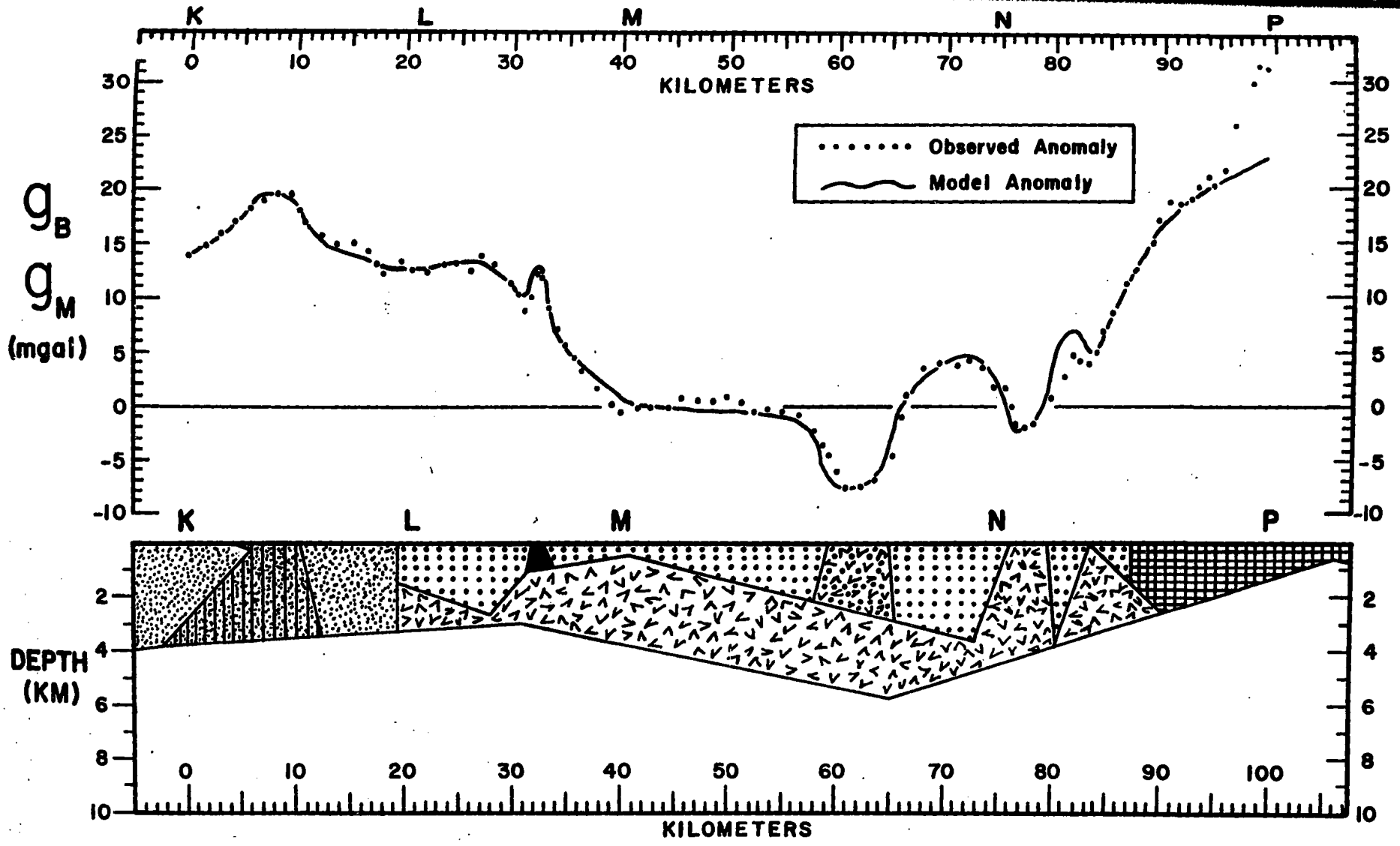

FIGURE 5.3.2 BOUGUER ANOMALY PROFILE WITH MODEL CROSS-SECTION (K to P). g_B and g_M are observed and model anomalies, respectively. Numbers 29-36 refer to geologic subdivision shown in Figures A5.2.1 - A5.2.6.

CHAPTER SIX

SUMMARY AND CONCLUSIONS

6.1 Summary and conclusions.

A gravity profile, consisting of 970 stations (with 0.8 km spacing) and 13 sub-bases, has been established along the Trans-Canada highway between Port-aux-Basques on the west coast and Come-by-Chance on the east coast of Newfoundland. Bouguer anomalies have been determined for all of the stations and most of the sub-bases. The standard deviation in this quantity averages about ±0.30 mgal.

Station elevations have been determined as follows: 60% by barometric altimetry; 36% by precise (spirit) levelling; 2½% by placement on bench-marks; 1½% from highway profile plans.

Improvement in elevation accuracy was achieved by means of the following modifications to the traditional "one-base" method of barometric altimetry: (i) numerical smoothing of base readings; (ii) a barometric field calibration; (iii) use of a weighting scheme, based on barometric error analyses, for determining the mean value of each station elevation.

144 rock samples, from 106 sites, have been collected and catalogued. These sites yield a mean density of 2.73 gm/cm^3, and an r.m.s. deviation of ±0.11 gm/cm^3 about this.

Graphs for estimating errors due to departures of the geologic structures from two-dimensionality have been plotted, and two of these are included for illustrative purposes.

A technique has been introduced for estimating (roughly) the error associated with the representation of an oblique geologic structure

by a perpendicular model. A convenient method has been devised to permit the making of end corrections at the "input" to the two-dimensional model study (computer) program. A "winding-route" anomaly effect has been recognized and discussed, and a technique for partially removing it has been suggested. The author has developed these topics only to the extent required for interpretation of this profile.

The Bouguer anomaly profile has been shown graphically with relevant geologic and geographic information.

As a prelude to more quantitative studies, most of the profile has been subjected to a general (qualitative) interpretation. The section between Notre Dame Junction and Traytown has been examined in more detail and a model representation of the geologic structure in that region has been presented.

A number of preliminary geologic observations have been made. These include the following:

(i) Rough calculations suggest that the overall anomaly low in south-western Newfoundland can be explained by reasonable geologic thicknesses for the Carboniferous sediments in that region.

(ii) Because of the orientations of the route near the Cabot fault, this study does not contribute to an understanding of that feature.

(iii) A large body of intermediate to basic rocks seems to underly the region around South Brook. Similar rocks which are mapped over a large area to the north of Badger appear to have little depth.

(iv) The region between Glenwood and Gambo is underlain by a large body of granite, whose cross-sectional shape suggests a distorted lopolith.
(v) There is a gravitational anomaly symmetry across the central Paleozoic mobile belt in northeastern Newfoundland.

6.2 Recommendations.

It is recommended that: (i) model studies of other sections of this profile be undertaken; (ii) techniques for model study error estimation be further investigated; (iii) more gravity work be done in the regions of the Cabot Fault and across the Hermitage Flexure; (iv) the region between Notre Dame Junction and Traytown be further investigated by means of electrical, magnetic, and seismic studies; (v) the gravitational anomaly symmetry across the central belt be further studied; (vi) isostatic anomalies be calculated, and the extent of the island's isostatic compensations be further investigated.

APPENDIX 1

GRAVITY METER CHECK AND SCALE CONSTANT REDETERMINATION

A1.1 Gravity meter used in 1966 survey.

A Model CG-2 Canadian gravity meter, No. 192, was purchased by the Physics Department of Memorial University in 1966 and given a field check soon after its arrival from the manufacturer. This consisted of a comparison of the gravity difference determined by this instrument with that obtained by the Gravity Division of the Dominion Observatory, using LaCoste and Romberg gravity meters, between their control stations 9211-64 (Memorial University) and 9513-63 (St. John's airport). Table A1.1, in which the interpolated values are obtained by assuming a linear drift in instrument readings between successive occupations of a base, contains the check results. Division of the LaCoste and Romberg gravity difference, 12.09 ± 0.10 mgal, by the Model CG-2 instrumental scale difference, 118.1 ± 0.3 div, yields 0.1024 ± 0.0009 mgal/div for the scale constant, S, of meter 192, compared with 0.10360 mgal/div specified by the manufacturer.

A second check, following the same procedure, was carried out between control stations 9175-64 (South Brook) and 9198 (Badger), where the maximum adjacent base gravity difference was encountered in 1966. Here the Dominion Observatory's gravity difference, 82.60 ± 0.10 mgal, and the Model CG-2 instrumental scale difference, 805.9 ± 0.3 div, gave a value of 0.1025 ± 0.0001 mgal/div for S.

The use of the manufacturer's scale constant in the reduction of the South Brook to Badger gravity data would have resulted in a profile anomaly discontinuity of approximately 0.8 mgal at the meeting point of traverses from the two bases.

On October 26 and 27, 1966, the gravity meter was given a tilt-table check by the Gravity Division of the Dominion Observatory. They obtained a value of 0.10260 ± 0.00009 mgal/div for S, and this was used in the reduction of the 1966 data.

A1.2 Gravity meter used in 1965 survey.

The scale constant discrepancy for the 1966 instrument brought about a reconsideration of the values used in reducing the 1965 and 1964 data. Similar differences would have resulted in profile anomaly discontinuities of up to 1.0 mgal for the 1965 survey and up to 0.2 mgal for the work done in 1964.

Two checks on the 1965 scale constant, S, were made. The first was between control stations 9202-64 (Port-aux-Basques) and 9201-64 (Corner Brook). The division of the LaCoste and Romberg gravity difference, 103.33 ± 0.10 mgal, by the 1965 instrumental scale difference, 1041 ± 3 div, gave a value of 0.0993 ± 0.0003 mgal/div for S. A similar check between the Dominion Observatory control station 9173-64 (Gander) and the Physics Department's sub-base 9101 (Notre-Dame Junction) yielded a value of 0.0990 ± 0.0004 mgal/div. Here the gravity and scale differences were 39.14 ± 0.10 mgal and 395.5 ± 1.0 div, respectively. The

mean value thus obtained for the 1965 instrument scale constant was 0.0991 ± 0.0003 mgal/div, whereas the manufacturer's determination had been 0.10010 mgal/div.

A1.3 Gravity meter used in 1964 survey.

No direct traverses between Dominion Observatory bases were made during the 1964 survey, and hence the methods previously described cannot now be used to determine its scale constant.

However, a comparison (Table A1.2) of three gravity meters has suggested that constants quoted by Sharpe Instruments of Canada are systematically larger, by 0.0010 mgal (approximately 1%), than those obtained either at the Dominion Observatory's Gravity Division or within that Division's Newfoundland base network. Two of the instruments were those used in 1965 and 1966 on this project, and the third, also Model CG-2, belonged to the Dominion Observatory. Information on the latter was obtained from Mr. A. C. Hamilton of the Observatory's Gravity Division (Personal conversation, September, 1966).

On the basis of these results the 1964 gravity meter has been assigned a scale constant of 0.1015 ± 0.0002 mgal/div, obtained by subtracting 0.0010 mgal/div from the value, 0.10252 mgal/div, quoted by the manufacturer.

Table A1.1 Calibration check on Model CG-2 Gravity Meter 192, June 24 and 27, 1966.

Time of Reading (hr, min)	Reading at 9211-64[1] Direct	Reading at 9211-64[1] Interpolated	Reading at 9513-63[2] Direct	Reading at 9513-63[2] Interpolated	Difference Between Base Readings
June 24					
1509	524.67				
1535		524.53	406.09		118.44
1640	524.18				
June 27					
1023	517.25				
1110		516.94	399.24		117.70
1152	516.66				
1327	517.35				
1405		517.14	399.34		117.80
1428	517.01			398.98	118.03
1458		516.92	398.52		118.40
1533	516.81				

Average reading difference = 118.07 ± 0.34 div.

[1]Observed gravity at control station 9211-64 (Memorial University) = 980.83541 ± 0.00007 gal.

[2]Observed gravity at control station 9513-63 (St. John's airport) = 980.82348 ± 0.00007 gal. Observed gravity at height of meter 192 = 980.82332 ± 0.00007 gal.

Observed gravity refers to Dominion Observatory measurements with LaCoste and Romberg gravity meters in 1963 and 64.

Table A1.2 Recheck of gravity meter constants quoted by manufacturer

Model CG-2 gravity meter	Gravity meter scale constant, S (mgal/div)			
	Specified by[1] manufacturer (M)	Determined at[2] Dom. Observatory (D)	Determined from Dom. Obs. bases (D)	Difference (M-D)
No. 183 (1965)	0.10010 ±0.00010		0.0991 ±0.0003	0.0010 ±0.0003
No. 192 (1966)	0.10360 ±0.00010	0.10260 ±0.00009		0.00100 ±0.00013
Dom. Obs. meter	0.10249 ±0.00010	0.10135 ±0.00010		0.00114 ±0.00014

Mean difference = $0.0010 \pm 0.000_3$ mgal/div

[1] Precision in manufacturer's value is not known. However, on the assumption that it would not differ greatly from the standard deviation of ±0.00009 mgal/div, obtained in the Dominion Observatory's check of gravity meter No. 192, an uncertainty of ±0.00010 mgal/div has been assigned.

[2] A scale constant uncertainty of ±0.00010 mgal/div has been assigned to the Dom. Obs. meter (S = 0.10135) on the assumption that it would not differ greatly from that obtained for Meter No. 192.

APPENDIX 2

GRAVITY BASE AND SUB-BASE INFORMATION

A2.1 The gravity base network.

The main base network was established in 1963 and 64 by the Gravity Division of the Dominion Observatory, using LaCoste and Romberg gravity meters. A brief description of the methods used and the errors involved in setting it up has been given by Weaver (1967). He states that most of the observed gravity residuals after a least squares adjustment of the Newfoundland control network were less than 0.05 mgal. From an interpretation of Weaver's value as the probable error associated with the observed gravity at any base, the corresponding standard deviation was calculated to be ±0.07 mgal.

Although elevation uncertainties have not been given specifically for these bases, Weaver (1967) does give an elevation error break-down for the whole of the 1964 regional gravity survey in Newfoundland. These errors are approximately as follows: majority of bench marks, ±0.3 m; sea-level observations, ±2 m; barometric determinations, ±5 m; and elevations supplied by the Surveys and Mapping Branch of the Department of Energy, Mines and Resources, ±7 m. Latitude and longitude determinations are accurate to ±0.1 min.

Table A2.1 contains the principal facts, as provided by the Gravity Division, for these bases. Bouguer anomalies have been calculated for those bases along the present project's profile, and these have been included with the principal facts for stations (Appendix 3).

A2.2 The establishment of sub-base 9101.

The date for the establishment of this sub-base, located at Notre Dame Junction, from Base 9001 (Dominion Observatory control station 9147, Bishop's Falls) is given in Table A2.2 as an illustration of the general procedure followed in determining sub-base gravity.

Substitution of the mean instrumental scale reading difference, 76.42 ± 0.15 div, and the gravity meter scale constant, 0.10260 ± 0.00009 mgal/div, into equation 2.1.1 yields 7.84 ± 0.02 mgal as the amount by which observed gravity at 9101 exceeds that at 9001.

Substitution of this value of Δg_{obs}, 0.00784 gal, and the observed gravity at base 9001, 980.99137 ± 0.00007 gal, into equation 2.1.2 gives 980.99921 ± 0.00007 gal for the observed gravity at sub-base 9101.

A2.3 Sub-base data.

Table A2.3 contains the principal facts for the gravity sub-bases. Bouguer anomalies have been calculated for those sub-bases along the traverse for which sufficient data exist, and these are listed with the principal facts for stations (Appendix 3).

The error in sub-base gravity is a composite of the error in the base gravity (section A2.1) and that in the gravity difference between base and sub-base. In all cases this latter error is less than or equal to ± 0.02 mgal, resulting in a standard deviation of less than ±0.08 mgal for observed sub-base gravity.

Discussion of the sub-base latitude, longitude, and elevation error is incorporated into the general station data error considerations (Chapter 2), in which latitude errors very from ±0.05 min to ±0.10 min, longitude uncertainty is ±0.15 min, and elevation errors vary from ±0.1 m to ±2 m.

Table A2.1 Principal facts for the gravity bases.

Base number Phys. Dept.	Dom. Obs.	W. Long (deg min)	N. Lat. (deg min)	Elev.[1] (m)	Observed gravity (gal)	Location
9001	9174-64	55 28.7	49 01.0	17.4	980.99137	CNR Stn, Bishop's Falls
9002	9198-64	56 02.3	48 58.7	100.6	980.97830	CNR Stn, Badger
9003	9201-64	57 56.6	48 57.4	3.1	980.98259	CNR Stn, Corner Brook
9004	9200-64	57 38.5	49 00.7	8.2	980.99668	Nat. Base on Deer Lake
9005	9199-64	57 25.6	49 10.2	30.2	981.01183	CNR Stn, Deer Lake
9006	9202-64	59 08.3	47 35.0	2.4	980.87926	CNR Stn, Port-aux-Basques
9007	9173-64	54 33.4	48 57.0	135.7	980.96007	CNR Stn, Gander
9008	9211-64	52 42.0	47 34.5	60.7	980.83541	Memorial University
9009	9513-63	52 44.6	47 36.8	132.6	980.82348	St. John's airport
9011	9180-64	53 57.8	48 10.3	19.5	980.91421	CNT Bldg., Clarenville
9012	9175-64	56 05.2	49 25.9	1.8	981.06091	Wharf, South Brook
9013	9177-64	54 00.4	48 26.1	1.2	980.95345	Wharf, Charlottetown

[1]Elevation initially quoted to the nearest foot (1 ft = 0.3 m).

Table A2.2 The establishment of sub-base 9101 from base 9001, August 29, 1966.

Time (hr, min)	Reading at Base 9001[1] (R_{bs})		Reading at sub-base 9101 (R_{sb})		Reading Difference
	Direct	Interpolated	Direct	Interpolated	(R_{sb}-R_{bs})
1534			505.11		
1756	429.49			505.78	76.29
1843		429.53	506.00		76.47
1926	429.57			506.05	76.48
2012		429.41	506.11		76.70
2118	429.18			505.51	76.33
2210		428.74	505.03		76.29
2309	428.24			504.60	76.36
2445		503.91	503.91		

Mean of reading differences: 76.42 ± 0.15 div

Corresponding gravity difference: 7.84 ± 0.02 mgal

[1]Observed gravity at 9001 (Bishop's Falls) = 980.99137 ± 0.0007 gal (obtained with LaCoste and Romberg gravity meters).

Table A2.3 Principal facts for the gravity sub-bases.

Sub-base number	W. Long. (deg min)	N. Lat. (deg min)	Elevation (m)	Observed gravity (gal)	Location
9101	55 05.4	49 07.64	76.2	980.99921	Crossing of Lewisporte road & CNR main line at Notre-Dame Junction
9102	55 15.9	49 05.41	14.1	981.01055	CNR Stn, Norris Arm
9103	58 05.7	48 46.74	unknown	980.93305	Bridge, Rock Brook, South of Corner Brook
9104	58 16.2	48 30.85	9.6	980.92979	Bridge, South West Brook, North of St. George's
9105	58 32.8	48 18.74	139.1	980.88550	On Trans-Canada highway, between stns 30300 & 10302, North of Fischel's Brook
9106	58 46.5	48 10.39	unknown	980.89660	Bridge, Crabbs River
9107	58 57.9	47 56.91	43.1	980.88299	On highway, between stns 10377 & 10379, South of South Branch
9108	unknown	unknown	unknown	980.86837	Bridge over Campbell Brook
9109	54 52.0	48 59.78	31.2	980.99480	Queen Elizabeth Bridge over Gander River
9110	54 17.8	58 48.26	51.5	980.96498	Entrance to Square Pond Provincial Park
9111	54 04.2	48 39.91	unknown	980.95943	Intersection of road to Glovertown with Trans-Canada highway
9113	56 40.4	49 20.47	94.1	981.00198	Bridge, Sheffield Brook
9114	56 58.1	49 22.41	113.3	981.02602	Bridge, Main Brook, North of Sandy Lake

APPENDIX 3

PRINCIPAL FACTS FOR GRAVITY STATIONS

A3.1 Gravity determinations at station 10825.

This station, approximately 8 km west of South Brook, was established from base 9012 on July 21, 1966. Its gravity value, g_{obs}, is obtained by substituting the following information (symbols defined in section 2.1) into equations 2.1.2 and 2.1.1:

$t' = 1824$ hrs $\qquad R'_{bs} = 620.05$ div

$t = 1920$ hrs $\qquad R_s = 469.30$ div

$t'' = 2030$ hrs $\qquad R''_{bs} = 621.66$ div

$$\begin{aligned} S &= 0.10260 \text{ mgal/div} \\ g_{bs} &= 981.06091 \text{ gal} \\ g_{obs} &= 981.04537 \text{ gal} \\ &\quad \pm 0.00009 \text{ gal} \end{aligned} \qquad \text{(A3.1)}$$

The error in g_{obs} is given in section 2.1.

Substituting the station elevation, h, into equation 1.3.1 gives the combined free-air and Bouguer correction, $\Delta g_{fc} + \Delta g_{bc}$,

$$\begin{aligned} h &= (83.4 \pm 1.1) \text{ m} \\ \Delta g_{fc} + \Delta g_{bc} &= (16.40 \pm 0.22) \text{ mgal} \end{aligned} \qquad \text{(A3.2)}$$

The theoretical gravity, g_{th}, is obtained by substituting the latitude, ϕ, into equation 1.3.2.

$$\phi = (49^{o}\ 26.91' \pm 0.07') \text{ North}$$

$$g_{th} = (981.02949 \pm 0.00011) \text{ gal} \qquad \text{(A3.3)}$$

Use of Bible's correction tables (Section 2.4) with the topographic map of this region yields the terrain correction, Δg_t

$$\Delta g_t = (0.20 \pm 0.06) \text{ mgal} \qquad \text{(A3.4)}$$

Substitution of equations A3.1 to A3.4 into equation 1.3.3 gives the Bouguer anomaly, g_B

$$g_B = (+\ 32.48 \pm 0.27) \text{ mgal}$$

A3.2 Gravity station information.

Table A3.1 gives the principal facts for the gravity stations in this survey. The symbols used are explained as follows: LOC, location on Figures 1.1.1 and A5.2.1 to A5.2.6; STN, station number; D PAB, distance along route from Port-aux-Basques; ELEV, station elevation; G OBS, observed acceleration due to gravity; TERC, terrain correction; G BOUG, Bouguer anomaly. The errors associated with the quoted values of latitude and elevation may be obtained from Figures 2.3.1 and 2.2.1, respectively. Errors in terrain correction and Bouguer anomaly values are given in Table 2.5.1.

The author's field notes contain location descriptions for all gravity stations in this survey. No problems would be encountered in attempts to re-occupy the majority of these during the next several years.

TABLE A3.1 PRINCIPAL FACTS FOR GRAVITY STATIONS

LOC	STN	C PAB (KM)	LONGITUDE (DEG MIN)	LATITUDE (DEG MIN)	ELEV (M)	G OBS (GAL)	TERC (MGAL)	G BOUG (MGAL)
A	10455	0.8	59 9.6	47 35.35	15.19	980.87795	0.30	18.39
	10454	1.6	59 9.9	47 35.59	8.02	980.87983	0.30	18.50
	10453	2.4	59 9.8	47 35.98	37.12	980.87476	0.31	18.58
	10452	3.2	59 10.3	47 36.26	27.54	980.87568	0.32	17.20
	10451	4.0	59 10.8	47 36.52	17.48	980.87747	0.32	16.62
	10450	4.8	59 11.4	47 36.65	21.14	980.87643	0.33	16.12
	10449	5.6	59 12.0	47 36.67	31.75	980.87338	0.34	15.14
	10448	6.4	59 12.7	47 36.74	15.59	980.87571	0.35	14.19
	10447	7.2	59 12.9	47 36.96	20.40	980.87264	0.35	11.74
	10446	8.0	59 13.4	47 37.13	24.19	980.87119	0.37	10.80
	10445	8.9	59 13.8	47 37.37	19.89	980.87062	0.39	9.04
	10444	9.7	59 14.3	47 37.59	36.39	980.86815	0.42	9.52
	10443	10.5	59 14.2	47 38.00	64.42	980.86282	0.45	9.12
	10442	11.3	59 14.2	47 38.46	54.26	980.86555	0.50	9.21
	10441	12.1	59 14.2	47 38.89	96.53	980.85868	0.55	10.06
	10440	12.9	59 14.5	47 39.21	110.01	980.85600	0.65	9.66
	10439	13.7	59 15.2	47 39.43	95.01	980.86000	0.85	10.57
	10438	14.5	59 15.8	47 39.61	65.33	980.86540	1.10	10.12
	10437	15.3	59 16.5	47 39.61	59.60	980.86608	1.30	9.87
	10436	16.1	59 16.8	47 39.91	52.58	980.86626	1.50	8.42
	10435	16.9	59 17.1	47 40.17	29.95	980.86879	1.35	5.96
	10434	17.7	59 17.6	47 40.41	18.30	980.86919	1.00	3.36
	10433	18.5	59 17.8	47 40.70	14.76	980.87177	0.80	4.61
	10432	19.3	59 17.8	47 41.11	37.36	980.86845	0.65	4.97
	10431	20.1	59 18.4	47 41.37	43.34	980.86927	0.60	6.52
	10430	20.9	59 18.7	47 41.76	44.10	980.86900	0.50	5.72
	10429	21.7	59 18.7	47 42.22	18.54	980.87169	0.45	2.64
	10428	22.5	59 18.6	47 42.67	25.50	980.86842	0.50	0.12
	10427	23.3	59 18.3	47 43.09	32.15	980.86535	0.50	-2.28
	10426	24.1	59 18.1	47 43.50	29.62	980.86511	0.55	-3.58
	10425	24.9	59 17.8	47 43.80	26.53	980.86412	0.55	-5.62
	10424	25.8	59 17.2	47 44.04	40.56	980.86160	0.60	-5.69
	10423	26.6	59 16.8	47 44.41	33.18	980.86040	0.60	-8.90
	10422	27.4	59 16.7	47 44.80	24.74	980.86032	0.60	-11.23
	10421	28.2	59 16.4	47 45.22	21.50	980.86145	0.65	-11.31

TABLE SYMBOLS EXPLAINED IN SECTION A3.2.

....continued

TABLE A3.1, CONTINUED

LOC	STN	C PAB (KM)	LONGITUDE (DEG MIN)	LATITUDE (DEG MIN)	ELEV (M)	G OBS (GAL)	TERC (MGAL)	G BOUG (MGAL)
	10420	29.0	59 16.2	47 45.61	13.36	980.86486	0.70	-10.04
	10419	29.8	59 15.9	47 45.96	4.82	980.86810	0.70	-9.00
	10418	30.6	59 15.5	47 46.30	4.45	980.86931	0.75	-8.32
	10417	31.4	59 15.1	47 46.52	8.57	980.86877	0.75	-8.38
	10416	32.2	59 14.5	47 46.70	14.64	980.86799	0.80	-8.19
	10415	33.0	59 14.0	47 47.00	16.04	980.86696	0.85	-9.34
	10414	33.8	59 13.6	47 47.43	13.69	980.86589	0.80	-11.57
	10413	34.6	59 13.8	47 47.61	6.25	980.86770	0.70	-11.59
	10412	35.4	59 13.8	47 47.98	9.00	980.86817	0.60	-11.24
	10411	36.2	59 13.2	47 48.28	13.57	980.86697	0.60	-11.99
	10410	37.0	59 12.9	47 48.61	19.00	980.86675	0.55	-11.68
	104C9	37.8	59 12.5	47 48.93	12.44	980.86921	0.50	-11.04
	104C8	38.6	59 12.1	47 49.20	20.80	980.86943	0.50	-9.58
B	104C7	39.4	59 11.7	47 49.61	31.51	980.86835	0.50	-9.17
	104C6	40.2	59 11.2	47 49.87	37.06	980.86771	0.50	-9.11
	104C5	41.1	59 10.7	47 50.17	50.02	980.86593	0.50	-8.79
	104C4	41.9	59 10.4	47 50.46	50.87	980.86628	0.50	-8.70
	10403	42.7	59 9.8	47 50.61	58.62	980.86424	0.50	-9.44
	10402	43.5	59 9.3	47 50.87	63.84	980.86322	0.50	-9.83
	10401	44.3	59 8.7	47 51.13	64.69	980.86309	0.55	-10.13
	10400	45.1	59 8.3	47 51.41	65.94	980.86320	0.55	-10.19
	10399	45.9	59 7.8	47 51.76	30.23	980.87134	0.55	-9.60
	10398	46.7	59 7.3	47 52.00	17.99	980.87468	0.60	-8.98
	10397	47.5	59 6.8	47 52.22	21.81	980.87428	0.60	-8.96
	10396	48.3	59 6.5	47 52.65	22.78	980.87566	0.60	-8.03
	10395	49.1	59 6.3	47 53.04	38.28	980.87451	0.60	-6.72
	10394	49.9	59 5.8	47 53.35	35.38	980.87615	0.60	-6.11
	10393	50.7	59 5.1	47 53.57	25.80	980.87838	0.65	-6.04
	10392	51.5	59 4.5	47 53.57	33.09	980.87729	0.65	-5.70
	10391	52.4	59 3.9	47 53.61	44.50	980.87531	0.70	-5.45
	10390	53.2	59 3.3	47 53.72	61.55	980.87242	0.65	-5.20
	10389	53.9	59 2.8	47 53.96	64.84	980.87240	0.65	-4.93
	10388	54.7	59 2.3	47 54.13	62.59	980.87398	0.60	-4.10
	10387	55.5	59 1.8	47 54.48	62.10	980.87506	0.60	-3.64
	10386	56.5	59 1.6	47 54.74	44.10	980.87893	0.55	-3.75

TABLE SYMBOLS EXPLAINED IN SECTION A3.2.

... continued

TABLE A3.1, CONTINUED

LOC	STN	C PAB (KM)	LONGITUDE (DEG MIN)	LATITUDE (DEG MIN)	ELEV (M)	G OBS (GAL)	TERC (MGAL)	G BOUG (MGAL)
	10385	57.3	59 1.1	47 54.96	43.04	980.87969	0.55	-3.52
	10384	58.1	59 0.5	47 55.09	60.15	980.87711	0.60	-2.88
	10383	58.9	58 59.9	47 55.35	58.47	980.87790	0.60	-2.81
	10382	59.7	58 59.8	47 55.78	36.54	980.88221	0.55	-3.51
	10381	60.5	58 59.4	47 56.09	39.89	980.88173	0.50	-3.84
	10380	61.3	58 58.8	47 56.33	44.47	980.88174	0.50	-3.29
	10379	62.1	58 58.3	47 56.57	45.51	980.88250	0.45	-2.74
	10378	62.9	58 57.9	47 56.91	43.13	980.88299	0.40	-3.28
	10377	63.7	58 57.6	47 57.28	46.91	980.88194	0.40	-4.14
	10376	64.7	58 57.6	47 57.70	106.66	980.87000	0.35	-5.00
	10375	65.5	58 57.8	47 58.09	147.25	980.86170	0.34	-5.91
	10374	66.1	58 58.0	47 58.48	155.15	980.86058	0.33	-6.07
	10373	67.0	58 57.9	47 58.91	119.10	980.86819	0.33	-6.19
	10372	67.8	58 57.7	47 59.35	121.76	980.86894	0.33	-5.58
	10371	68.6	58 57.7	47 59.74	135.82	980.86589	0.35	-6.43
	10370	69.3	58 57.2	48 0.04	140.30	980.86554	0.40	-6.30
	10369	69.8	58 56.8	48 0.17	132.89	980.86702	0.40	-6.47
	10368	70.4	58 56.4	48 0.33	137.04	980.86664	0.45	-6.22
	10367	71.2	58 55.9	48 0.57	123.49	980.86969	0.45	-6.20
	10366	72.4	58 55.6	48 1.04	146.98	980.86604	0.45	-5.93
	10365	73.1	58 55.6	48 1.43	156.71	980.86712	0.50	-3.47
	10364	74.0	58 55.8	48 1.83	153.35	980.86814	0.50	-3.71
	10363	74.8	58 55.5	48 2.22	144.39	980.87042	0.50	-3.78
	10362	75.6	58 55.3	48 2.70	143.53	980.86995	0.55	-5.08
	10361	76.4	58 54.9	48 3.04	158.36	980.86782	0.60	-4.76
	10360	77.2	58 54.5	48 3.37	161.71	980.86797	0.55	-4.49
	10359	78.1	58 53.9	48 3.57	176.87	980.86399	0.50	-5.84
	10358	78.9	58 53.4	48 3.78	173.33	980.86524	0.50	-5.60
	10357	79.7	58 52.8	48 3.98	180.50	980.86437	0.50	-5.36
	10356	80.5	58 52.2	48 4.22	172.14	980.86649	0.50	-5.24
C	10355	81.3	58 51.5	48 4.43	161.99	980.86727	0.60	-6.67
	10354	82.1	58 50.8	48 4.52	171.29	980.86593	0.70	-6.22
	10353	82.9	58 50.2	48 4.61	180.07	980.86610	0.80	-4.35
	10352	83.7	58 49.5	48 4.72	205.78	980.86253	1.00	-2.83
	10351	84.5	58 49.0	48 4.83	186.87	980.86702	0.90	-2.32

TABLE SYMBOLS EXPLAINED IN SECTION A3.2.

.... continued

TABLE A3.1, CONTINUED

LOC	STN	D PAB (KM)	LONGITUDE (DEG MIN)	LATITUDE (DEG MIN)	ELEV (M)	G OBS (GAL)	TERC (MGAL)	G BOUG (MGAL)
	10350	85.3	58 48.6	48 4.96	197.91	980.86589	0.70	-1.68
	10349	86.1	58 48.2	48 5.26	182.85	980.86841	0.55	-2.72
	10348	86.9	58 47.8	48 5.52	144.84	980.87441	0.45	-4.68
	10347	87.7	58 47.4	48 5.83	111.23	980.88114	0.35	-5.13
	10346	88.5	58 47.0	48 6.13	96.72	980.88427	0.27	-5.39
	10345	89.3	58 46.9	48 6.50	78.14	980.88971	0.20	-4.22
	10344	90.1	58 47.1	48 6.96	80.67	980.89000	0.20	-4.12
	10343	90.9	58 47.0	48 7.39	76.52	980.89170	0.19	-3.89
	10342	91.7	58 46.9	48 7.87	101.69	980.88755	0.18	-3.82
	10341	92.5	58 47.0	48 8.35	114.07	980.88611	0.18	-3.54
	10340	93.3	58 47.1	48 8.74	143.44	980.87993	0.17	-4.54
	10339	94.1	58 46.8	48 9.13	151.19	980.87751	0.17	-6.02
	10338	95.0	58 46.5	48 9.51	127.83	980.88212	0.16	-6.58
	10337	95.8	58 46.5	48 9.93	100.31	980.88623	0.16	-8.51
	10336	96.6	58 46.5	48 10.35	52.58	980.89462	0.15	-10.15
	10335	97.4	58 46.6	48 10.76	47.00	980.89545	0.15	-11.03
	10334	98.2	58 47.0	48 11.09	78.02	980.88760	0.13	-13.30
	10333	99.0	58 47.5	48 11.35	63.20	980.88872	0.12	-15.49
	10332	99.8	58 47.6	48 11.65	48.89	980.89203	0.11	-15.45
	10331	100.6	58 47.6	48 12.00	68.08	980.88983	0.10	-14.41
	10330	101.4	58 47.2	48 12.28	88.85	980.88735	0.10	-13.23
	10329	102.2	58 46.7	48 12.54	70.15	980.89208	0.10	-12.56
	10328	103.0	58 46.3	48 12.93	83.30	980.89079	0.10	-11.85
	10327	103.8	58 45.9	48 13.35	66.46	980.89526	0.09	-11.33
	10326	104.6	58 45.4	48 13.65	43.25	980.90199	0.09	-9.61
	10325	105.4	58 44.9	48 13.87	52.28	980.90042	0.09	-9.74
	10324	106.2	58 44.4	48 14.17	40.41	980.90430	0.09	-8.64
	10323	107.0	58 44.0	48 14.50	41.88	980.90494	0.08	-8.22
	10322	107.8	58 43.4	48 14.57	61.64	980.90197	0.08	-7.40
	10321	108.6	58 42.8	48 14.57	80.12	980.89852	0.08	-7.22
	10320	109.4	58 42.2	48 14.76	87.47	980.89733	0.08	-7.24
	10319	110.2	58 41.7	48 15.00	106.32	980.89466	0.08	-6.57
	10318	111.0	58 41.2	48 15.33	124.44	980.89194	0.08	-6.22
	10317	111.9	58 40.8	48 15.65	141.18	980.88931	0.08	-6.03
	10316	112.7	58 40.4	48 16.00	147.74	980.88925	0.08	-5.32

TABLE SYMBOLS EXPLAINED IN SECTION A3.2.

... CONTINUED

TABLE A3.1, CONTINUED

LOC	STN	D PAB (KM)	LONGITUDE (DEG MIN)	LATITUDE (DEG MIN)	ELEV (M)	G OBS (GAL)	TERC (MGAL)	G BOUG (MGAL)
	10315	113.5	58 40.0	48 16.30	142.10	980.89074	0.08	-5.39
	10314	114.3	58 39.4	48 16.57	127.12	980.89305	0.08	-6.43
	10313	115.1	58 38.9	48 16.86	125.90	980.89309	0.08	-7.07
	10312	115.9	58 38.4	48 17.13	113.15	980.89476	0.08	-8.31
	10311	116.7	58 38.0	48 17.43	102.42	980.89671	0.10	-8.90
	10310	117.5	58 38.0	48 17.87	80.34	980.90260	0.10	-8.01
	10309	118.3	58 37.6	48 18.17	78.29	980.90295	0.08	-8.53
	10308	119.1	58 37.2	48 18.48	80.52	980.90173	0.08	-9.78
	10307	119.9	58 36.5	48 18.37	97.75	980.89722	0.08	-10.73
	10306	120.7	58 35.9	48 18.20	117.82	980.89175	0.08	-12.00
	10305	121.5	58 35.2	48 18.17	120.11	980.89077	0.08	-12.48
	10304	122.3	58 34.5	48 18.13	139.72	980.88425	0.08	-15.09
	10303	123.1	58 33.9	48 18.28	147.62	980.87988	0.08	-18.13
	10302	123.9	58 33.3	48 18.50	153.84	980.88038	0.08	-16.73
	10301	124.7	58 32.8	48 18.74	139.08	980.88550	0.08	-14.87
	10300	125.5	58 32.3	48 19.00	176.93	980.88096	0.08	-12.36
	10299	126.3	58 31.8	48 19.28	195.17	980.87778	0.08	-12.37
	10298	127.1	58 31.4	48 19.57	215.70	980.87540	0.08	-11.14
	10297	127.9	58 30.8	48 19.83	215.63	980.87712	0.08	-9.82
	10296	128.8	58 30.3	48 20.09	218.14	980.87690	0.08	-9.94
	10295	129.6	58 29.9	48 20.46	210.08	980.88001	0.08	-8.97
	10294	130.4	58 29.8	48 20.87	201.39	980.88182	0.08	-9.48
	10293	131.2	58 29.7	48 21.26	162.14	980.88984	0.09	-9.76
	10292	132.0	58 29.5	48 21.65	141.79	980.89429	0.11	-9.87
	10291	132.8	58 28.9	48 21.96	112.88	980.89978	0.12	-10.52
	10290	133.6	58 28.4	48 22.18	69.33	980.90736	0.12	-11.84
	10289	134.4	58 28.4	48 22.57	70.21	980.90848	0.10	-11.15
	10288	135.2	58 28.2	48 22.98	68.93	980.90990	0.10	-10.59
	10287	136.0	58 27.8	48 23.22	76.80	980.90853	0.10	-10.77
	10286	136.8	58 27.2	48 23.41	81.80	980.90755	0.12	-11.03
	10285	137.6	58 26.8	48 23.61	105.13	980.90310	0.15	-11.16
	10284	138.4	58 26.6	48 23.98	100.77	980.90426	0.15	-11.41
	10283	139.2	58 26.6	48 24.37	109.22	980.90388	0.14	-10.73
	10282	140.0	58 26.6	48 24.74	103.24	980.90563	0.14	-10.70
	10281	140.8	58 26.6	48 25.17	113.83	980.90303	0.13	-11.88

TABLE SYMBOLS EXPLAINED IN SECTION A3.2.

... continued

TABLE A3.1, CONTINUED

LOC	STN	D PAB (KM)	LONGITUDE (DEG MIN)	LATITUDE (DEG MIN)	ELEV (M)	G OBS (GAL)	TERC (MGAL)	G BOUG (MGAL)
	10280	141.6	58 26.3	48 25.57	95.62	980.90682	0.13	-12.27
	10279	142.4	58 25.9	48 25.87	79.79	980.91024	0.12	-12.42
	10278	143.2	58 24.9	48 26.39	45.38	980.91746	0.12	-12.74
	10277	144.0	58 24.9	48 26.39	30.10	980.92059	0.12	-12.62
	10276	144.8	58 24.3	48 26.63	15.71	980.92338	0.12	-13.02
	10275	145.7	58 23.8	48 26.87	29.68	980.92020	0.12	-13.81
D	10274	146.5	58 23.3	48 27.09	24.92	980.92110	0.12	-14.18
	10273	147.3	58 22.7	48 27.30	35.96	980.91975	0.11	-13.68
	10272	148.1	58 22.0	48 27.57	23.88	980.92257	0.11	-13.64
	10271	148.7	58 21.6	48 27.74	39.56	980.91964	0.11	-13.74
	10270	149.5	58 20.8	48 27.87	41.51	980.91943	0.11	-13.76
	10269	150.3	58 20.1	48 28.00	50.39	980.91774	0.11	-13.90
	10268	151.1	58 19.6	48 28.17	61.27	980.91580	0.12	-13.94
	10267	151.9	58 19.0	48 28.37	95.65	980.90954	0.13	-13.72
	10266	152.7	58 18.4	48 28.61	110.65	980.90730	0.14	-13.36
	10265	153.5	58 17.9	48 28.86	116.48	980.90699	0.14	-12.90
	10264	154.3	58 17.4	48 29.14	117.64	980.90776	0.13	-12.33
	10263	155.1	58 17.2	48 29.50	101.93	980.91185	0.12	-11.88
	10262	155.9	58 17.2	48 29.84	109.34	980.91021	0.11	-12.58
	10261	156.8	58 16.9	48 30.17	49.81	980.92244	0.10	-12.56
	10260	157.6	58 16.5	48 30.47	25.19	980.92762	0.10	-12.67
	10259	158.4	58 16.2	48 30.85	9.61	980.92979	0.10	-14.14
	10258	159.3	58 16.1	48 31.39	25.41	980.92745	0.11	-14.16
	10257	160.1	58 16.1	48 31.84	48.53	980.92370	0.11	-14.04
	10256	160.9	58 16.1	48 32.20	33.85	980.92696	0.12	-14.19
	10255	161.7	58 16.0	48 32.69	85.80	980.91757	0.13	-14.09
	10254	162.5	58 16.0	48 33.78	117.06	980.91199	0.13	-15.14
	10253	163.3	58 16.0	48 33.59	133.25	980.90977	0.14	-13.89
	10252	164.1	58 15.9	48 34.01	130.72	980.91062	0.14	-14.16
	10251	164.9	58 15.8	48 34.40	153.41	980.90694	0.15	-13.95
	10250	165.6	58 15.5	48 34.67	142.62	980.91002	0.16	-13.39
	10249	166.4	58 14.9	48 35.02	150.55	980.90974	0.18	-12.61
	10248	167.2	58 14.5	48 35.30	159.42	980.90939	0.19	-11.62
	10247	168.0	58 14.2	48 35.61	162.26	980.91052	0.20	-10.39
	10246	168.8	58 14.1	48 36.00	150.36	980.91414	0.20	-9.69

TABLE SYMBOLS EXPLAINED IN SECTION A3.2.

... continued

TABLE A3.1, CONTINUED

LOC	STN	C PAB (KM)	LONGITUDE (DEG MIN)	LATITUDE (DEG MIN)	ELEV (M)	G OBS (GAL)	TERC (MGAL)	G BOUG (MGAL)
	10245	169.6	58 14.1	48 36.47	103.61	980.92439	0.20	-9.34
	10244	170.4	58 14.0	48 36.79	135.82	980.91957	0.20	-8.30
	10243	171.2	58 13.7	48 37.06	144.30	980.91927	0.20	-7.34
	10242	172.0	58 13.2	48 37.39	158.14	980.91828	0.20	-6.09
	10241	172.8	58 13.1	48 37.78	171.75	980.91670	0.22	-5.56
	10240	173.7	58 12.6	48 38.17	176.02	980.91731	0.24	-4.67
	10239	174.5	58 12.3	48 38.48	177.63	980.91786	0.26	-4.25
	10238	175.3	58 12.2	48 38.91	206.94	980.91264	0.24	-4.36
	10237	176.0	58 12.0	48 39.30	198.13	980.91502	0.24	-4.30
	10236	176.8	58 11.6	48 39.70	203.19	980.91526	0.24	-3.66
	10235	177.6	58 11.4	48 40.09	208.99	980.91489	0.24	-3.47
	10234	178.3	58 11.3	48 40.40	188.92	980.91910	0.24	-3.68
	10233	179.1	58 10.8	48 40.62	147.77	980.92780	0.24	-3.40
	10232	179.9	58 10.2	48 40.85	122.61	980.93251	0.24	-3.98
	10231	180.7	58 9.9	48 41.26	124.53	980.93375	0.26	-2.96
	10230	181.5	58 9.6	48 41.70	147.53	980.92945	0.30	-3.35
	10229	182.3	58 9.2	48 42.02	143.29	980.93004	0.35	-4.02
	10228	183.1	58 9.0	48 42.39	148.87	980.93008	0.42	-3.36
	10227	184.0	58 8.9	48 42.91	191.60	980.92157	0.65	-4.01
	10226	184.7	58 8.7	48 43.30	206.39	980.91960	0.55	-3.76
	10225	185.6	58 8.6	48 43.83	198.52	980.92123	0.50	-4.52
	10224	186.4	58 8.4	48 44.22	194.04	980.92297	0.45	-4.29
	10223	187.1	58 8.1	48 44.55	208.56	980.92096	0.35	-4.04
	10222	187.9	58 7.8	48 44.98	218.72	980.91946	0.30	-4.23
	10221	188.5	58 7.8	48 45.30	226.61	980.91823	0.25	-4.43
	10220	189.2	58 7.7	48 45.70	216.55	980.92065	0.25	-4.59
	10219	190.1	58 7.3	48 46.04	195.78	980.92526	0.25	-4.57
	10218	191.0	58 6.9	48 46.39	167.26	980.93128	0.25	-4.69
	10217	191.8	58 6.3	48 46.61	152.77	980.93386	0.25	-5.29
	10216	192.6	58 5.7	48 46.74	163.11	980.93402	0.25	-3.29
	10215	193.4	58 5.2	48 47.04	189.34	980.92988	0.25	-2.71
	10214	194.2	58 4.8	48 47.39	190.90	980.92999	0.25	-2.82
	10213	195.0	58 4.3	48 47.68	195.29	980.93035	0.24	-2.04
	10212	195.8	58 3.7	48 47.87	175.13	980.93445	0.23	-2.20
	10211	196.6	58 3.0	48 48.04	188.31	980.93227	0.22	-2.05

TABLE SYMBOLS EXPLAINED IN SECTION A3.2.

... continued

TABLE A3.1, CONTINUED

LOC	STN	D PAB (KM)	LONGITUDE (DEG MIN)	LATITUDE (DEG MIN)	ELEV (M)	G OBS (GAL)	TERC (MGAL)	G BOUG (MGAL)
	10210	197.4	58 2.5	48 48.15	181.26	980.93443	0.22	-1.44
	10209	198.2	58 2.0	48 48.28	190.53	980.93334	0.20	-0.92
	10208	199.0	58 1.3	48 48.39	230.15	980.92581	0.20	-0.82
	10207	199.8	58 0.8	48 48.65	223.35	980.92849	0.20	0.13
	10206	200.5	58 0.3	48 48.91	221.95	980.92909	0.20	0.07
	10205	201.6	57 59.8	48 49.15	199.68	980.93416	0.18	0.38
	10204	202.4	57 59.2	48 49.46	221.58	980.93071	0.18	0.78
	10203	203.3	57 58.6	48 49.70	257.21	980.92439	0.18	1.11
	10202	204.0	57 58.3	48 49.97	257.76	980.92473	0.18	1.15
	10201	204.8	57 58.0	48 50.30	261.60	980.92473	0.16	1.40
	10200	205.8	57 57.5	48 50.70	261.05	980.92604	0.16	2.00
	10199	206.6	57 57.1	48 51.04	278.16	980.92342	0.16	2.24
	10198	207.3	57 56.8	48 51.33	288.50	980.92218	0.16	2.60
	10197	207.9	57 56.6	48 51.57	301.19	980.92008	0.16	2.64
	10196	208.6	57 56.4	48 51.93	303.05	980.92052	0.14	2.89
	10195	209.5	57 56.1	48 52.37	314.33	980.91938	0.14	3.31
	10194	210.3	57 55.8	48 52.74	274.87	980.92778	0.13	3.39
	10193	211.3	57 55.4	48 53.26	273.77	980.92917	0.13	3.79
	10192	212.0	57 55.1	48 53.59	284.66	980.92771	0.14	3.98
	10191	212.8	57 54.8	48 53.91	271.88	980.93084	0.13	4.11
	10190	213.4	57 54.5	48 54.17	258.30	980.93411	0.13	4.33
	10189	214.2	57 54.0	48 54.52	246.32	980.93668	0.13	4.02
	10188	215.0	57 53.7	48 54.76	233.32	980.93984	0.15	4.28
	10187	215.8	57 53.4	48 55.25	229.36	980.94236	0.16	5.30
	10186	216.6	57 54.0	48 55.46	218.35	980.94345	0.17	3.92
	10185	217.4	57 54.5	48 55.83	200.96	980.94601	0.20	2.54
	10184	218.4	57 54.9	48 56.20	138.87	980.95729	0.24	1.09
	10183	219.2	57 55.3	48 56.59	131.88	980.95914	0.28	1.03
	10182	220.0	57 55.8	48 56.83	60.79	980.97144	0.35	-0.95
	10181	220.8	57 56.4	48 57.00	29.71	980.97704	0.42	-1.64
E	10180	221.6	57 56.8	48 57.15	16.96	980.97949	0.43	-1.92
	10696	222.2	57 56.7	48 57.40	2.99	980.98259	0.43	-1.94
	10060	222.8	57 56.2	48 57.68	4.24	980.98264	0.43	-2.06
	10059	223.6	57 55.8	48 57.85	11.41	980.98180	0.44	-1.73
	10058	224.4	57 55.2	48 57.94	10.10	980.98300	0.46	-0.90

TABLE SYMBOLS EXPLAINED IN SECTION A3.2.

... continued

TABLE A3.1, CONTINUED

LOC	STN	C PAB (KM)	LONGITUDE (DEG MIN)	LATITUDE (DEG MIN)	ELEV (M)	G OBS (GAL)	TERC (MGAL)	G BOUG (MGAL)
	10C66	225.3	57 54.7	48 57.78	4.42	980.98368	0.48	-1.08
	10C65	226.4	57 54.0	48 57.55	7.14	980.98336	0.50	-0.51
	10110	226.9	57 53.7	48 57.40	7.62	980.98360	0.70	0.25
	10C61	227.2	57 53.5	48 57.27	5.09	980.98361	1.00	0.26
	10C62	228.0	57 52.8	48 57.00	16.13	980.98097	1.35	0.55
	10108	228.5	57 52.6	48 57.00	16.71	980.98136	1.70	1.40
	10C63	229.3	57 52.1	48 56.77	16.81	980.98002	2.00	0.72
	10109	229.7	57 51.8	48 56.70	21.87	980.98328	2.05	5.13
	10C67	230.5	57 51.3	48 56.61	14.82	980.97985	2.20	0.60
	10C68	231.4	57 50.7	48 56.70	10.34	980.98187	2.30	1.70
	10C64	232.2	57 49.9	48 57.06	11.07	980.98313	2.15	2.42
	10C69	232.7	57 49.7	48 57.21	8.45	980.98475	2.15	3.30
	10C70	233.7	57 48.9	48 57.52	21.99	980.98285	2.40	3.85
	10C72	234.5	57 48.5	48 57.85	11.77	980.98440	2.40	2.90
	10C71	235.2	57 48.2	48 58.07	22.75	980.98529	2.20	5.42
	10C73	236.3	57 47.7	48 58.35	10.06	980.98697	2.00	3.99
	10C74	237.1	57 47.1	48 58.55	14.33	980.98679	2.20	4.55
	10075	237.9	57 46.4	48 58.77	15.92	980.98656	2.20	4.30
	10C76	238.8	57 45.8	48 58.91	17.20	980.98560	2.20	3.39
	10C78	239.6	57 45.1	48 59.09	24.19	980.98469	2.10	3.48
	10077	240.4	57 44.4	48 59.10	33.85	980.98431	2.10	4.99
	10C84	241.2	57 43.5	48 59.30	35.04	980.98509	2.00	5.61
	10C85	242.2	57 42.9	48 59.59	30.35	980.98789	1.80	6.85
	10102	242.9	57 42.4	48 59.85	24.49	980.98985	1.70	7.17
	10C86	243.3	57 42.1	48 59.98	14.98	980.99215	1.60	7.30
	10C87	243.7	57 41.8	49 0.13	14.85	980.99131	1.50	6.12
	10C83	244.5	57 40.9	49 0.18	15.92	980.99117	1.50	6.11
	10C82	245.5	57 40.3	49 0.24	19.34	980.99154	1.45	7.01
	10C80	246.3	57 39.5	49 0.34	22.42	980.99228	1.40	8.16
	10C81	247.3	57 38.8	49 0.52	22.42	980.99351	1.35	9.07
	10695	248.0	57 38.4	49 0.70	8.23	980.99668	1.00	8.83
	10C88	248.7	57 38.0	49 0.95	20.68	980.99714	0.90	11.27
	10C79	249.5	57 37.6	49 1.06	19.09	980.99780	0.80	11.35
	10C89	250.2	57 37.3	49 0.75	35.62	980.99490	0.80	12.17
	10C90	251.0	57 36.8	49 0.75	17.87	980.99704	0.75	10.77

TABLE SYMBOLS EXPLAINED IN SECTION A3.2.

... continued

TABLE A3.1, CONTINUED

LOC	STN	C PAB (KM)	LONGITUDE (DEG MIN)	LATITUDE (DEG MIN)	ELEV (M)	G OBS (GAL)	TERC (MGAL)	G BOUG (MGAL)
	10C92	251.8	57 36.0	49 0.83	29.89	980.99366	0.60	9.48
	10C91	252.8	57 35.6	49 1.16	31.60	980.99316	0.50	8.72
	10C94	253.6	57 35.3	49 1.50	27.79	980.99460	0.45	8.86
	10C95	254.3	57 35.0	49 1.86	41.88	980.99201	0.40	8.45
	10C96	255.1	57 34.7	49 2.26	21.62	980.99655	0.40	8.41
	10C93	256.0	57 34.6	49 2.70	12.41	980.99954	0.40	8.94
	10103	256.7	57 34.1	49 3.07	27.85	980.99721	0.40	9.09
	10C97	257.5	57 33.9	49 3.53	19.86	980.99962	0.40	9.24
	10104	258.3	57 33.6	49 3.94	23.48	980.99976	0.40	9.49
	10C98	259.1	57 33.4	49 4.36	40.66	980.99766	0.40	10.14
	10105	259.9	57 32.9	49 4.73	51.58	980.99667	0.40	10.74
	10C99	260.7	57 32.5	49 5.02	36.45	981.00017	0.45	10.89
	10106	261.5	57 32.4	49 5.45	41.85	980.99990	0.45	11.04
	10100	262.3	57 32.0	49 5.84	84.33	980.99490	0.40	13.76
	10107	263.0	57 31.7	49 6.13	84.88	980.99576	0.40	14.30
	10101	263.9	57 31.2	49 6.53	56.94	981.00138	0.45	13.88
	10118	264.6	57 30.8	49 6.82	28.82	981.00703	0.45	13.56
	10117	265.2	57 30.7	49 6.99	13.42	981.01010	0.45	13.35
	10116	265.8	57 30.2	49 7.13	39.22	981.00605	0.45	14.17
	10119	266.6	57 29.9	49 7.46	40.75	981.00676	0.50	14.74
	10115	267.4	57 29.4	49 7.84	32.76	981.00926	0.45	15.05
	10122	268.0	57 29.1	49 8.08	19.52	981.01299	0.40	15.77
	10123	268.6	57 28.8	49 8.26	24.28	981.01113	0.40	14.57
	10114	268.9	57 28.6	49 8.39	22.14	981.01183	0.40	14.66
	10121	270.0	57 27.9	49 8.87	32.70	981.01044	0.35	14.58
	10113	270.8	57 27.5	49 9.15	34.59	981.01061	0.35	14.71
	10120	271.7	57 26.9	49 9.54	31.99	981.01158	0.30	14.53
	10112	272.4	57 26.6	49 9.80	18.21	981.01451	0.30	14.37
F	10111	273.0	57 25.8	49 10.20	10.03	981.01660	0.30	14.25
	10924	273.6	57 26.0	49 10.39	11.16	981.01672	0.25	14.26
	10925	274.4	57 26.0	49 10.82	12.54	981.01669	0.21	13.82
	10926	275.1	57 26.0	49 11.12	20.80	981.01537	0.17	13.64
	10927	275.9	57 25.5	49 11.42	17.29	981.01647	0.15	13.58
	10928	276.7	57 25.0	49 11.52	14.76	981.01720	0.13	13.65
	10929	277.5	57 24.4	49 11.48	28.21	981.01374	0.11	12.87

TABLE SYMBOLS EXPLAINED IN SECTION A3.2.

... continued

TABLE A3.1, CONTINUED

LOC	STN	D PAB (KM)	LONGITUDE (DEG MIN)	LATITUDE (DEG MIN)	ELEV (M)	G OBS (GAL)	TERC (MGAL)	G BOUG (MGAL)
	10930	278.4	57 23.7	49 11.52	34.13	981.01288	0.10	13.11
	10931	279.3	57 23.3	49 11.83	37.64	981.01238	0.10	12.83
	10932	280.0	57 22.9	49 12.13	42.64	981.01176	0.10	12.75
	10933	280.8	57 22.5	49 12.30	45.32	981.01116	0.10	12.43
	10934	281.7	57 21.9	49 12.52	46.94	981.01016	0.10	11.42
	10935	282.4	57 21.4	49 12.63	52.25	981.00836	0.10	10.50
	10936	282.9	57 21.0	49 12.61	53.37	981.00753	0.10	9.92
	10937	283.7	57 20.3	49 12.75	48.16	981.00797	0.10	9.12
	10938	283.8	57 20.0	49 12.96	48.13	981.00800	0.10	8.83
	10939	284.6	57 19.6	49 13.21	51.27	981.00766	0.10	8.74
	10940	285.3	57 19.0	49 13.35	47.85	981.00836	0.10	8.56
	10941	286.2	57 18.5	49 13.52	44.38	981.00912	0.15	8.43
	10942	287.0	57 18.0	49 13.70	59.26	981.00682	0.10	8.74
	10943	287.8	57 17.5	49 13.91	59.41	981.00738	0.09	9.01
	10944	288.6	57 16.8	49 13.91	68.69	981.00591	0.09	9.36
	10945	289.4	57 16.2	49 13.91	75.79	981.00540	0.09	10.25
	10946	290.2	57 15.7	49 13.65	80.46	981.00050	0.09	8.63
	10947	291.0	57 15.3	49 13.38	85.86	980.99957	0.09	7.19
	10948	291.8	57 14.6	49 13.22	89.76	980.99821	0.09	6.84
	10949	292.6	57 14.0	49 13.25	102.33	980.99605	0.09	7.10
	10950	293.4	57 13.3	49 13.39	119.47	980.99304	0.09	7.26
	10951	294.2	57 12.9	49 13.65	130.91	980.99166	0.09	7.74
	10952	295.0	57 12.6	49 13.96	134.44	980.99174	0.09	8.06
	10953	295.8	57 12.1	49 14.25	128.04	980.99391	0.09	8.53
	10954	296.6	57 11.7	49 14.59	131.03	980.99433	0.09	9.04
	10955	297.4	57 11.0	49 14.86	125.08	980.99492	0.09	8.05
	10956	298.2	57 10.5	49 15.09	118.95	980.99501	0.09	6.59
	10957	299.0	57 9.9	49 15.24	126.39	980.99354	0.09	6.37
	10958	299.8	57 9.3	49 15.39	134.20	980.99170	0.09	5.84
	10985	300.0	57 9.1	49 15.42	137.01	980.99135	0.09	6.00
	10984	300.8	57 8.5	49 15.45	143.14	980.99034	0.09	6.15
	10983	301.6	57 7.9	49 15.57	148.69	980.98994	0.09	6.66
	10982	302.5	57 7.2	49 15.80	152.59	980.98981	0.10	6.97
	10981	303.2	57 6.8	49 15.98	150.67	980.99029	0.10	6.80
	10980	304.1	57 6.0	49 16.00	154.51	980.98984	0.10	7.08

TABLE SYMBOLS EXPLAINED IN SECTION A3.2.

... continued

TABLE A3.1, CONTINUED

LOC	STN	C PAB (KM)	LONGITUDE (DEG MIN)	LATITUDE (DEG MIN)	ELEV (M)	G CBS (GAL)	TERC (MGAL)	G BOUG (MGAL)
	10979	304.9	57 5.4	49 15.89	153.26	980.98853	0.10	5.68
	10978	305.8	57 4.8	49 15.96	136.76	980.99038	0.10	4.18
	10977	306.6	57 4.4	49 16.30	141.31	980.99061	0.11	4.81
	10976	307.5	57 4.0	49 16.67	141.52	980.99189	0.11	5.58
	10975	308.3	57 3.7	49 17.00	143.17	980.99310	0.12	6.64
	10974	309.1	57 3.3	49 17.30	140.15	980.99515	0.12	7.64
	10973	309.9	57 3.0	49 17.65	131.30	980.99785	0.12	8.08
	10972	310.7	57 2.7	49 17.96	126.54	980.99999	0.12	8.83
	10971	311.5	57 2.4	49 18.35	123.52	981.00201	0.12	9.67
	10970	312.3	57 2.0	49 18.76	104.37	981.00742	0.12	10.70
	10969	313.0	57 1.9	49 19.09	107.02	981.00853	0.13	11.85
	10968	313.8	57 1.5	49 19.52	115.63	981.00862	0.13	13.00
	10967	314.7	57 1.3	49 19.98	115.32	981.01015	0.13	13.78
	10966	315.5	57 1.2	49 20.39	114.89	981.01209	0.13	15.03
	10965	316.3	57 1.0	49 20.74	117.88	981.01218	0.13	15.18
	10964	317.1	57 0.9	49 21.10	116.81	981.01391	0.13	16.17
	10963	317.9	57 0.5	49 21.49	113.19	981.01638	0.14	17.35
	10962	318.7	57 0.1	49 21.89	106.72	981.01929	0.14	18.40
	10961	319.5	56 59.7	49 22.25	103.09	981.02164	0.14	19.50
	10960	320.4	56 59.4	49 22.65	95.04	981.02438	0.15	20.07
	10959	321.2	56 58.9	49 22.87	91.65	981.02786	0.15	22.55
	10923	322.0	56 58.3	49 22.75	125.69	981.02438	0.15	25.95
	9114	322.8	56 58.1	49 22.41	113.31	981.02602	0.15	25.66
	10921	323.6	56 58.0	49 22.04	109.68	981.02597	0.15	25.45
	10920	324.4	56 58.0	49 21.60	94.37	981.02754	0.15	24.66
	10919	325.2	56 57.8	49 21.17	94.82	981.02612	0.15	23.97
	10918	326.1	56 57.8	49 20.73	107.97	981.02198	0.15	23.07
	10917	326.9	56 57.4	49 20.38	108.73	981.02024	0.15	22.00
	10916	327.7	56 57.0	49 20.02	106.93	981.01875	0.15	20.69
	10915	328.6	56 56.8	49 19.70	113.49	981.01537	0.15	19.08
	10914	329.4	56 56.4	49 19.35	106.29	981.01469	0.15	17.50
	10913	330.2	56 56.0	49 19.04	98.48	981.01370	0.15	15.44
	10912	330.9	56 55.8	49 18.77	99.12	981.01129	0.16	13.57
	10911	331.6	56 55.5	49 18.47	104.77	981.00855	0.16	12.38
	10910	332.4	56 55.1	49 18.10	102.63	981.00733	0.17	11.30

TABLE SYMBOLS EXPLAINED IN SECTION A3.2.

... continued

TABLE A3.1, CONTINUED

LOC	STN	C PAB (KM)	LONGITUDE (DEG MIN)	LATITUDE (DEG MIN)	ELEV (M)	G OBS (GAL)	TERC (MGAL)	G BOUG (MGAL)
	10SC9	333.1	56 54.8	49 17.81	101.05	981.00638	0.17	10.47
	10SC8	334.0	56 54.2	49 17.62	107.79	981.00515	0.18	10.86
	10SC7	334.8	56 53.7	49 17.53	102.57	981.00576	0.19	10.59
	10SC6	335.6	56 53.0	49 17.43	89.49	981.00956	0.20	11.97
	10S05	336.4	56 52.3	49 17.28	91.93	981.00926	0.23	12.41
	10S04	337.2	56 51.9	49 17.00	93.51	981.00782	0.27	11.74
	10S03	337.9	56 51.5	49 16.76	94.09	981.00578	0.34	10.24
G	10S02	338.9	56 50.7	49 16.65	117.79	980.99883	0.37	8.14
	10S01	339.7	56 50.0	49 16.63	104.00	981.00084	0.40	7.50
	10S00	340.5	56 49.2	49 16.69	94.64	981.00098	0.45	5.76
	1C899	341.4	56 48.6	49 16.91	102.57	980.99825	0.50	4.31
	1C898	342.2	56 48.0	49 17.20	98.51	980.99967	0.50	4.50
	10897	343.0	56 47.5	49 17.48	101.93	980.99818	0.50	3.27
	1C896	343.8	56 47.0	49 17.74	113.46	980.99458	0.50	1.55
	1C895	344.6	56 46.5	49 18.00	133.28	980.99051	0.50	0.99
	1C894	345.4	56 45.9	49 18.32	111.26	980.99471	0.50	0.38
	1C893	346.2	56 45.4	49 18.61	100.04	980.99700	0.45	-0.02
	1C892	347.0	56 44.8	49 18.74	102.33	980.99706	0.40	0.25
	1C891	347.8	56 44.2	49 18.93	126.57	980.99199	0.40	-0.33
	1C890	348.6	56 43.8	49 19.13	117.06	980.99364	0.39	-0.86
	1C889	349.4	56 43.1	49 19.35	108.12	980.99581	0.39	-0.78
	1C888	350.2	56 42.6	49 19.54	109.10	980.99611	0.38	-0.58
	10887	351.1	56 42.0	49 19.74	109.34	980.99621	0.38	-0.73
	10886	351.8	56 41.5	49 19.97	112.54	980.99590	0.37	-0.76
	1C885	352.7	56 41.0	49 20.26	115.26	980.99600	0.37	-0.56
	1C884	353.5	56 40.4	49 20.48	112.24	980.99749	0.36	0.00
	9113	354.3	56 40.4	49 20.47	94.06	981.00198	0.36	0.93
	1C861	355.1	56 39.8	49 20.54	98.67	981.00210	0.35	1.84
	1C862	355.9	56 39.1	49 20.63	94.43	981.00303	0.34	1.79
	1C863	356.7	56 38.6	49 20.78	95.28	981.00325	0.32	1.94
	1C864	357.5	56 38.0	49 21.00	96.84	981.00376	0.31	2.42
	1C865	358.3	56 37.6	49 21.35	95.80	981.00460	0.30	2.52
	1C866	359.1	56 37.2	49 21.70	102.85	981.00513	0.30	3.92
	1C867	359.9	56 36.9	49 22.06	104.89	981.00636	0.30	5.01
	1C868	360.7	56 36.4	49 22.35	109.68	981.00661	0.30	5.77

TABLE SYMBOLS EXPLAINED IN SECTION A3.2.

... continued

TABLE A3.1, CONTINUED

LOC STN	C PAB (KM)	LONGITUDE (DEG MIN)	LATITUDE (DEG MIN)	ELEV (M)	G OBS (GAL)	TERC (MGAL)	G BOUG (MGAL)
10869	361.5	56 35.9	49 22.61	108.88	981.00774	0.30	6.36
10870	362.3	56 35.4	49 22.87	104.98	981.00948	0.30	6.95
10871	363.0	56 34.8	49 23.13	105.71	981.00972	0.30	6.94
10872	363.8	56 34.3	49 23.38	101.90	981.01134	0.30	7.44
10873	364.6	56 33.8	49 23.65	108.88	981.01072	0.30	7.79
10874	365.4	56 33.3	49 23.88	113.49	981.01124	0.30	8.88
10875	366.2	56 32.8	49 24.15	99.43	981.01559	0.30	10.06
10876	367.0	56 32.3	49 24.43	96.38	981.01693	0.30	10.38
10877	367.8	56 31.8	49 24.67	90.62	981.01937	0.29	11.32
10878	368.6	56 31.3	49 24.96	84.79	981.02119	0.28	11.55
10879	369.4	56 30.7	49 25.20	79.67	981.02294	0.27	11.93
10880	370.2	56 30.2	49 25.43	69.08	981.02614	0.26	12.70
10881	371.0	56 29.7	49 25.67	61.52	981.02915	0.25	13.85
10882	371.9	56 29.1	49 25.92	66.03	981.02923	0.24	14.44
10883	372.7	56 28.7	49 26.20	70.27	981.02849	0.23	14.10
10860	373.6	56 28.1	49 26.46	68.56	981.02976	0.22	14.64
10859	374.5	56 27.6	49 26.76	69.14	981.02977	0.21	14.31
10858	375.3	56 27.0	49 27.00	60.15	981.03261	0.21	15.02
10857	376.1	56 26.5	49 27.22	60.60	981.03331	0.20	15.47
10856	376.9	56 25.9	49 27.38	58.74	981.03454	0.20	16.10
10855	377.7	56 25.3	49 27.54	58.74	981.03541	0.19	16.72
10854	378.5	56 24.8	49 27.70	69.54	981.03443	0.19	17.63
10853	379.3	56 24.1	49 27.85	77.10	981.03267	0.19	17.13
10852	380.1	56 23.6	49 27.93	91.19	981.02927	0.20	16.40
10851	380.9	56 23.0	49 28.00	80.52	981.03014	0.20	15.06
10850	381.7	56 22.4	49 28.06	76.40	981.03014	0.20	14.16
10849	382.5	56 21.8	49 28.07	78.05	981.02941	0.20	13.74
10848	383.3	56 21.1	49 27.96	78.42	981.02942	0.20	13.99
10847	384.0	56 21.6	49 27.87	79.97	981.03014	0.20	15.15
10846	384.8	56 20.0	49 27.74	81.13	981.03180	0.20	17.23
10845	385.6	56 19.3	49 27.61	57.13	981.03755	0.20	18.45
10844	386.4	56 18.6	49 27.50	61.43	981.03809	0.20	20.00
10843	387.2	56 17.9	49 27.62	79.36	981.03590	0.20	21.16
10842	387.9	56 17.4	49 27.85	76.52	981.03700	0.20	21.36
10841	388.8	56 16.9	49 28.11	72.13	981.03862	0.20	21.73

TABLE SYMBOLS EXPLAINED IN SECTION A3.2.

... continued

TABLE A3.1, CONTINUED

LOC	STN	C PAB (KM)	LONGITUDE (DEG MIN)	LATITUDE (DEG MIN)	ELEV (M)	G OBS (GAL)	TERC (MGAL)	G BOUG (MGAL)
	1C840	389.6	56 16.5	49 28.34	68.69	981.04071	0.20	22.80
	1C839	390.4	56 15.9	49 28.54	65.79	981.04148	0.20	22.70
	1C838	391.1	56 15.4	49 28.63	63.78	981.04214	0.20	22.83
	10837	391.9	56 14.8	49 28.65	58.56	981.04438	0.20	24.02
	1C836	392.6	56 14.2	49 28.61	35.01	981.04959	0.20	24.65
	10835	393.5	56 13.5	49 28.78	41.91	981.04911	0.20	25.28
	10834	394.2	56 13.1	49 29.03	36.69	981.04900	0.20	23.77
	10833	395.0	56 12.6	49 29.09	35.59	981.05060	0.20	25.06
	10832	395.8	56 11.9	49 28.98	54.11	981.04821	0.20	26.48
	10831	396.5	56 11.5	49 28.82	64.14	981.04682	0.20	27.30
	10830	397.3	56 11.2	49 28.47	67.34	981.04654	0.20	28.17
	1C829	398.1	56 10.9	49 28.07	86.07	981.04413	0.20	30.04
	1C828	398.9	56 10.9	49 27.70	96.87	981.04154	0.20	30.12
	1C827	399.7	56 10.5	49 27.41	78.81	981.04476	0.20	30.22
	1C826	400.6	56 9.9	49 27.20	73.08	981.04665	0.20	31.30
	1C825	401.2	56 9.8	49 26.91	83.39	981.04537	0.20	32.48
	10824	402.0	56 9.7	49 26.50	105.93	981.04132	0.20	33.47
	1C823	402.8	56 9.4	49 26.22	91.80	981.04371	0.20	33.50
	1C822	403.6	56 9.0	49 25.87	64.63	981.04678	0.20	31.74
	1C821	404.3	56 8.8	49 25.57	48.83	981.04836	0.20	30.66
	10820	405.1	56 8.4	49 25.26	11.28	981.05698	0.20	32.36
	1C819	405.9	56 7.7	49 25.22	16.35	981.05723	0.21	33.67
	1C818	406.7	56 7.0	49 25.37	14.88	981.05693	0.22	32.87
	1C817	407.5	56 6.4	49 25.52	15.68	981.05620	0.23	32.09
	1C816	408.3	56 5.8	49 25.54	19.15	981.05630	0.25	32.86
H	1C77C	409.0	56 5.4	49 25.28	13.76	981.05744	0.27	33.34
	1C771	410.0	56 5.0	49 24.83	17.60	981.06037	0.30	37.73
	1C772	410.8	56 4.9	49 24.40	19.15	981.06238	0.27	40.66
	10773	411.8	56 4.8	49 23.91	16.29	981.06492	0.24	43.33
	1C774	412.6	56 4.8	49 23.47	23.94	981.06358	0.21	44.12
	10775	413.5	56 5.1	49 23.02	21.93	981.06332	0.18	44.11
	1C776	414.4	56 5.4	49 22.52	22.87	981.06178	0.18	43.50
	10777	415.3	56 5.7	49 22.01	22.66	981.06085	0.17	43.27
	1C778	416.1	56 5.9	49 21.61	24.55	981.06048	0.17	43.87
	1C779	416.9	56 6.2	49 21.15	27.24	981.05941	0.16	44.00

TABLE SYMBOLS EXPLAINED IN SECTION A3.2.

... continued

TABLE A3.1, CONTINUED

LOC	STN	D PAB (KM)	LONGITUDE (DEG MIN)		LATITUDE (DEG MIN)		ELEV (M)	G OBS (GAL)	TERC (MGAL)	G BOUG (MGAL)
	1C78C	417.7	56	6.3	49	20.74	28.55	981.05765	0.16	43.11
	1C781	418.5	56	6.5	49	20.30	32.27	981.05580	0.15	42.64
	1C782	419.3	56	6.6	49	19.87	39.16	981.05326	0.15	42.09
	1C783	420.1	56	6.7	49	19.39	52.19	981.04989	0.14	41.99
	1C784	420.9	56	6.8	49	18.96	44.83	981.04977	0.14	41.06
	1C785	421.7	56	6.9	49	18.54	52.37	981.04660	0.13	39.99
	1C786	422.5	56	6.9	49	18.09	50.14	981.04639	0.13	40.01
	1C787	423.4	56	7.0	49	17.60	56.12	981.04497	0.12	40.49
	1C788	424.2	56	7.0	49	17.17	73.44	981.04075	0.12	40.32
	1C789	425.0	56	6.9	49	16.74	79.73	981.03689	0.12	38.33
	1C790	425.8	56	6.9	49	16.31	82.41	981.03252	0.12	35.13
	1C791	426.6	56	6.9	49	16.00	84.45	981.02994	0.12	33.41
	1C792	427.4	56	6.9	49	15.65	94.98	981.02605	0.12	32.12
	1C793	428.2	56	7.0	49	15.15	115.66	981.02061	0.12	31.49
	1C794	429.0	56	7.1	49	14.89	126.73	981.01763	0.12	31.07
	1C795	429.8	56	7.0	49	14.48	131.18	981.01513	0.11	30.05
	1C796	430.6	56	6.9	49	14.13	138.35	981.01296	0.10	29.80
	1C797	431.4	56	6.6	49	13.80	145.94	981.00982	0.10	28.65
	1C798	432.2	56	6.6	49	13.41	144.87	981.00790	0.10	27.10
	1C799	433.0	56	6.4	49	13.10	143.65	981.00446	0.10	23.88
	1C800	433.8	56	6.0	49	12.83	140.39	981.00165	0.10	20.83
	1C801	434.6	56	5.8	49	12.48	149.66	980.99701	0.10	18.53
	1C802	435.4	56	5.8	49	12.08	154.21	980.99399	0.10	17.00
	1C803	436.2	56	5.8	49	11.65	181.69	980.98668	0.10	15.74
	1C804	437.0	56	5.8	49	11.22	187.61	980.98304	0.10	13.90
	1C805	437.8	56	5.8	49	10.83	184.10	980.98223	0.10	12.99
	1C806	438.6	56	5.9	49	10.43	185.53	980.98002	0.10	11.65
	1C807	439.4	56	6.0	49	10.04	190.20	980.97746	0.10	10.59
	1C808	440.3	56	6.1	49	9.22	199.74	980.97403	0.10	10.26
	1C809	441.0	56	6.2	49	9.26	191.78	980.97443	0.10	9.04
	1C810	441.8	56	6.3	49	8.87	187.97	980.97424	0.10	8.68
	1C811	442.7	56	6.1	49	8.46	195.54	980.97165	0.10	8.19
	10812	443.5	56	5.8	49	8.04	182.51	980.97360	0.10	8.20
	10813	444.2	56	5.6	49	7.74	147.71	980.97949	0.10	7.69
	1C814	444.9	56	5.3	49	7.41	142.13	980.98000	0.10	7.59

TABLE SYMBOLS EXPLAINED IN SECTION A3.2.

... continued

TABLE A3.1, CONTINUED

LOC	STN	C PAB (KM)	LONGITUDE (DEG MIN)		LATITUDE (DEG MIN)		ELEV (M)	G OBS (GAL)	TERC (MGAL)	G BOUG (MGAL)
	10815	445.7	56	4.9	49	7.11	125.17	980.98330	0.10	8.01
	10671	446.5	56	4.7	49	6.73	133.71	980.98215	0.10	9.10
	10670	447.3	56	4.6	49	6.28	137.22	980.98069	0.10	9.00
	10669	448.1	56	4.6	49	5.89	130.63	980.98080	0.10	8.40
	10668	448.9	56	4.8	49	5.49	130.45	980.97962	0.10	7.78
	10667	449.7	56	4.9	49	5.05	131.97	980.97857	0.10	7.68
	10666	450.6	56	4.8	49	4.66	128.22	980.97756	0.10	6.52
	10665	451.1	56	4.9	49	4.31	136.79	980.97533	0.10	6.49
	10664	451.9	56	5.0	49	3.93	128.77	980.97681	0.10	6.96
	10663	452.7	56	5.2	49	3.54	128.68	980.97584	0.10	6.56
	10662	453.5	56	5.2	49	3.12	127.49	980.97561	0.10	6.72
	10661	454.3	56	4.8	49	2.82	132.77	980.97395	0.10	6.54
	10660	455.1	56	4.7	49	2.43	128.50	980.97441	0.10	6.74
	10659	455.9	56	4.8	49	2.03	134.29	980.97323	0.09	7.29
	10658	456.7	56	4.7	49	1.66	134.08	980.97302	0.08	7.58
	10657	457.6	56	4.3	49	1.35	131.15	980.97336	0.07	7.80
	10656	458.4	56	3.8	49	1.08	121.24	980.97507	0.06	7.95
	10655	459.2	56	3.3	49	0.81	112.24	980.97721	0.06	8.72
	10654	460.0	56	2.9	49	0.47	109.49	980.97721	0.06	8.69
	10653	460.9	56	2.8	49	0.02	104.65	980.97792	0.06	9.11
	10652	461.7	56	2.7	48	59.58	102.17	980.97789	0.06	9.25
I	10651	462.5	56	2.4	48	59.14	100.77	980.97806	0.06	9.80
	10769	463.3	56	2.1	48	58.78	101.90	980.97806	0.06	10.56
	10768	464.2	56	1.7	48	58.57	106.54	980.97725	0.06	10.98
	10767	464.7	56	1.3	48	58.40	102.08	980.97823	0.06	11.34
	10766	465.4	56	0.8	48	58.28	108.12	980.97725	0.06	11.72
	10765	466.4	56	0.2	48	58.09	113.73	980.97628	0.06	12.14
	10764	467.2	55	59.5	48	57.91	122.85	980.97470	0.06	12.62
	10763	468.0	55	58.9	48	57.78	126.18	980.97391	0.06	12.68
	10762	468.9	55	58.3	48	57.61	118.31	980.97565	0.06	13.13
	10761	469.6	55	57.7	48	57.41	111.78	980.97712	0.06	13.61
	10760	470.5	55	57.1	48	57.24	106.23	980.97820	0.06	13.85
	10759	471.2	55	56.6	48	57.20	109.43	980.97787	0.06	14.21
	10758	471.7	55	56.2	48	57.17	104.04	980.97911	0.06	14.43
	10757	472.6	55	55.6	48	57.13	105.53	980.97900	0.06	14.68

TABLE SYMBOLS EXPLAINED IN SECTION A3.2.

... continued

TABLE A3.1, CONTINUED

LOC	STN	C PAB (KM)	LONGITUDE (DEG MIN)	LATITUDE (DEG MIN)	ELEV (M)	G OBS (GAL)	TERC (MGAL)	G BOUG (MGAL)
	1C756	473.6	55 54.8	48 57.13	88.57	980.98260	0.06	15.02
	1C755	474.3	55 54.2	48 57.12	94.12	980.98167	0.06	15.12
	1C754	475.2	55 53.4	48 57.09	96.96	980.98121	0.06	15.26
	1C753	475.8	55 52.9	48 57.08	95.62	980.98168	0.06	15.48
	1C752	476.6	55 52.4	48 57.04	85.61	980.98343	0.06	15.32
	1C751	477.3	55 51.8	48 57.03	83.39	980.98375	0.06	15.22
	1C750	478.0	55 51.2	48 57.00	81.43	980.98427	0.06	15.40
	1C749	479.0	55 50.5	48 56.87	86.19	980.98311	0.06	15.37
	1C748	479.9	55 49.9	48 56.72	80.67	980.98385	0.06	15.25
	1C747	480.6	55 49.4	48 56.61	79.39	980.98374	0.06	15.05
	1C746	481.1	55 48.8	48 56.61	86.99	980.98219	0.06	14.99
	1C745	482.0	55 48.4	48 56.65	85.86	980.98288	0.06	15.40
	1C744	482.9	55 47.7	48 56.74	100.53	980.98043	0.06	15.70
	10743	483.6	55 47.1	48 56.72	82.35	980.98418	0.06	15.91
	1C742	484.5	55 46.5	48 56.64	71.71	980.98599	0.06	15.74
	10741	485.3	55 45.8	48 56.57	72.35	980.98688	0.06	16.86
	1C740	486.2	55 45.0	48 56.50	72.16	980.98619	0.06	16.24
	10739	487.0	55 44.4	48 56.46	72.59	980.98453	0.06	14.73
	1C738	487.9	55 43.7	48 56.43	75.27	980.98386	0.06	14.63
	1C737	488.8	55 43.0	48 56.50	73.20	980.98414	0.06	14.40
	1C736	489.6	55 42.3	48 56.58	79.97	980.98267	0.06	14.14
	1C735	490.3	55 41.7	48 56.65	81.95	980.98179	0.06	13.55
	1C734	491.0	55 41.1	48 56.73	82.38	980.98072	0.06	12.44
	1C733	491.6	55 40.7	48 56.74	73.69	980.98269	0.06	12.68
	10732	492.3	55 40.2	48 56.74	78.51	980.98084	0.06	11.78
J	10C18	492.7	55 40.0	48 56.83	76.31	980.98170	0.06	12.08
	10CC6	493.0	55 39.9	48 56.85	79.76	980.98143	0.06	12.45
	10CC7	493.8	55 39.6	48 56.45	84.45	980.97821	0.06	10.76
	10C03	494.6	55 38.8	48 56.28	103.52	980.97252	0.06	9.07
	10C17	495.4	55 38.2	48 56.53	118.28	980.96985	0.06	8.93
	10C16	496.2	55 37.5	48 56.78	110.26	980.97132	0.06	8.45
	10C15	497.0	55 37.0	48 56.97	105.32	980.97236	0.06	8.23
	10C13	497.7	55 36.3	48 57.34	111.39	980.97091	0.06	7.43
	10C14	498.5	55 35.9	48 57.76	106.90	980.97158	0.06	6.59
	10C12	499.2	55 35.6	48 58.11	99.31	980.97337	0.06	6.36

TABLE SYMBOLS EXPLAINED IN SECTION A3.2.

... continued

TABLE A3.1, CONTINUED

LOC	STN	C PAB (KM)	LONGITUDE (DEG MIN)	LATITUDE (DEG MIN)	ELEV (M)	G OBS (GAL)	TERC (MGAL)	G BOUG (MGAL)
	10C11	500.0	55 34.7	48 58.51	87.32	980.97550	0.06	5.54
	10CC9	500.8	55 34.1	48 58.83	66.52	980.97934	0.06	4.81
	10C1C	501.6	55 33.6	48 59.07	45.11	980.98358	0.06	4.48
	10CC5	502.4	55 33.1	48 59.34	24.70	980.98761	0.06	4.09
	10C02	503.1	55 32.5	48 59.30	21.50	980.98844	0.06	4.35
	10C04	503.8	55 32.0	48 59.43	20.19	980.98925	0.06	4.71
	10CC8	504.5	55 31.6	48 59.74	19.43	980.98973	0.06	4.58
	10C01	505.2	55 30.9	48 59.92	19.28	980.99028	0.06	4.83
	10179	506.0	55 29.8	49 0.70	18.60	980.99187	0.06	5.12
	10178	506.9	55 29.1	49 0.96	20.71	980.99232	0.06	5.60
	10177	507.8	55 28.5	49 1.11	18.60	980.99367	0.06	6.31
	10176	508.5	55 28.0	49 1.16	12.63	980.99494	0.06	6.33
	10175	509.2	55 27.5	49 1.40	17.45	980.99508	0.07	7.07
	10174	510.0	55 27.0	49 1.41	8.14	980.99679	0.07	6.94
	10173	510.7	55 26.5	49 1.26	17.29	980.99567	0.08	7.85
	10172	511.5	55 25.8	49 1.40	16.41	980.99645	0.08	8.25
	10171	512.2	55 25.2	49 1.54	17.72	980.99713	0.09	8.99
	10170	513.0	55 24.6	49 1.50	14.52	980.99809	0.09	9.38
	10169	513.9	55 24.0	49 1.70	12.14	980.99865	0.10	9.18
	10168	514.7	55 23.7	49 1.98	12.29	980.99917	0.10	9.31
	10167	515.4	55 23.3	49 2.33	11.50	980.99938	0.10	8.85
	10166	516.1	55 23.1	49 2.67	13.18	980.99972	0.10	9.01
	10165	516.9	55 22.8	49 3.00	10.92	981.00131	0.10	9.66
	10164	517.6	55 22.2	49 3.20	7.96	981.00259	0.10	10.06
	10163	518.5	55 21.4	49 3.50	9.67	981.00328	0.10	10.64
	10162	519.3	55 21.0	49 3.85	5.52	981.00510	0.10	11.13
	10161	520.2	55 20.4	49 4.11	3.57	981.00601	0.10	11.26
	10160	521.0	55 19.9	49 4.43	3.96	981.00720	0.10	12.05
	10159	521.9	55 19.3	49 4.61	4.67	981.00847	0.10	13.19
	10158	522.6	55 18.8	49 4.35	4.36	981.00879	0.10	13.84
	10157	523.4	55 18.3	49 4.13	5.86	981.01035	0.11	16.03
	10156	524.2	55 17.8	49 4.33	9.49	981.01001	0.12	16.12
	10155	525.1	55 17.4	49 4.64	14.00	981.01030	0.14	16.86
	10154	525.8	55 16.9	49 4.96	11.96	981.01054	0.16	16.24
	10153	526.7	55 16.4	49 5.22	12.38	981.01036	0.18	15.77

TABLE SYMBOLS EXPLAINED IN SECTION A3.2.

... continued

TABLE A3.1, CONTINUED

LOC	STN	D PAB (KM)	LONGITUDE (DEG MIN)	LATITUDE (DEG MIN)	ELEV (M)	G OBS (GAL)	TERC (MGAL)	G BOUG (MGAL)
	10152	527.5	55 15.9	49 5.41	14.06	981.01055	0.18	16.01
	10151	528.3	55 15.4	49 5.65	21.90	981.00900	0.19	15.65
	10150	529.0	55 14.8	49 5.97	19.18	981.00960	0.19	15.24
	10149	529.7	55 14.2	49 6.20	16.53	981.00978	0.17	14.54
	10148	530.5	55 13.5	49 6.30	18.15	981.00968	0.15	14.59
	10147	531.4	55 12.8	49 6.49	47.55	981.00413	0.13	14.52
	10146	532.1	55 12.1	49 6.61	61.82	981.00122	0.12	14.23
	10145	533.0	55 11.8	49 6.88	81.65	980.99739	0.11	13.89
	10144	533.8	55 11.1	49 7.00	71.67	980.99938	0.10	13.73
	10143	534.6	55 10.4	49 7.08	79.15	980.99823	0.10	13.93
	10142	535.4	55 9.7	49 7.16	94.15	980.99532	0.10	13.85
	10141	536.2	55 9.1	49 7.25	115.05	980.99168	0.09	14.17
	10140	536.9	55 8.4	49 7.35	116.75	980.99171	0.09	14.39
	10139	537.7	55 7.8	49 7.30	114.34	980.99254	0.08	14.81
	10138	538.6	55 7.2	49 7.28	100.04	980.99520	0.08	14.69
	10137	539.4	55 6.5	49 7.25	89.97	980.99727	0.07	14.81
K	10136	540.3	55 5.8	49 7.30	91.44	980.99660	0.07	14.36
	10523	541.2	55 5.5	49 7.26	83.42	980.99758	0.06	13.81
	10522	542.0	55 4.8	49 7.09	84.33	980.99754	0.06	14.20
	10521	542.9	55 4.3	49 6.91	87.63	980.99725	0.06	14.83
	10520	543.7	55 3.7	49 6.80	83.87	980.99809	0.06	15.09
	10519	544.5	55 3.3	49 6.51	83.81	980.99833	0.06	15.75
	10518	545.3	55 2.9	49 6.12	87.53	980.99725	0.06	15.99
	10517	546.1	55 2.9	49 5.67	93.06	980.99657	0.06	17.06
	10516	546.9	55 2.5	49 5.35	98.30	980.99582	0.06	17.82
	10515	547.7	55 2.0	49 5.09	105.59	980.99446	0.06	18.28
	10514	548.5	55 1.7	49 4.76	100.92	980.99451	0.06	17.91
	10513	549.3	55 1.6	49 4.37	113.98	980.99249	0.06	19.04
	10512	550.1	55 1.3	49 4.04	117.42	980.99190	0.06	19.62
	10511	550.9	55 0.9	49 3.72	117.39	980.99144	0.06	19.63
	10510	551.7	55 0.7	49 3.36	97.57	980.99498	0.06	19.80
	10509	552.5	55 0.4	49 3.01	112.39	980.99133	0.06	19.59
	10508	553.3	54 59.9	49 2.83	112.15	980.98975	0.06	18.23
	10507	554.1	54 59.4	49 2.64	101.72	980.99001	0.06	16.72
	10506	554.9	54 58.9	49 2.45	91.35	980.99119	0.06	16.15

TABLE SYMBOLS EXPLAINED IN SECTION A3.2.

... continued

TABLE A3.1, CONTINUED

LOC	STN	C PAB (KM)	LONGITUDE (DEG MIN)	LATITUDE (DEG MIN)	ELEV (M)	G OBS (GAL)	TERC (MGAL)	G BOUG (MGAL)
	10505	555.7	54 58.4	49 2.27	89.67	980.99084	0.06	15.73
	10504	556.5	54 57.9	49 2.09	96.41	980.98872	0.06	15.21
	10503	557.3	54 57.5	49 1.87	96.87	980.98788	0.06	14.79
	10502	558.1	54 56.9	49 1.65	82.62	980.99056	0.06	14.99
	10501	558.9	54 56.4	49 1.43	78.75	980.99113	0.06	15.13
	10500	559.7	54 55.9	49 1.21	75.27	980.99101	0.06	14.65
	10499	560.6	54 55.5	49 0.93	65.27	980.99206	0.06	14.15
	10498	561.4	54 55.1	49 0.63	56.67	980.99231	0.06	13.16
	10497	562.2	54 54.7	49 0.35	56.42	980.99068	0.06	11.90
	10496	563.0	54 54.3	49 0.04	58.99	980.98959	0.06	11.77
	10495	563.8	54 53.8	48 59.85	58.32	980.98992	0.06	12.25
	10494	564.6	54 53.1	48 59.87	43.22	980.99329	0.06	12.62
	10493	565.4	54 52.5	48 59.86	33.76	980.99501	0.06	12.50
L	10492	566.2	54 52.0	48 59.78	31.23	980.99480	0.06	11.91
	10491	567.0	54 51.6	48 59.52	58.71	980.98936	0.06	12.26
	10490	567.8	54 51.3	48 59.15	92.45	980.98271	0.06	12.80
	10489	568.6	54 51.0	48 58.78	94.31	980.98204	0.06	13.05
	10488	569.2	54 50.9	48 58.43	81.95	980.98378	0.06	12.88
	10487	570.2	54 50.6	48 58.06	85.19	980.98284	0.06	13.13
	10486	571.0	54 50.1	48 57.91	77.20	980.98458	0.06	13.52
	10485	571.8	54 49.6	48 57.76	83.54	980.98203	0.06	12.44
	10484	572.7	54 49.0	48 57.70	100.99	980.97959	0.06	13.52
	10483	573.5	54 48.5	48 57.85	108.79	980.97862	0.06	13.87
	10482	574.3	54 48.0	48 57.87	100.44	980.98024	0.06	13.81
	10481	575.1	54 47.3	48 57.78	94.00	980.98059	0.06	13.03
	10480	575.9	54 46.7	48 57.75	78.17	980.98323	0.06	12.60
	10479	576.7	54 46.1	48 57.62	55.69	980.98600	0.06	11.14
	10478	577.5	54 45.5	48 57.49	65.45	980.98300	0.06	10.26
	10477	578.3	54 44.9	48 57.39	79.85	980.97834	0.06	8.58
	10476	579.1	54 44.4	48 57.41	78.69	980.98008	0.07	10.07
	10475	579.9	54 43.9	48 57.57	82.81	980.98166	0.07	12.22
	10474	580.8	54 43.4	48 57.91	87.35	980.98135	0.08	12.31
	10473	581.6	54 42.9	48 58.13	83.42	980.98179	0.08	11.65
	10472	582.4	54 42.3	48 58.04	88.48	980.97788	0.09	8.88
	10471	583.2	54 41.7	48 57.91	81.86	980.97714	0.09	7.03

TABLE SYMBOLS EXPLAINED IN SECTION A3.2.

... continued

TABLE A3.1, CONTINUED

LOC	STN	D PAB (KM)	LONGITUDE (DEG MIN)	LATITUDE (DEG MIN)	ELEV (M)	G OBS (GAL)	TERC (MGAL)	G BOUG (MGAL)
	10470	584.0	54 40.9	48 57.87	115.87	980.96905	0.10	5.70
	10469	584.8	54 40.3	48 57.80	133.16	980.96432	0.10	4.47
	10468	585.7	54 39.6	48 57.72	119.47	980.96564	0.11	3.23
	10467	586.5	54 39.0	48 57.67	117.55	980.96492	0.11	2.21
	10466	587.4	54 38.4	48 57.61	134.60	980.96095	0.12	1.69
	10465	588.2	54 37.9	48 57.52	139.35	980.95882	0.12	0.63
	10464	589.0	54 37.5	48 57.26	124.90	980.96085	0.12	0.20
M	10463	589.8	54 37.0	48 57.00	124.01	980.96022	0.12	-0.21
	10565	590.6	54 36.8	48 56.87	119.53	980.96074	0.12	-0.38
	10564	591.4	54 36.4	48 56.65	112.42	980.96191	0.12	-0.28
	10563	592.2	54 35.9	48 56.37	111.66	980.96183	0.12	-0.09
	10562	593.0	54 35.5	48 56.09	113.22	980.96067	0.12	-0.53
	10561	593.8	54 35.0	48 55.80	125.26	980.95835	0.12	-0.05
	10560	594.6	54 34.8	48 55.50	126.27	980.95794	0.12	0.19
	10559	595.4	54 34.5	48 55.20	115.17	980.95934	0.12	-0.15
	10558	596.2	54 34.0	48 55.00	111.66	980.96080	0.12	0.92
	10557	597.0	54 33.6	48 54.62	111.81	980.96003	0.12	0.75
	10556	597.8	54 33.3	48 54.26	114.37	980.95893	0.12	0.69
	10555	598.6	54 32.9	48 53.96	123.52	980.95654	0.12	0.54
	10554	599.4	54 32.4	48 53.70	130.63	980.95470	0.12	0.49
	10553	600.2	54 31.9	48 53.51	124.87	980.95546	0.12	0.40
	10552	601.0	54 31.3	48 53.35	105.53	980.95923	0.12	0.60
	10551	601.8	54 30.8	48 53.24	90.01	980.96233	0.12	0.81
	10550	602.6	54 30.2	48 53.26	92.17	980.96154	0.12	0.42
	10549	603.4	54 29.7	48 53.21	91.96	980.96131	0.12	0.22
	10548	604.2	54 29.0	48 53.10	82.38	980.96258	0.12	-0.23
	10547	605.1	54 28.5	48 53.17	69.54	980.96507	0.12	-0.37
	10546	605.9	54 27.9	48 53.33	42.88	980.97080	0.12	-0.12
	10545	606.7	54 27.2	48 53.46	37.06	980.97203	0.12	-0.23
	10544	607.5	54 26.6	48 53.41	40.96	980.97107	0.12	-0.35
	10543	608.3	54 26.0	48 53.34	37.06	980.97174	0.12	-0.34
	10542	609.1	54 25.4	48 53.20	40.35	980.97083	0.12	-0.39
	10541	609.9	54 24.9	48 53.04	34.62	980.97142	0.12	-0.69
	10540	610.7	54 24.4	48 52.70	51.15	980.96673	0.12	-1.62
	10539	611.5	54 23.9	48 52.50	66.52	980.96271	0.12	-2.32

TABLE SYMBOLS EXPLAINED IN SECTION A3.2.

... continued

TABLE A3.1, CONTINUED

LOC	STN	C PAB (KM)	LONGITUDE (DEG MIN)	LATITUDE (DEG MIN)	ELEV (M)	G OBS (GAL)	TERC (MGAL)	G BOUG (MGAL)
	10538	612.3	54 23.2	48 52.39	80.06	980.95933	0.12	-2.87
	10537	613.1	54 22.9	48 52.04	73.84	980.95828	0.12	-4.63
	10536	613.9	54 22.4	48 51.76	59.69	980.95937	0.12	-5.90
	10535	614.7	54 22.0	48 51.43	30.04	980.96321	0.12	-7.40
	10534	615.5	54 21.7	48 51.11	68.41	980.95523	0.12	-7.36
	10533	616.3	54 21.4	48 50.74	97.66	980.94891	0.12	-7.37
	10532	617.1	54 21.0	48 50.39	123.16	980.94347	0.12	-7.27
	10531	617.9	54 20.6	48 50.07	126.24	980.94284	0.12	-6.82
	10530	618.7	54 20.3	48 49.76	124.71	980.94339	0.12	-6.11
	10529	619.5	54 19.9	48 49.40	136.46	980.94205	0.12	-4.60
	10528	620.3	54 19.6	48 49.06	145.18	980.94353	0.12	-0.90
	10527	621.1	54 19.3	48 48.74	96.50	980.95461	0.12	1.09
	10526	622.0	54 18.8	48 48.52	56.30	980.96342	0.14	2.34
	10525	622.8	54 18.3	48 48.39	49.90	980.96554	0.12	3.37
	10524	623.6	54 17.8	48 48.26	51.48	980.96498	0.12	3.32
	10603	624.4	54 17.3	48 48.13	80.34	980.95967	0.13	3.89
	10601	625.8	54 16.3	48 47.87	57.37	980.96435	0.15	4.46
	10600	626.6	54 16.0	48 47.65	57.37	980.96330	0.16	3.74
	10599	627.4	54 15.8	48 47.26	58.35	980.96258	0.17	3.81
	10598	628.2	54 15.7	48 46.91	68.32	980.96062	0.18	4.34
	10597	629.0	54 15.1	48 46.87	88.27	980.95640	0.19	4.12
	10596	629.9	54 14.6	48 46.80	97.33	980.95383	0.20	3.44
	10595	630.6	54 14.1	48 46.52	111.45	980.94975	0.20	2.56
	10594	631.5	54 14.2	48 46.13	92.60	980.95216	0.20	1.84
N	10593	632.3	54 14.4	48 45.78	70.49	980.95607	0.19	1.92
	10592	633.1	54 14.4	48 45.40	74.21	980.95442	0.18	1.55
	10591	633.9	54 14.5	48 44.91	42.46	980.96023	0.17	1.84
	10590	634.7	54 14.5	48 44.50	10.52	980.96509	0.16	1.02
	10589	635.4	54 14.6	48 44.10	12.81	980.96308	0.15	0.05
	10588	636.2	54 14.1	48 44.13	8.23	980.96231	0.15	-1.67
	10587	637.0	54 13.5	48 44.26	6.62	980.96257	0.15	-1.92
	10586	637.8	54 12.9	48 44.39	10.98	980.96255	0.15	-1.28
	10585	638.6	54 12.3	48 44.50	24.74	980.95979	0.15	-1.49
	10584	639.4	54 11.7	48 44.43	33.06	980.95891	0.15	-0.63
	10583	640.2	54 11.1	48 44.30	25.47	980.96168	0.15	0.84

TABLE SYMBOLS EXPLAINED IN SECTION A3.2.

... continued

TABLE A3.1, CONTINUED

LOC	STN	D PAB (KM)	LONGITUDE (DEG MIN)	LATITUDE (DEG MIN)	ELEV (M)	G OBS (GAL)	TERC (MGAL)	G BOUG (MGAL)
	10582	641.0	54 10.7	48 44.06	21.96	980.96306	0.15	1.89
	10581	641.8	54 10.3	48 43.78	37.33	980.96045	0.15	2.72
	10580	642.6	54 9.9	48 43.52	39.16	980.96168	0.15	4.70
	10579	643.4	54 9.5	48 43.22	33.61	980.96189	0.15	4.26
	10578	644.2	54 9.0	48 42.89	20.05	980.96250	0.15	3.88
	10577	645.0	54 8.7	48 42.59	35.38	980.96164	0.15	5.30
	10576	645.9	54 8.1	48 42.39	51.91	980.95970	0.15	6.91
	10575	646.7	54 7.5	48 42.30	57.64	980.96017	0.15	8.64
	10574	647.5	54 7.0	48 42.20	72.01	980.95790	0.15	9.35
	10573	648.3	54 6.6	48 42.00	83.57	980.95730	0.15	11.32
	10572	649.1	54 6.6	48 41.61	87.11	980.95563	0.15	10.93
	10571	649.9	54 6.6	48 41.14	117.42	980.95041	0.15	12.38
	10570	650.7	54 6.4	48 40.80	144.72	980.94521	0.15	13.05
	10569	651.5	54 5.9	48 40.48	143.47	980.94680	0.15	14.88
	10568	652.3	54 5.4	48 40.24	146.40	980.94783	0.15	16.84
	10567	653.1	54 4.8	48 40.07	128.10	980.95313	0.15	18.79
	11158	654.0	54 3.8	48 39.83	77.59	980.96197	0.15	18.06
	11157	654.9	54 3.3	48 39.43	50.93	980.96769	0.15	19.13
	11156	655.7	54 3.1	48 39.09	40.44	980.97008	0.15	19.96
	11155	656.6	54 2.5	48 38.70	17.38	980.97499	0.15	20.92
	11154	657.5	54 2.1	48 38.35	10.06	980.97531	0.15	20.32
	11153	658.5	54 1.5	48 38.09	18.30	980.97472	0.15	21.74
	11152	659.5	54 1.0	48 38.22	26.32	980.97553	0.15	23.93
	11151	660.3	54 0.5	48 38.43	56.42	980.97218	0.15	26.19
	11150	661.2	53 59.8	48 38.43	65.94	980.97171	0.15	27.59
	11149	662.0	53 59.1	48 38.43	89.67	980.96931	0.15	29.86
	11148	662.8	53 58.5	48 38.43	91.96	980.97082	0.15	31.82
P	11147	663.6	53 57.8	48 38.28	74.21	980.97378	0.15	31.51
	11146	664.4	53 57.8	48 37.89	44.29	980.97835	0.15	30.78
	11145	665.3	53 58.2	48 37.48	21.69	980.98088	0.15	29.48
	11144	666.1	53 58.5	48 37.04	35.53	980.97698	0.15	28.96
	11143	666.8	53 58.6	48 36.76	12.20	980.97957	0.15	27.38
	11142	667.7	53 58.5	48 36.17	66.58	980.96606	0.15	25.45
	11141	668.5	53 58.4	48 35.70	80.82	980.96237	0.15	25.26
Q	11140	669.3	53 58.2	48 35.30	68.69	980.96581	0.15	26.91

TABLE SYMBOLS EXPLAINED IN SECTION A3.2.

... continued

TABLE A3.1, CONTINUED

LOC STN	C PAB (KM)	LONGITUDE (DEG MIN)	LATITUDE (DEG MIN)	ELEV (M)	G OBS (GAL)	TERC (MGAL)	G BOUG (MGAL)
11139	670.2	53 58.0	48 34.87	45.26	980.96963	0.15	26.76
11138	670.9	53 58.3	48 34.50	33.70	980.97119	0.15	26.60
11137	671.8	53 58.6	48 34.43	84.79	980.95833	0.15	23.90
11136	672.6	53 58.8	48 33.67	87.35	980.95690	0.15	24.11
11135	673.3	53 58.9	48 33.35	96.88	980.95314	0.15	23.09
11134	674.3	53 59.1	48 32.85	77.93	980.95549	0.15	22.07
11133	675.1	53 59.4	48 32.39	27.45	980.96294	0.14	20.26
11132	676.0	53 59.7	48 32.00	35.81	980.96021	0.14	19.76
11131	676.9	54 0.0	48 31.65	38.40	980.95869	0.14	19.27
11130	677.7	54 0.1	48 31.22	32.97	980.95859	0.14	18.75
11129	678.6	53 59.9	48 30.70	81.56	980.94847	0.14	18.96
11128	679.4	53 59.6	48 30.03	107.18	980.94254	0.14	19.07
11127	680.3	53 59.6	48 29.94	127.67	980.93761	0.14	18.31
11126	681.1	53 59.6	48 29.54	113.95	980.93942	0.14	18.02
11125	682.1	53 59.8	48 29.13	101.53	980.94013	0.14	16.90
11124	682.9	54 0.0	48 28.70	93.18	980.94095	0.14	16.72
11123	683.8	54 0.1	48 28.26	69.66	980.94350	0.14	15.30
11122	684.6	54 0.3	48 27.89	71.43	980.94191	0.14	14.61
11121	685.4	54 0.6	48 27.50	98.79	980.93623	0.14	14.89
11120	686.3	54 0.9	48 27.11	102.14	980.93528	0.14	15.19
11119	687.1	54 1.4	48 26.76	67.10	980.94300	0.14	16.54
11118	687.9	54 1.7	48 26.43	73.72	980.94177	0.14	17.10
11117	688.6	54 2.0	48 26.15	86.19	980.93896	0.14	17.16
11116	689.3	54 2.3	48 25.87	112.30	980.93370	0.14	17.46
11115	690.0	54 2.6	48 25.63	108.67	980.93397	0.14	17.37
11114	690.8	54 3.1	48 25.35	106.14	980.93538	0.14	18.70
11113	691.6	54 3.6	48 25.30	131.76	980.92989	0.14	18.33
11112	692.4	54 4.3	48 25.30	138.90	980.92792	0.14	17.76
11111	693.2	54 4.9	48 25.26	114.86	980.93246	0.14	17.63
11110	694.0	54 5.4	48 25.30	84.42	980.93776	0.14	16.89
11109	694.8	54 5.9	48 25.43	42.82	980.94478	0.14	15.53
111C8	695.5	54 6.0	48 25.57	17.96	980.94957	0.14	15.22
111C7	696.4	54 7.0	48 25.78	29.58	980.94717	0.14	14.79
111C6	697.2	54 7.5	48 25.57	34.56	980.94516	0.14	14.07
111C5	697.8	54 7.9	48 25.39	32.18	980.94474	0.14	13.45

TABLE SYMBOLS EXPLAINED IN SECTION A3.2.

... continued

TABLE A3.1, CONTINUED

LOC	STN	C PAB (KM)	LONGITUDE (DEG MIN)	LATITUDE (DEG MIN)	ELEV (M)	G OBS (GAL)	TERC (MGAL)	G BOUG (MGAL)
	11104	698.5	54 8.2	48 25.11	26.93	980.94474	0.14	12.84
	11103	699.3	54 8.5	48 24.72	10.31	980.94724	0.14	12.65
	11102	700.1	54 8.9	48 24.39	11.89	980.94636	0.14	12.58
	11101	700.9	54 9.3	48 24.04	14.82	980.94557	0.14	12.89
	11100	701.7	54 9.7	48 23.74	16.96	980.94463	0.14	12.82
	11099	702.4	54 10.2	48 23.52	17.69	980.94379	0.14	12.45
R	11098	703.1	54 10.8	48 23.52	16.07	980.94323	0.14	11.57
	11097	704.1	54 11.4	48 23.70	25.47	980.94034	0.14	10.26
	11096	705.0	54 12.1	48 23.70	27.75	980.93987	0.14	10.24
	11095	705.9	54 12.4	48 23.26	51.00	980.93515	0.14	10.75
	11094	706.8	54 12.3	48 22.83	45.23	980.93699	0.14	12.10
	11093	707.7	54 11.7	48 22.72	14.40	980.94317	0.14	12.38
	11092	708.5	54 11.1	48 22.48	32.09	980.94033	0.14	13.38
	11091	709.3	54 10.6	48 22.13	49.96	980.93717	0.14	14.25
	11090	710.2	54 10.3	48 21.67	42.36	980.93858	0.14	14.86
	11089	711.0	54 10.4	48 21.30	26.78	980.94138	0.14	15.15
	11088	711.8	54 10.5	48 20.87	39.59	980.93830	0.14	15.23
	11087	712.6	54 10.6	48 20.48	60.51	980.93329	0.14	14.92
	11086	713.5	54 10.5	48 20.04	73.20	980.92985	0.14	14.63
	11085	714.3	54 10.5	48 19.61	48.28	980.93381	0.15	14.34
	11084	715.1	54 10.5	48 19.24	38.52	980.93501	0.15	14.18
	11083	715.9	54 10.5	48 18.87	12.26	980.93994	0.16	14.50
	11082	716.7	54 10.5	48 18.41	17.26	980.93897	0.18	15.22
	11081	717.6	54 10.8	48 18.00	36.11	980.93442	0.20	15.02
	11080	718.3	54 10.8	48 17.63	35.72	980.93350	0.18	14.55
	11079	719.1	54 10.8	48 17.22	49.71	980.93028	0.16	14.68
	11078	719.8	54 10.5	48 16.87	59.32	980.92799	0.15	14.79
	11077	720.6	54 10.0	48 16.87	98.27	980.92140	0.14	15.85
	11076	721.4	54 9.5	48 16.96	111.39	980.91999	0.14	16.89
	11075	722.1	54 8.8	48 16.76	112.85	980.91997	0.14	17.46
	11074	722.9	54 8.4	48 16.57	108.24	980.91953	0.14	16.39
	11073	723.7	54 7.8	48 16.35	111.17	980.91884	0.14	16.61
	11072	724.6	54 7.4	48 16.09	130.30	980.91383	0.14	15.75
	11071	725.4	54 6.8	48 16.83	142.07	980.91051	0.14	13.64
	11070	726.2	54 6.1	48 16.63	148.11	980.90751	0.14	12.13

TABLE SYMBOLS EXPLAINED IN SECTION A3.2.

... continued

TABLE A3.1, CONTINUED

LOC	STN	C PAB (KM)	LONGITUDE (DEG MIN)	LATITUDE (DEG MIN)	ELEV (M)	G OBS (GAL)	TERC (MGAL)	G BOUG (MGAL)
	11C69	727.C	54 5.5	48 16.43	154.79	980.90341	0.14	9.64
	11C68	727.9	54 5.0	48 16.09	154.21	980.90225	0.14	8.87
	11C67	728.7	54 4.4	48 14.65	133.19	980.90493	0.14	9.57
	11C66	729.5	54 4.0	48 14.35	104.43	980.90929	0.16	8.74
	11C65	730.4	54 3.6	48 13.96	71.74	980.91451	0.20	8.16
	11C64	731.2	54 3.3	48 13.61	85.00	980.91095	0.22	7.75
	11C63	732.0	54 2.9	48 13.26	63.65	980.91352	0.24	6.66
	11C62	732.8	54 2.6	48 12.87	53.22	980.91359	0.26	5.28
	11C61	733.6	54 2.3	48 12.52	56.27	980.91210	0.28	4.94
	11C60	734.3	54 1.9	48 12.22	60.24	980.91039	0.30	4.48
	11C59	735.1	54 1.6	48 11.83	63.56	980.90862	0.30	3.94
	11C58	735.9	54 1.6	48 11.37	101.29	980.90223	0.28	5.64
	11C57	736.7	54 1.2	48 11.02	92.96	980.90486	0.25	7.13
	11C56	737.7	54 0.8	48 10.61	109.07	980.90130	0.20	7.30
	11C55	738.5	54 0.3	48 10.26	120.47	980.89905	0.20	7.82
	11C54	739.4	53 59.9	48 9.96	91.01	980.90312	0.20	6.54
	11C53	740.0	53 59.7	48 9.74	86.56	980.90385	0.20	6.72
	11C52	740.8	53 59.3	48 9.39	50.20	980.90924	0.20	5.49
	11C51	741.7	53 58.8	48 9.09	30.96	980.91191	0.20	4.82
	11C50	742.5	53 58.3	48 8.91	15.74	980.91349	0.20	3.67
	10731	743.5	53 57.5	48 8.70	55.27	980.90588	0.20	4.15
	10730	744.3	53 56.8	48 8.65	56.12	980.90281	0.20	1.33
	10729	745.1	53 56.6	48 8.26	29.13	980.90577	0.25	-0.39
	10728	746.0	53 56.2	48 7.91	50.60	980.89943	0.30	-1.93
	10727	746.8	53 55.9	48 7.52	71.80	980.89581	0.30	-0.80
	10726	747.5	53 55.9	48 7.09	56.46	980.89960	0.30	0.62
	10725	748.3	53 56.0	48 6.70	85.89	980.89378	0.30	1.17
	10724	749.1	53 56.0	48 6.28	79.18	980.89421	0.30	0.91
	10723	749.9	53 56.4	48 6.00	50.45	980.89977	0.30	1.24
S	10722	750.8	53 56.8	48 5.85	15.43	980.90725	0.30	2.05
	10721	751.6	53 56.7	48 5.59	42.55	980.90099	0.35	1.57
	10720	752.2	53 56.6	48 5.26	53.71	980.89800	0.30	1.22
	10719	752.8	53 56.5	48 4.96	44.71	980.89908	0.30	0.98
	10718	753.4	53 56.4	48 4.65	34.56	980.90024	0.30	0.60
	10717	754.0	53 56.2	48 4.35	23.09	980.90182	0.30	0.37

TABLE SYMBOLS EXPLAINED IN SECTION A3.2.

... continued

TABLE A3.1, CONTINUED

LOC	STN	C PAB (KM)	LONGITUDE (DEG MIN)	LATITUDE (DEG MIN)	ELEV (M)	G OBS (GAL)	TERC (MGAL)	G BOUG (MGAL)
	1C716	754.9	53 56.0	48 3.87	14.79	980.90178	0.40	-0.48
	1C715	755.9	53 55.9	48 3.35	22.17	980.89862	0.50	-1.31
	10714	756.7	53 55.9	48 2.96	28.82	980.89728	0.50	-0.76
	1C713	757.4	53 55.9	48 2.61	40.75	980.89424	0.40	-1.03
	1C712	758.1	53 56.0	48 2.26	50.87	980.89235	0.30	-0.50
	1C711	758.8	53 56.2	48 1.96	58.56	980.89139	0.28	0.48
	1C71C	759.3	53 56.5	48 1.83	42.30	980.89580	0.26	1.87
	107C9	760.0	53 57.0	48 1.93	33.58	980.89904	0.24	3.22
	1C7C8	760.7	53 57.5	48 1.87	15.34	980.90466	0.22	5.32
	1C7C7	761.5	53 57.8	48 1.70	30.93	980.90139	0.20	5.35
	1C7C6	762.4	53 57.7	48 1.22	63.56	980.89640	0.18	7.48
	1C705	763.3	53 57.3	48 0.78	113.31	980.88431	0.16	5.82
	1C7C4	763.7	53 57.3	48 0.61	121.08	980.88201	0.14	5.28
	1C7C3	764.5	53 57.3	48 0.17	124.93	980.88068	0.12	5.34
	1C7C2	765.3	53 57.4	47 59.76	132.98	980.87764	0.10	4.48
	107C1	766.1	53 57.5	47 59.33	112.91	98C.88039	0.10	3.93
	1C7CC	766.8	53 57.6	47 58.92	110.14	980.88015	0.10	3.76
T	1C699	767.9	53 57.8	47 58.35	115.84	980.87846	0.10	4.04
	11CC0	768.6	53 57.7	47 57.96	97.60	980.88128	0.10	3.86
	11C01	769.5	53 57.6	47 57.61	85.40	980.88250	0.10	3.20
	11CC2	770.3	53 57.3	47 57.09	74.11	980.88341	0.10	2.67
	11C03	770.9	53 57.1	47 56.83	67.40	980.88406	0.10	2.39
	11C04	771.7	53 57.0	47 56.48	67.71	980.88225	0.10	1.16
	11C05	772.6	53 57.0	47 56.09	95.16	980.87627	0.10	1.17
	11C06	773.2	53 57.1	47 55.78	79.30	980.87862	0.10	0.86
	11CC7	774.C	53 56.9	47 55.30	59.78	980.88098	0.10	0.10
	11CC8	774.8	53 5e.9	47 54.91	69.84	980.8787C	0.10	0.38
	11CC9	775.8	53 57.0	47 54.39	64.66	980.87942	0.10	0.86
	11C10	776.5	53 57.0	47 54.07	61.61	980.87920	0.10	0.52
	11C11	777.4	53 57.0	47 53.59	58.25	980.87937	0.10	0.75
	11C12	778.2	53 57.0	47 53.15	70.45	980.87618	0.10	0.62
	11C13	779.1	53 57.1	47 52.70	66.79	980.87713	0.10	1.52
	11C14	779.8	53 57.3	47 52.35	59.17	980.87731	0.10	0.73
	11C15	780.6	53 57.5	47 51.93	42.70	980.88022	0.10	1.03
U	11C16	781.4	53 57.7	47 51.46	70.76	980.87464	0.10	1.67

TABLE SYMBOLS EXPLAINED IN SECTION A3.2.

APPENDIX 4

BAROMETRIC ALTIMETRY

A4.1 Field equipment.

Three Type FA-181-4000 altimeters, manufactured by Wallace & Tiernan, Inc., were used in the altimetric determinations, and a fourth, Type FA-181-5000 by the same manufacturer, was read at base as a check on possible base altimeter malfunctions. Basically these are aneroid barometers, scaled directly in feet; calibrated for 10°C atmospheric temperature and 0% relative humidity; and so designed that equal pointer deflections correspond to equal changes in elevation. Table A4.1 contains the manufacturer's specifications for these instruments. Because these altimeters give elevation differences, they are used in conjunction with a network of bases of accurately known elevation (Section 2.2.1).

Temperature was measured with stationary mercury thermometers, and relative humidity with a wet and dry bulb hygrometer for the work west of Grand Falls, and a sling psychrometer for the remainder. These instruments had scale graduations and readability of 0.5°C and 0.2°C, respectively.

A4.2 One-base method of barometric altimetry.

Gravity stations were located between altimetry bases and visited

following the pattern illustrated in Figure A4.1. The lateral separation of adjacent bases was, on the average, about 12 km. The one-base method (Kissam, 1945) yielded an elevation value for each station visit. The majority of stations were occupied at least twice, and the accepted station elevation was the weighted mean of the individual visit determinations (Section A4.5).

At the beginning and end of a base occupation, at times t_1 and t_n, respectively, the base and roving altimeters were read together, giving values R_{b1} and R_{bn} for the base, and values R_{r1} and R_{rn} for the two roving instruments (averaged). The roving altimeters were referenced to the one at base by means of the index difference, D, given at time t by

$$D = (R_{b1} - R_{r1}) + \frac{(R_{bn} - R_{rn}) - (R_{b1} - R_{r1})}{(t_n - t_1)} (t - t_1) \qquad \text{(A4.1)}$$

Each station visit consisted of three readings at one-minute intervals on each roving altimeter, yielding for these six values an average, R_s. The index difference, D, at the average time, t, of the station readings was added to R_s to give an adjusted reading R_s'. Two stationary thermometers were also read at each station visited and their values averaged. Because of accidental breakages of psychrometers and hygrometers, relative humidity was recorded at only a few of the stations visited.

Base altimeter, thermometer, and psychrometer (or hygrometer) readings were recorded at five-minute intervals from times t_1 to t_n,

and smoothed by means of running averages (Section A4.2).

Where the times of base and station elevation readings did not coincide, base values at the time t of the station occupation were obtained by linear interpolation between those immediately before and after. Thus, for base altimeter values R_{bj} and R_{bk} at times t_j and t_k, just before and after t, respectively, the base value, R_b, at time t is given by

$$R_b = R_{bj} + \frac{R_{bk} - R_{bj}}{t_k - t_j} (t - t_j) \qquad \text{(A4.2)}$$

The altimeter difference, ΔR, between base and station is then

$$\Delta R = R_s' - R_b \qquad \text{(A4.3)}$$

The base and station temperatures for time t are averaged and combined with the base relative humidity to obtain, from a calibration chart provided with the altimeters, a factor, K, which corrects ΔR for non-calibration atmospheric conditions, giving the initial estimate of elevation difference, Δh_a.

$$\Delta h_a = K \Delta R \qquad \text{(A4.4)}$$

Δh_a is further corrected on the basis of field calibration equation A4.7, yielding Δh_c, which is then added to the base elevation, h_b, to give the station elevation, h_i.

$$h_i = h_b + \Delta h_c \qquad \text{(A4.5)}$$

A4.3 Smoothing base readings.

Base altimeter, thermometer, and hygrometer (or psychrometer) readings were smoothed by means of running averages, in which a value at time t was replaced, with the exception of the first and last readings, by the average of values at t-5 minutes, t, and t+5 minutes.

Initially, 120 barometric determinations, first with base data smoothing and then without smoothing, were made at 50 stations of known elevation. A "known" elevation is defined as one obtained by precise (spirit) levelling. A comparison of these techniques is obtained from a quantity, M, defined as the difference of two magnitudes by

$$M = |h_n - h_k| - |h_s - h_k| \qquad (A4.6)$$

where h_k is a known elevation, and h_s and h_n are the values obtained with and without base smoothing, respectively. The frequency distribution of M, given in Figure A4.2, shows slightly better results for smoothing of base values.

A4.4 Altimetry field calibration.

A field check of the altimeter scale calibration is complicated by the following factors: (i) the thermometers, hygrometer, and psychrometer were not checked against any absolute standard during the survey; (ii) the thermometers were read with their bulbs approximately 10 cm above ground, which may have been too close; and (iii) the altimeters

respond to atmospheric disturbances as well as to elevation changes. Thus any field calibration is essentially one of the whole apparatus, and may also include systematic atmospheric effects.

Table A4.2 gives 39 known elevation differences, $\Delta h'_c$, and the corresponding barometric determinations, $\Delta h'_a$. A regression line

$$\Delta h_c = A\ (\Delta h_a) + B \qquad (A4.7)$$

was fitted to this data by the method of least squares, as described by Topping (1957). Values of A = 0.996 and B = -0.41 m, with standard deviations $\sigma_A = \pm 0.005$ and $\sigma_B = \pm 0.23$ m, respectively, were obtained.

The departure of the slope from unity may be explained by a possible 1°C systematic temperature error; or, along with the offset of -0.41 m, it may be due to altimeter defects or miscalibration. A contribution from systematic weather patterns may also be present. LaFlamme and Pelletier[1], noticing similar altimeter behaviour in a laboratory check between comparable altimeters, attributed it to a "creep" in the altimeter needle linkage system.

A4.5 Weighting station elevation determinations.

The majority of stations were visited at least twice, usually under different atmospheric conditions and from different occupied bases; thus

---

[1] LaFlamme & Pelletier, Precise Barometric Leveling in Northern Quebec With the Help of Helicopters; paper presented before the Montreal Section, Canadian Institute of Surveying, December 11, 1957.

the elevation values for a given station tend to be associated with different errors. A final estimate of station elevation was obtained as a weighted mean of separate observations. Were sufficient statistics available, each determination would have been given a weight inversely proportional to the square of its standard deviation, as described in standard references (e.g., Beers, 1957). Instead, in this project, each elevation determination, h_i, was assigned a weight, w_i, which was proportional to the reciprocal of an error, d_i, not the standard deviation.

The error, d_i, is obtained from the larger of the differences, d_{max}, between the known and barometrically determined elevations at the second base visited at the beginning and end of each run. This base was at the opposite end of the traverse from the one occupied during station visits. Each stretch of stations was divided into three approximately equal sections, and values of d_i equal to (1/3) d_{max}, (1/2) d_{max}, and d_{max} were assigned to the stations in the sections near the occupied base, in the middle, and near the unoccupied base, respectively. This division, though somewhat arbitrary, is based on the assumption that the main errors are due to the lateral pressure variations associated with weather patterns, and that this variation is uniform.

The arithmetic mean of N determinations then gave the station elevation, h, as

$$h = \frac{\sum_{i=1}^{N} h_i/d_i^2}{\sum_{i=1}^{N} 1/d_i^2} \qquad \text{(A4.8)}$$

A comparison, based on a sample of 14 stations, of this weighting scheme with some others is given in Table A4.3, showing it to be superior

Most stations visited only once were situated approximately midway, in space and time, between two stations each of which was visited twice. As an example, consider the correction to the reading at station 5 in Figure A4.1. If h_4', h_5', and h_6' are the determinations at stations 4, 5, and 6 at 0910 hrs, 0916 hrs, and 0923 hrs, respectively; and h_4 and h_6 the weighted means at stations 4 and 6; then the corrected elevation at station 5 is given by

$$h_5 = h_5' + \frac{(h_4 - h_4') + (h_6 - h_6')}{2} \qquad \text{(A4.9)}$$

A4.6 Barometric altimetry error estimates.

Error uncertainty associated with pressure variations caused by changes in the weather systems prohibits the calculation of individual station elevation errors. A simple measure of elevation accuracy may, however, be obtained from a comparison of known station elevations, h_k, with the barometric determinations, h_i (equation A4.5). Let z be the difference given by

$$z = h_i - h_k \qquad \text{(A4.10)}$$

Table A4.4 gives the distribution of z values for 120 determinations at 50 stations (same stations as used in section A4.3), and yields a mean of zero with a standard deviation about the mean of ±1.6 m. The actual

standard deviation associated with the elevation determinations is expected to be less than this for two reasons: (i) the majority of stations were visited twice, making the standard deviation of the mean approximately $1/\sqrt{2}$ of that of an individual determination, and (ii) the majority of stations had a smaller separation between station and base than those used in the sample. The weighted results given in Table A4.3, indicating a standard deviation of ±0.60 m, confirm this conclusion. Standard deviations in barometric elevation determinations have been calculated for the various segments of the traverse, and are shown in Figure 2.2.1.

The modified "one-base" barometric method described in this Appendix represents an improvement over the traditional "one-base" method. The weighting scheme employed (Section A4.5) resulted in a standard deviation which is less than one-half that associated with the unit-weight method (Table A4.3). Systematic errors have been reduced by the field calibration and the smoothing of base data (Sections A4.4 and A4.3, respectively).

Table A4.1 Usage and manufacturer's specifications for survey altimeters.

Unit number	1	2	3	4
Serial number	MM13071	MM13070	MM13069	Wp64242
Usage (normally)	base	roving	roving	base check
Type	FA-181-4000			FA-181-5000
Range	-1000 to +3000 ft			-1000 to +4000 ft
Graduations	5 ft			10 ft
Readability	½ ft			3/4 ft
Sensitivity	1 part in 8000			
Accuracy	1 part in 1000			
Temperature effect	1 part in 3000 per 10°C temperature change			
Scale length	30 in (∿76 cm)			
Dial size	6 in (∿15 cm)			
Manufacturer	Wallace & Tiernan, Inc.			

Table A4.2 Comparison of known[1] elevation differences with barometrically determined differences.

Located between Bases[2]	Located in Section[3]	Known Difference $\Delta h'_c$ (m)	Barometric Difference[4] $\Delta h'_a$ (m)
5033-5030	F - G	0.31	0.52
480K-473K	A - B	1.16	3.36
5028-5030	F - G	1.53	1.83
5028-5033	F - G	1.83	2.38
5035-5037	G - H	3.29	5.40
5037-5040	G - H	3.36	4.67
5060-283K	K - L	4.85	4.91
473K-471K	A - B	6.53	6.16
318K-306K	I - J	7.81	7.08
473K-469K	A - B	8.48	8.17
5056-5057	I - J	8.72	9.42
5022-5029	F - G	8.78	8.78
5007-5008	C - D	10.16	10.92
5021-5023	F - G	12.44	12.41
5034-5035	G - H	12.90	13.79
5005-5006	A - B	12.96	12.81
284K-282K	K - L	13.94	14.24
5071-5072	R - S	15.01	16.90
5028-5032	F - G	16.71	17.96
5027-5022	F - G	18.76	19.70
5030-5034	F - G	23.49	24.61
5021-5024	F - G	24.22	23.52
5028-5031	F - G	24.40	24.67
5034-5036	G - H	25.96	27.02
280K-279K	K - L	27.33	28.00

[1] Obtained by precise (spirit) levelling.

[2] 5000 series numbers are secondary bench-marks; the reminder are geodetic bench-marks.

[3] The letters refer to Figure 1.1.1

[4] $\Delta h'_a$ corresponds to Δh_a given by equation A4.4

Table A4.2, continued [1]

Located between Bases	Located in Section	Known Difference $\Delta h'_c$ (m)	Barometric Difference $\Delta h'_a$ (m)
5057-318K	I - J	32.12	32.42
5073-5075	R - S	34.40	35.56
5022-5028	F - G	35.62	35.90
282K-280K	K - L	39.71	40.63
5040-5043	G - H	39.89	37.15
469K-5005	A - B	43.65	45.96
5070-5071	R - S	53.13	53.89
389K-5021	F - G	54.38	54.32
5021-5026	F - G	54.63	53.47
5021-5025	F - G	64.02	64.81
5072-5073	R - S	80.28	81.25
5021-5022	F - G	85.58	86.25
279K-5065	L - M	110.59	110.26
5065-259K	M - N	134.69	137.40

[1] See footnotes on first page of table.

Table A4.3 Comparison of station elevation weighting schemes.[1]

Station Number	Known Elevation h_k	Elevation comparison for values obtained with weights w_i = unity (h_k-h_m)	$\alpha\, 1/d_{max}^2$ (h_k-h_p)	$\alpha\, 1/d_i$ (h_k-h_w)	$\alpha\, 1/d_i^2$ (h_k-h)
5003	8.39	0.52	-0.10	0.17	-0.10
5006	37.12	-1.78	-1.57	-1.12	-0.78
5008	161.99	1.14	1.79	0.85	0.63
5011	35.96	-3.16	0.28	-0.05	0.49
5033	112.85	-0.05	-0.05	0.04	0.09
5039	98.09	0.90	0.90	0.90	0.90
5038	113.80	1.27	1.27	1.27	1.27
5041	110.38	0.11	0.56	0.11	0.11
5042	107.02	-1.48	-0.40	-0.40	-0.16
5045	104.22	1.24	0.64	0.24	-0.16
5044	84.91	0.49	-0.03	0.22	-0.03
5047	69.97	-0.56	0.35	0.10	0.35
5074	110.29	-0.35	-0.21	-0.28	-0.21
5076	55.63	-2.27	-1.96	-2.14	-1.96
Arithmetic Mean		-0.28	0.11	0.01	0.01
Standard Deviation		±1.43	±1.00	±0.89	±0.60

[1] h_m, h_p, h_w, and h are elevations obtained barometrically using the corresponding weighting schemes shown; h_k obtained by precise (spirit) levelling; d_{max}, d_i are maximum and weighted check-in errors, respectively (section A4.5).

Table A4.4 Comparison of known elevations with altimetric determinations.

Barometric determination - known elevation z (m)	Frequency f	$f z^2$ (m^2)
-5.0	1	25
-4.0	3	48
-3.0	2	18
-2.0	9	36
-1.0	25	25
0.0	44	0
1.0	19	19
2.0	9	36
3.0	4	36
4.0	3	48
5.0	1	25
Total	120	316
Mean = 0.0	Standard deviation = ± 1.6 m	

Run	Time (hrs)	Location of altimeters												
		Base 1	Section X				Section Y				Section Z				Base 2
			Station				Station				Station				
			1	2	3	4	5	6	7	8	9	10	11	12	
1	0800	A BC													
	0825														BC
	0850	A read at 5-minute intervals	BC												
	0855			BC											
	0902				BC										
	0910					BC									
	0916						BC								
	0923							BC							
	0930								BC						
	0940										BC				
	0948												BC		
	1000														BC
	1030	A BC													
2	1115														A BC
	1140	BC													
	1148			BC											
	1157					BC									
	1205							BC							
	1210								BC						
	1215									BC					
	1222										BC				
	1230											BC			
	1235												BC		
	1240													BC	
	1303	BC													A read at 5-minute intervals
	1325														A BC

Figure A4.1 Altimetric observations sequence at stations between two bases. X,Y,Z, are equal-length sections for weighting check-in errors. A,B,C, denote instruments used in observations: A, base altimeter; B,C, roving altimeters. The time intervals are typical for a base separation of about 10 km.

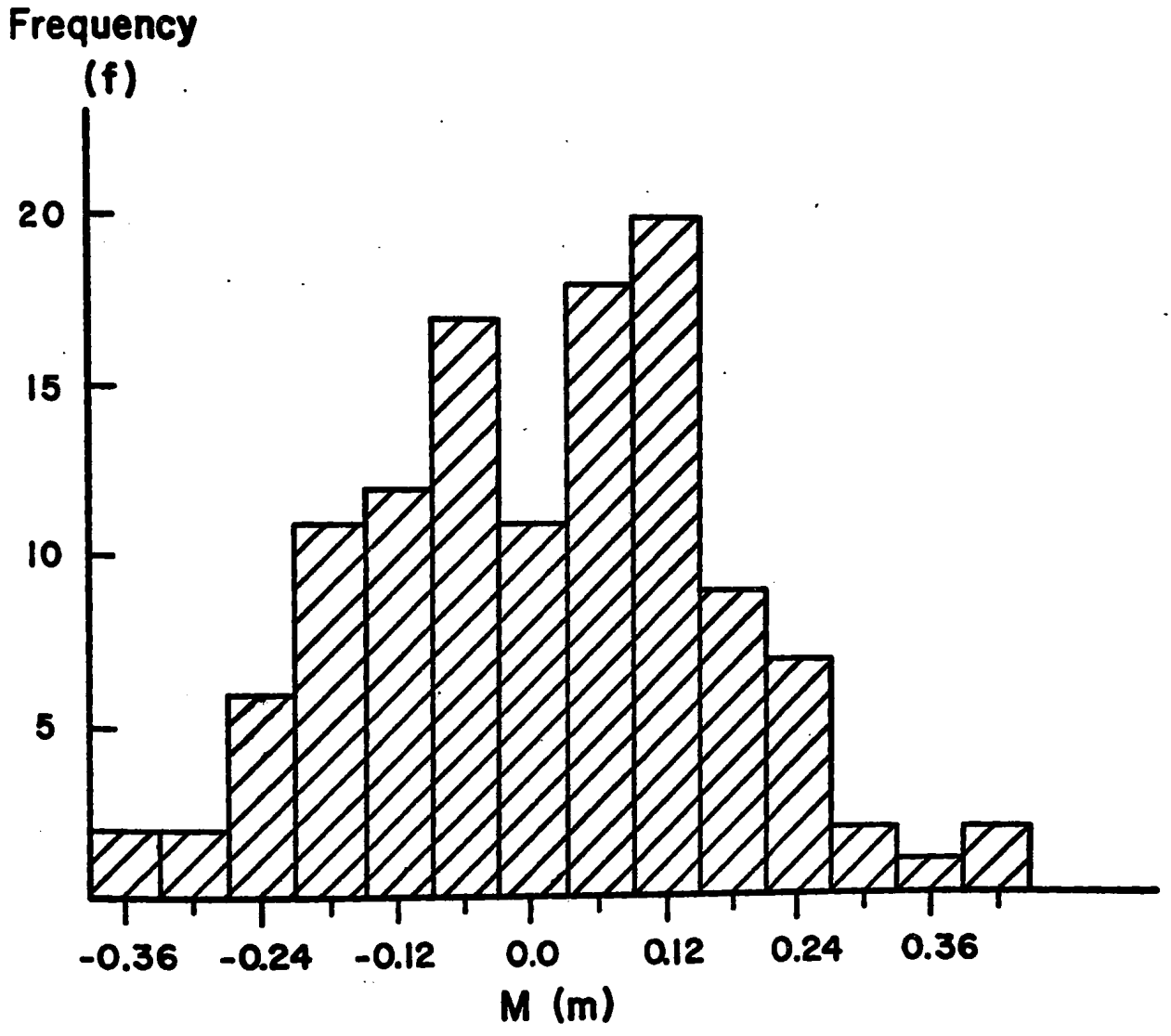

Figure A4.2 Comparison of results with base values smoothed and non-smoothed. M is defined by equation A4.6. Positive values of M indicate smoothed values are closer to known elevations than are non-smoothed values.

APPENDIX 5

BOUGUER ANOMALY PROFILE WITH SURFACE GEOLOGY AND STATION ELEVATION

A5.1 Presentation of data.

The Bouguer anomaly and station elevation profiles are given in Figures A5.2.1 to A5.2.6, inclusive. These figures also contain corresponding geologic and geographic information. Symbols are explained in Figure A5.1, and supplementary geologic information is given in Table A5.1.

FIGURE A5.1 LEGEND FOR FIGURES A5.2.1 TO A5.2.6

GEOLOGY — Subdivisions described in Table A5.1

ROCK SAMPLES } ρ_m SITE — Mean density at site. Mean subdivision density given in Table A5.1.

GENERAL

F_m : Faults shown Map 123 1A (Williams, 1967)

F_d, F_x, F_s : Faults (d - defined, x - approximate, s - assumed) shown on other geologic maps.

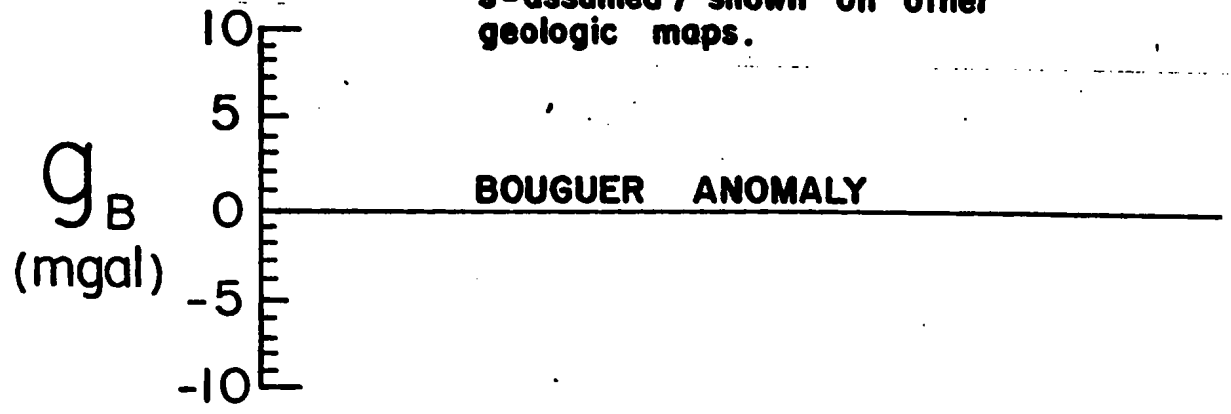

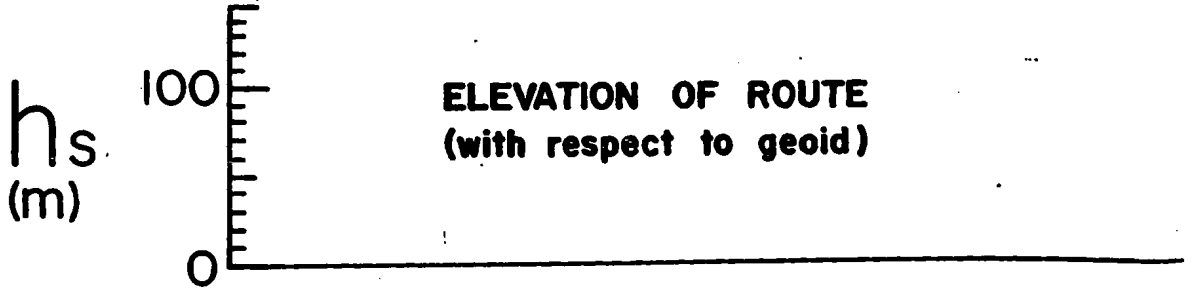

d_{PAB} (km) — Distance along route from Port - Aux - Basques.

DIRECTION — Along route away from Port-Aux-Basques. Angles measured from first to second compass points shown.

LOCATION — Refer Figure 1.1.1

FIGURE A5.2.1 BOUGUER ANOMALY PROFILE WITH SURFA

FACE GEOLOGY AND STATION ELEVATION. LOCATIONS A – D.

6	7	6	7	6	8	6	7	6	9

2.57
6

2.57
7

$F_x F_x$

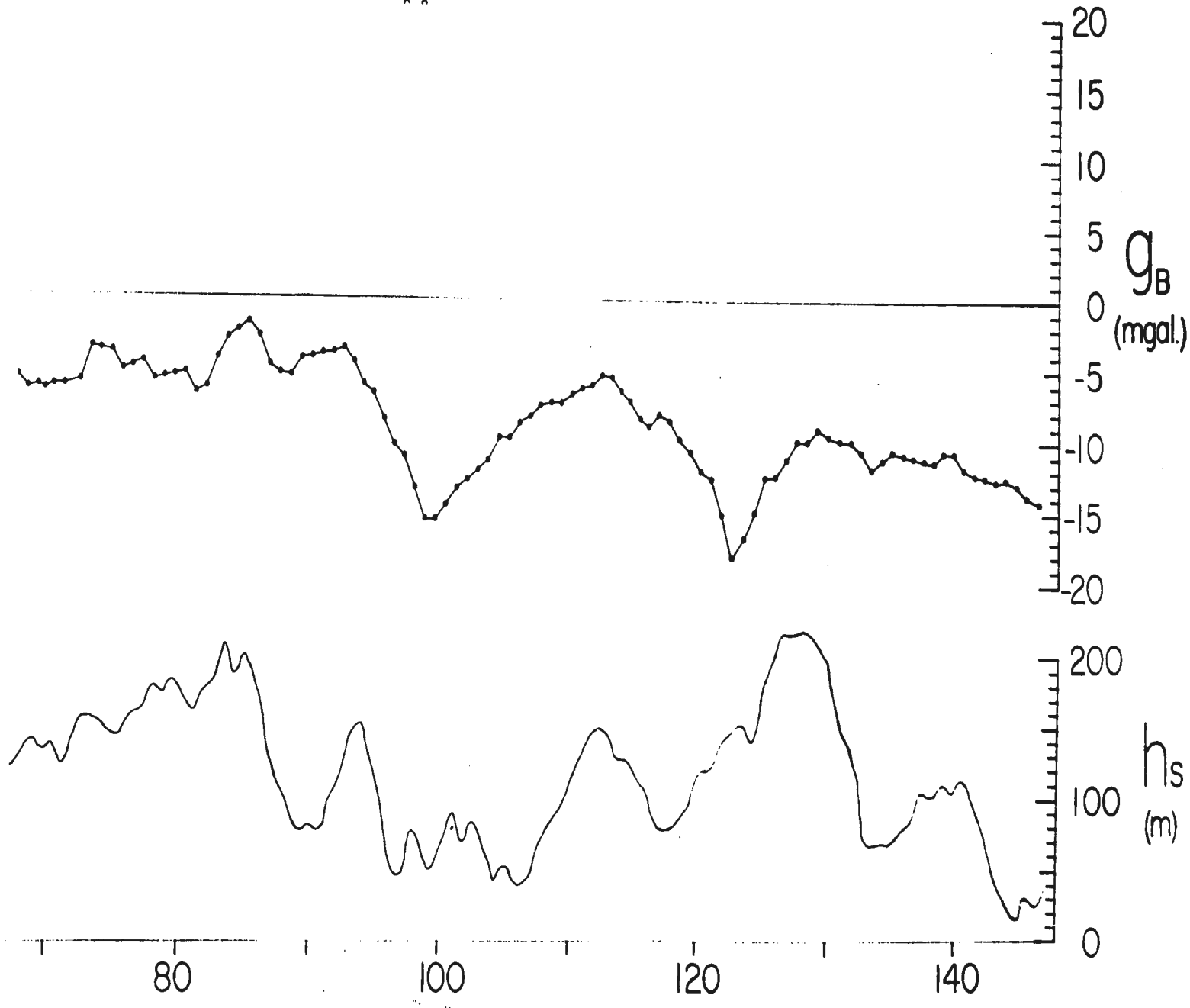

N50E	N	N25E	N60E	N80E	NE	N	N20E	W60N	N E	E	N40E	E	N50E	N35E	N	N55E

C D

FIGURE A5.2.2 BOUGUER ANOMALY PROFILE WITH SURFACE GEOL

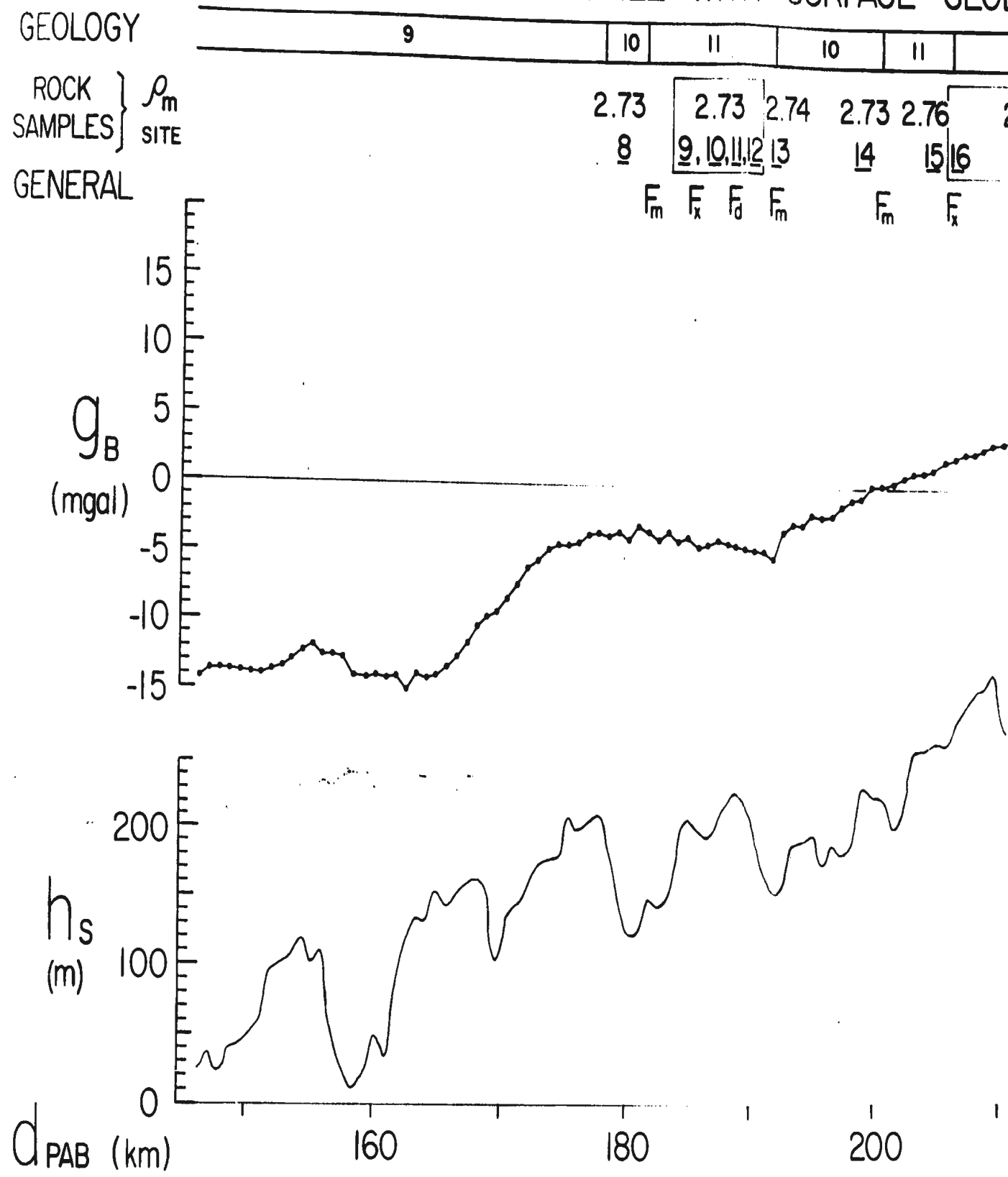

GEOLOGY AND STATION ELEVATION. LOCATIONS D–F.

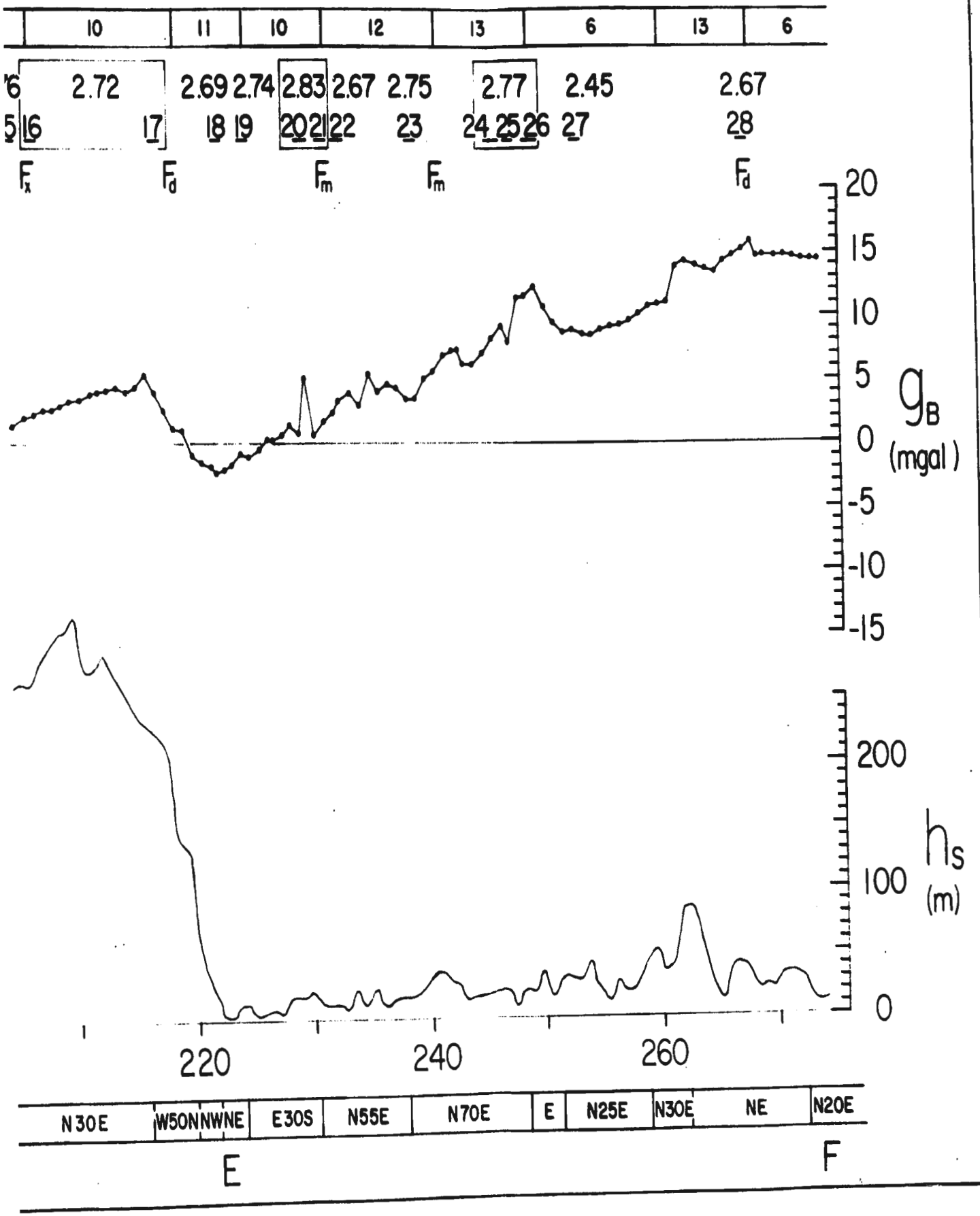

FIGURE A5.2.3 BOUGUER ANOMALY PROFILE WITH SURFACE GEOL

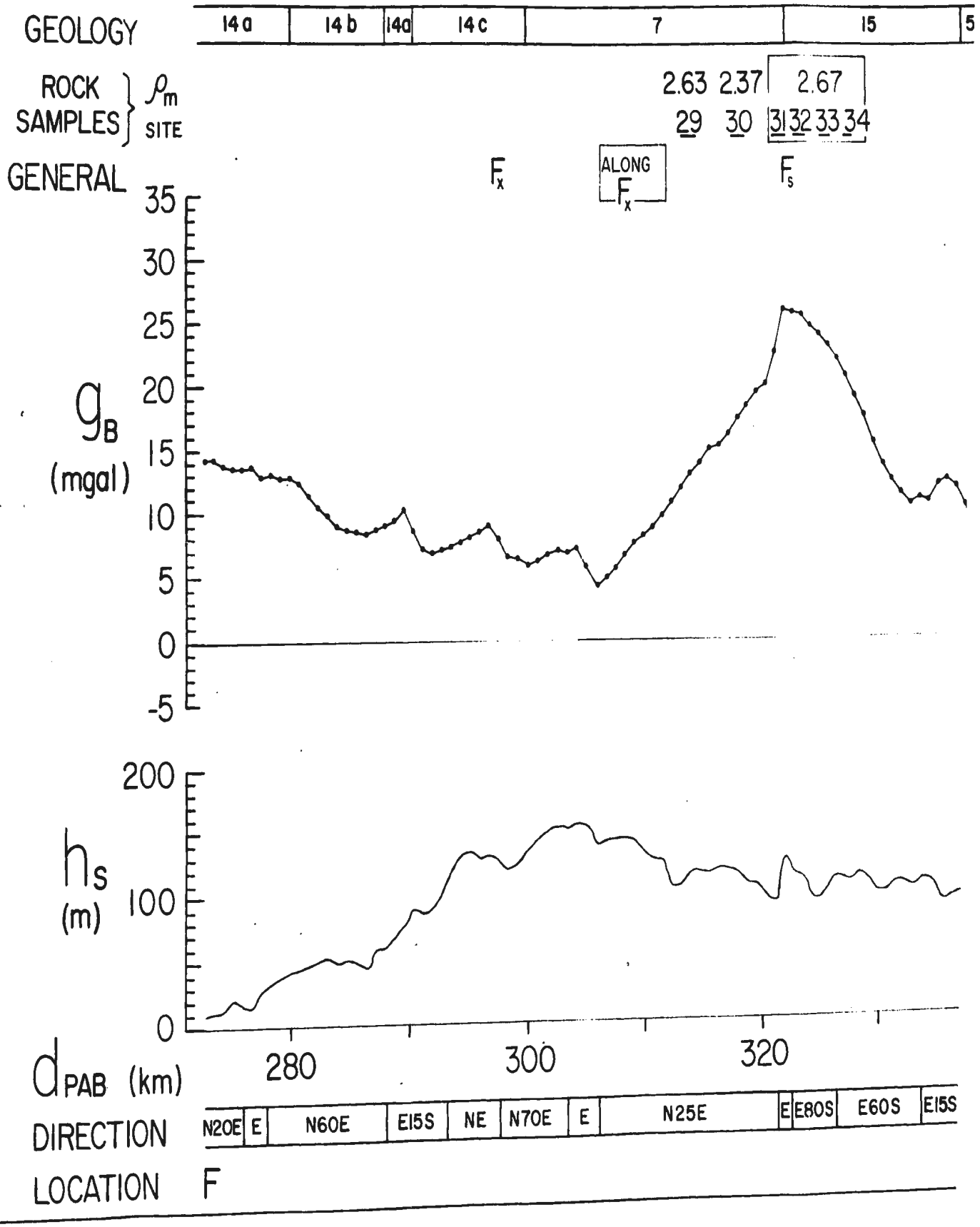

GEOLOGY AND STATION ELEVATION. LOCATIONS F–H.

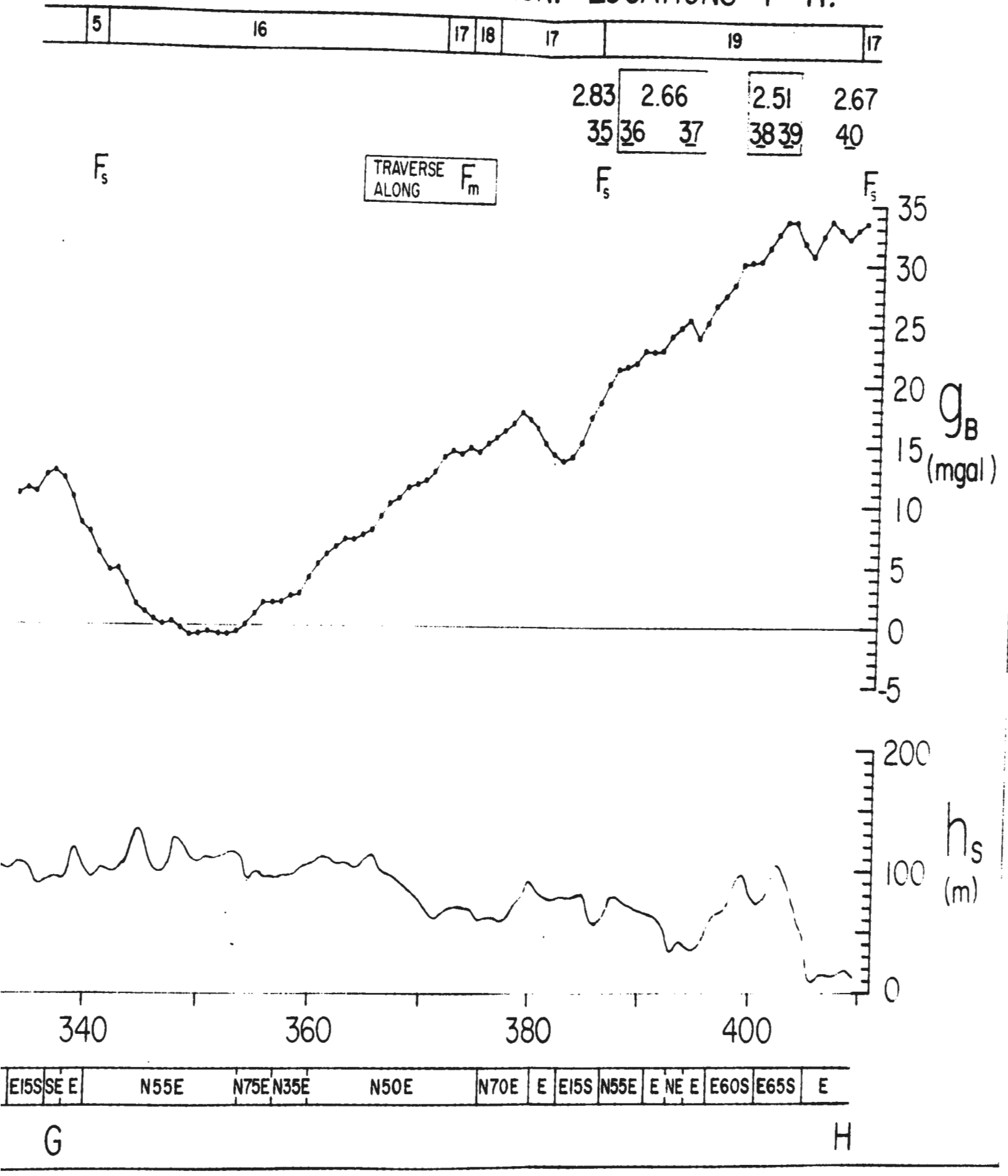

FIGURE A5.2.4 BOUGUER ANOMALY PROFILE WITH SURFACE GEOL

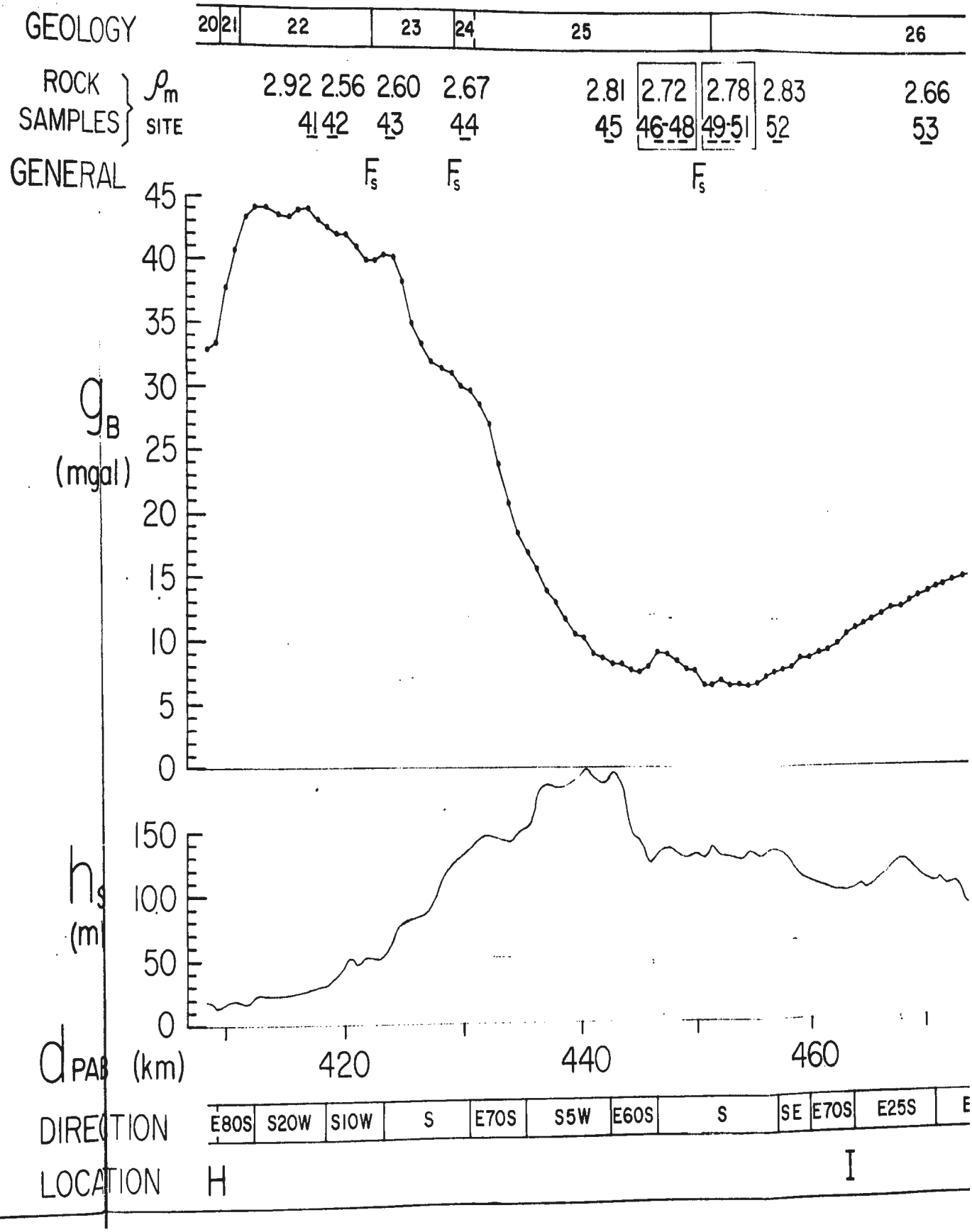

GEOLOGY AND STATION ELEVATION. LOCATIONS H-K.

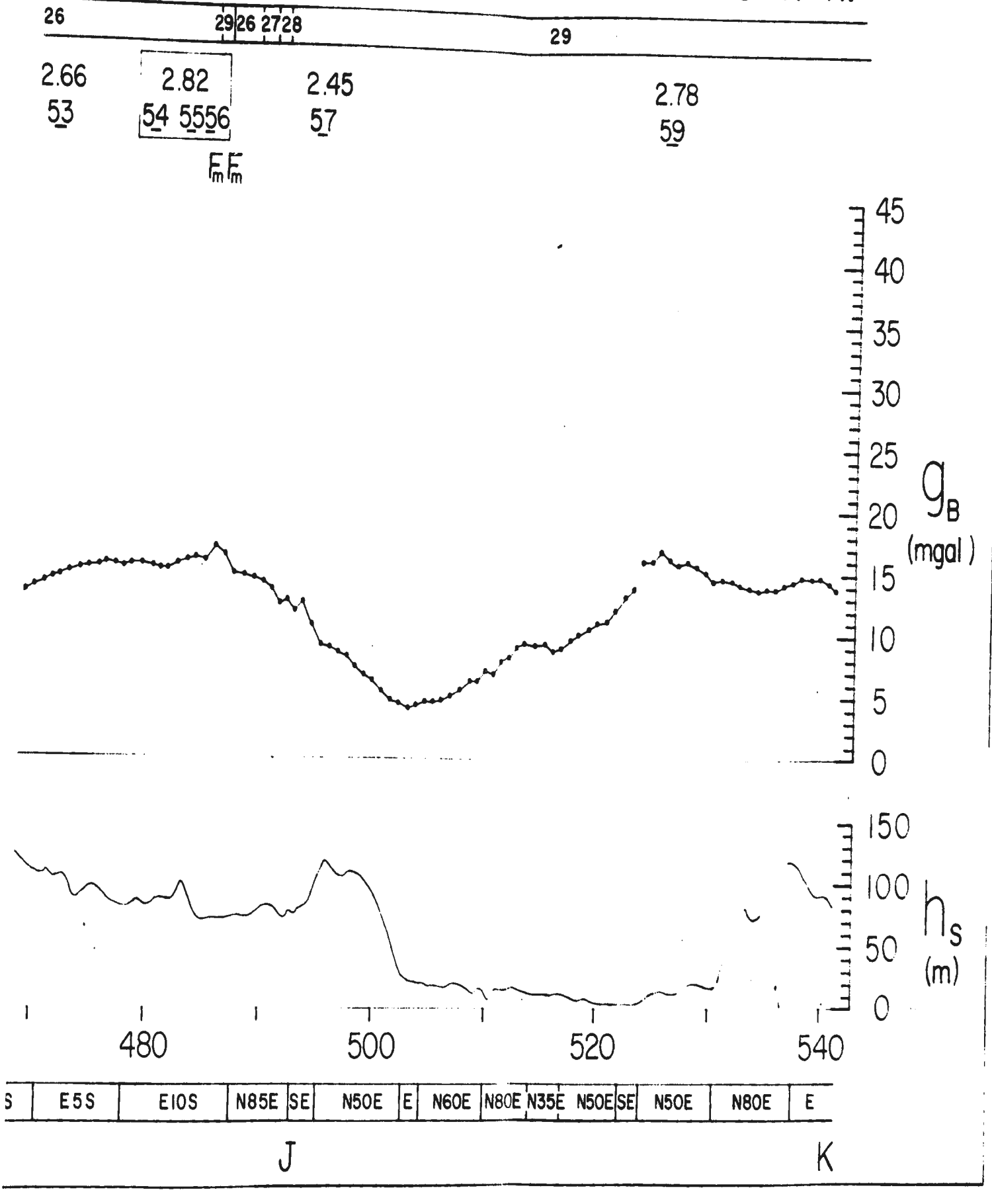

FIGURE A5.2.5 BOUGUER ANOMALY PROFILE WITH SURFACE GEOL

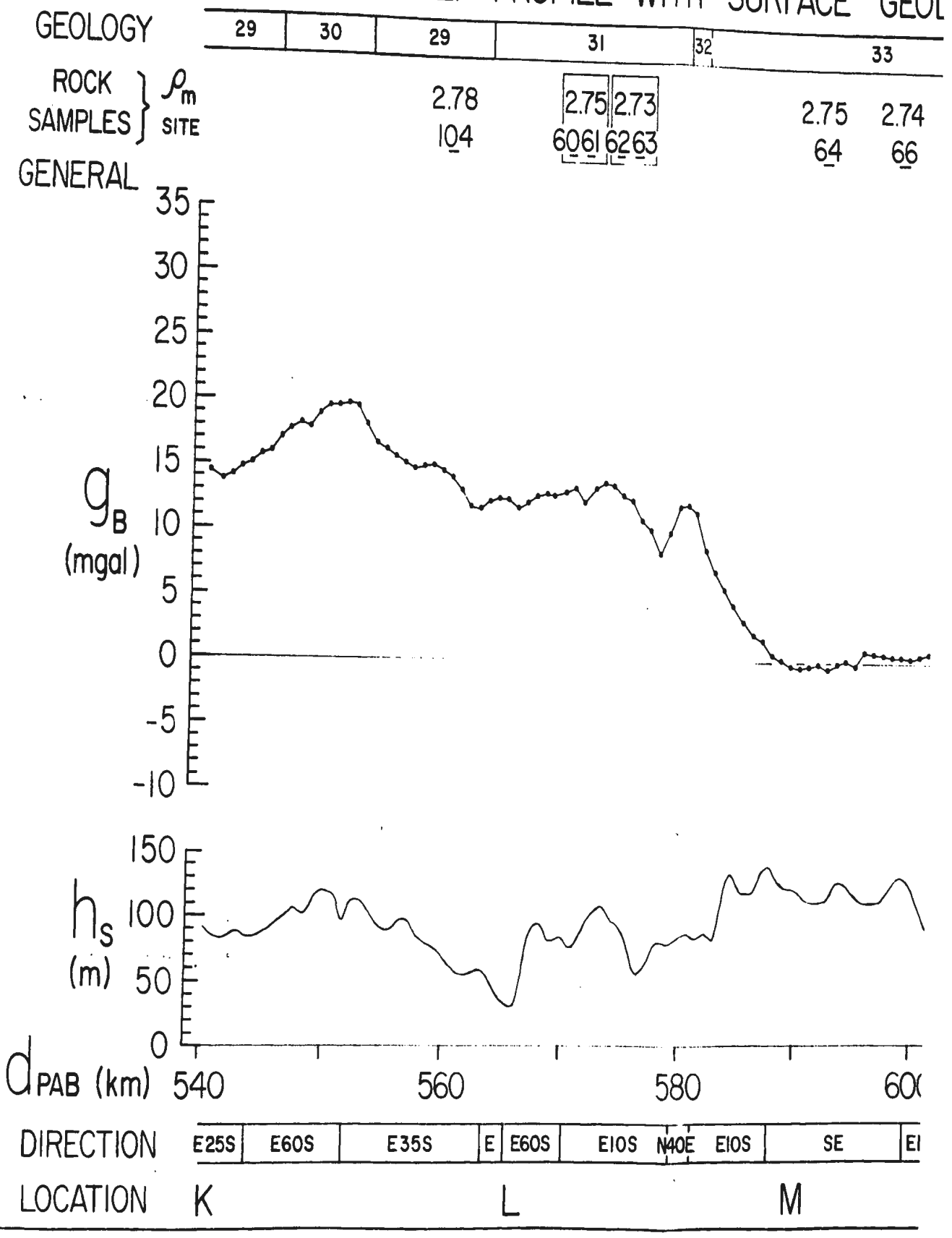

GEOLOGY AND STATION ELEVATION. LOCATIONS K–P.

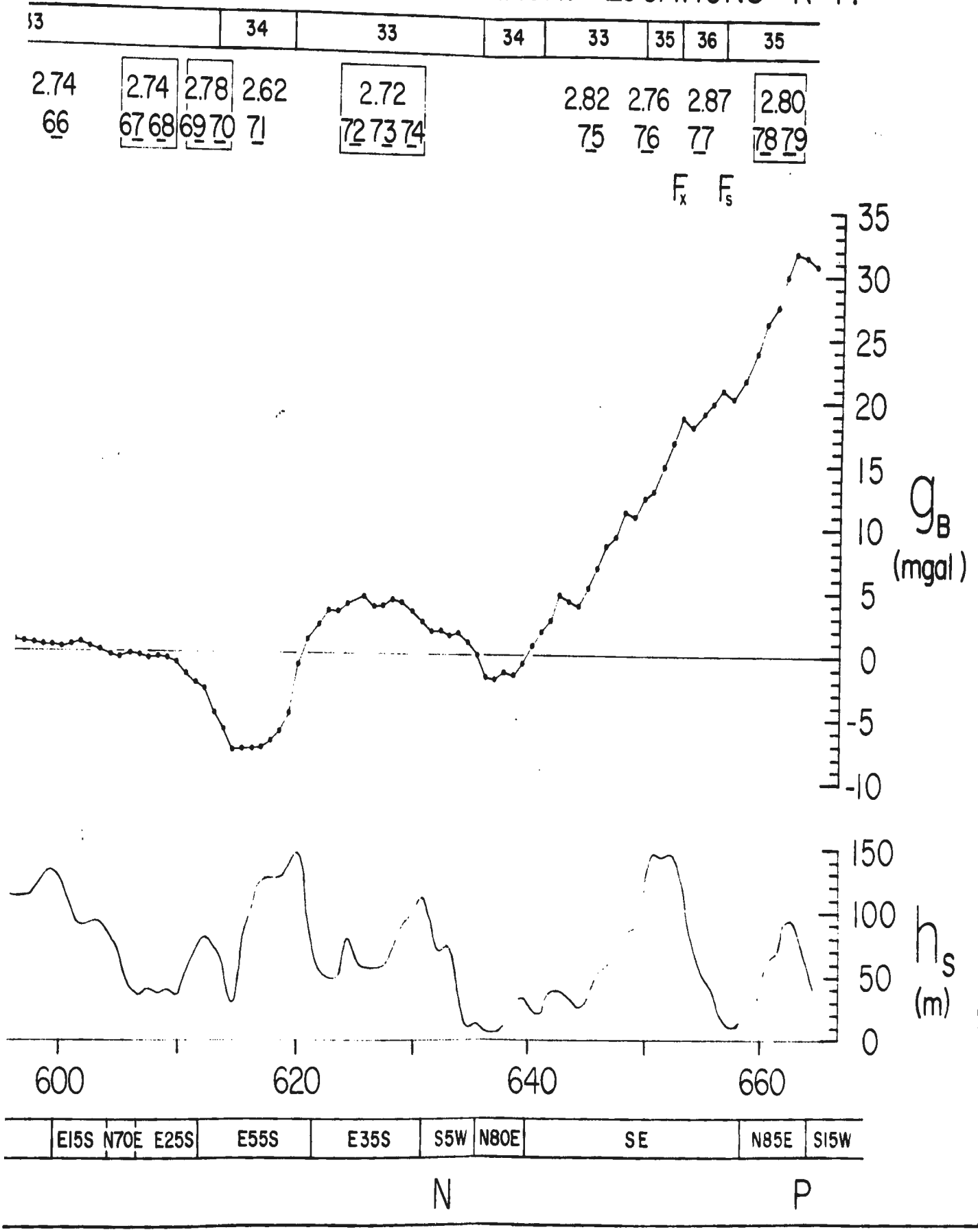

FIGURE A5.2.6 BOUGUER ANOMALY PROFILE WITH SURFACE GEO

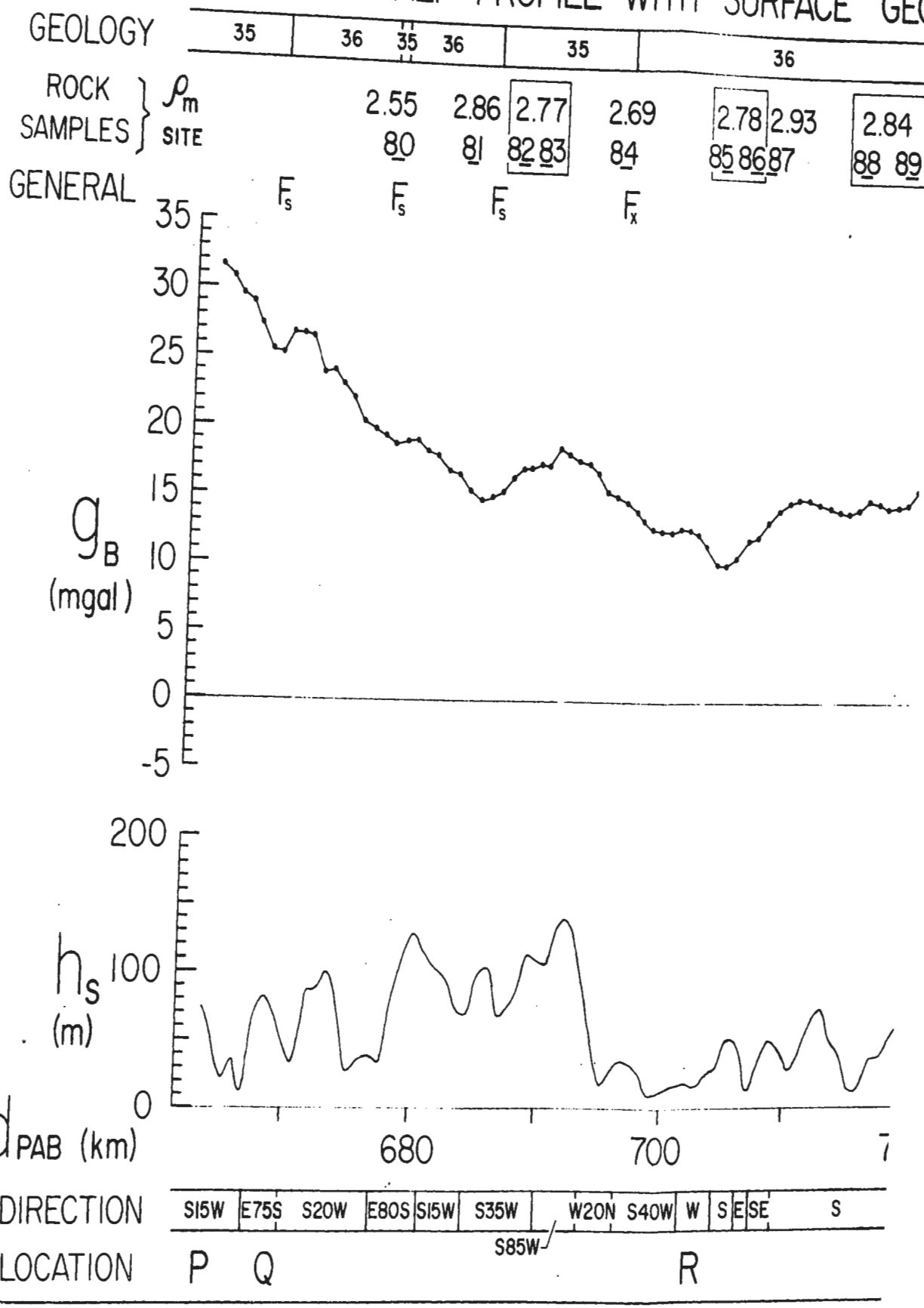

GEOLOGY AND STATION ELEVATION. LOCATIONS P-U.

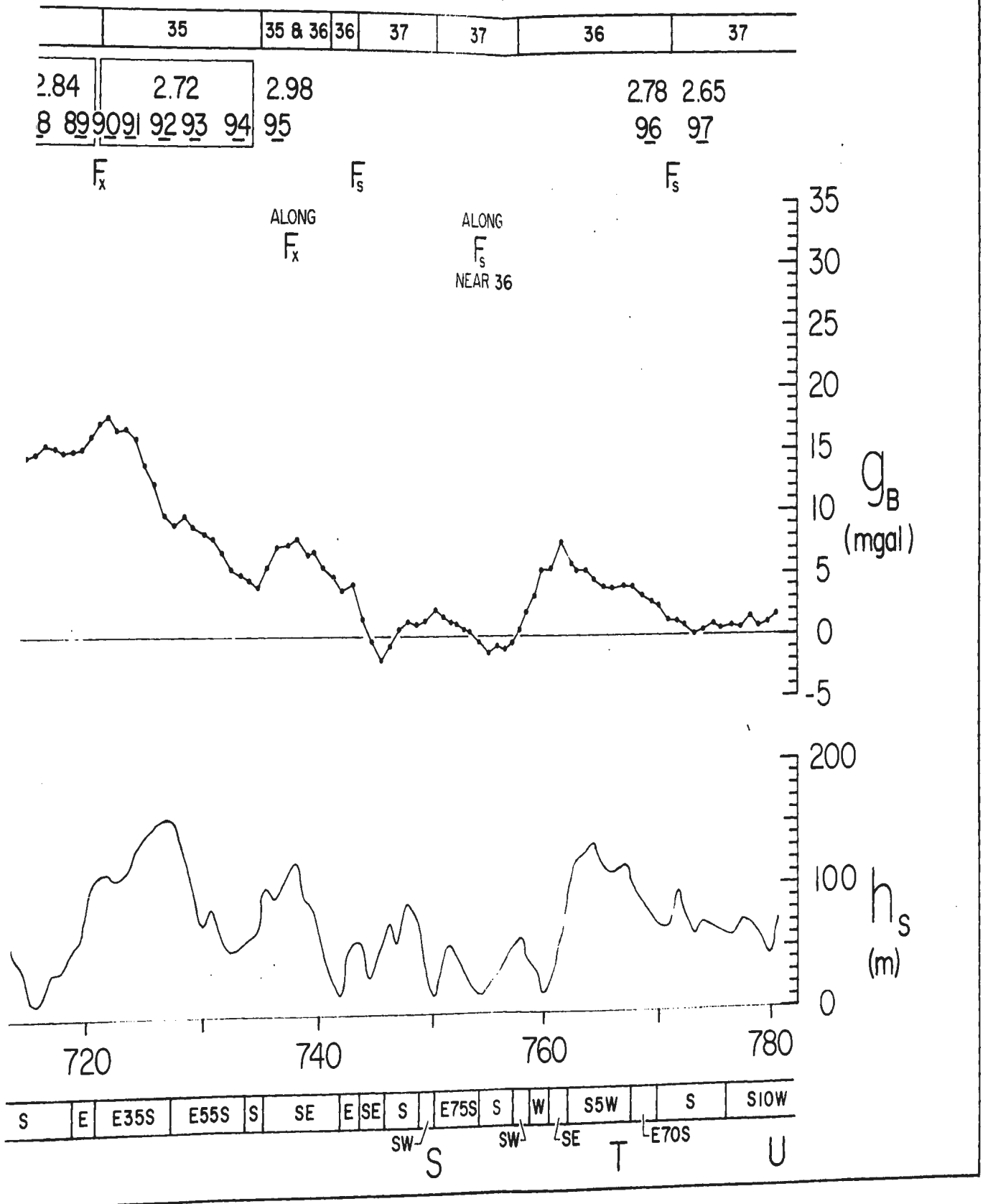

Table A5.1 Geologic information.

(1) Geologic sub-division[1]	(2) Age[2]	(3) General description[3]	(4) Rock sample data:[4] (a) number of sites; (b) rock types; and (c) mean density (gm/cm^3)	(5) See also sub-divs.[5]
1	O,S,D and earlier	Sandstone, slate, greywacke, conglomerate, acidic to mafic volcanic rocks and metamorphic equivalents.	(a) 5 (b) schist (c) 2.75	
2	O,S and earlier	Slate, greywacke, acidic to mafic volcanic rocks, quartzite; chert, limestone and metamorphic equivalents.		21
3	D and earlier	Granite, granodiorite, syenite, monzonite, quartz diorite and related rocks.		17, 20, 23
4	D (mainly) and Upper S(?)	Gabbro, diorite, pyroxenite, quartz diorite, granodiorite, mafic syenite and related rocks.		22, 25, 27
5	C	Conglomerate, sandstone, siltstone, shale, limestone, gypsum, anhydrite, some coal. Includes Barachois Group and Searston Beds (Upper C_m and C_p).		8
6	C_m (Upper and Middle)	Brown, red, green, and grey sandstone, commonly pebbly siltstone, conglomerate, limestone; gypsum. Codroy Group and probable equivalents.	(a) 2 (b) siltstone & sandstone (c) 2.51	14
7	C_m Lower	Limestone, conglomerate, grey sandstone, shale, siltstone. Anguille Group.	(a) 4 (b) sandstone, siltstone, shale, schist (c) 2.56	
8	C_p	Grey, some red, pebble, micaceous sandstone, grey siltstone; coal; conglomerate; minor shale, limestone, limestone conglomerate. Barachois Group.		5
9	C	Conglomerate, sandstone, siltstone, shale, limestone, gypsum, anhydrite, some coal.		5
10	O (Lower and Middle)	Massive grey, buff, and pink dolomite and limestone; minor shale and limestone conglomerate; some quartzite and sandstone. St. George's and Table Head Groups.	(a) 6 (b) limestone (c) 2.76	

1 A "sub-division" may be either a system, series, group, formation, or bed.

2 Symbols: PE, Precambrian; E, Cambrian; O, Ordovician; S, Silurian; D, Devonian; C, Carboniferous (with C_m, Mississippian; C_p, Pennsylvanian); (?) age uncertainty.

3 General description of the whole sub-division (and not just the part near the traverse). These were obtained primarily from maps published by the Geological Survey of Canada.

4 The mean density (arithmetic) is calculated by giving unit weight to each site.

5 Cross-reference to sub-divisions of approximately the same age and general description.

(1)	(2)	(3)
11	E,O	Shale, sandstone, slate, gre limestone, conglomerate, bas rocks. Possible Taconic Kli transported from east. Hum Group.
12	E	Limestone, quartzite, shale slate, with arkose, conglom basalt locally at base.
13	E or earlier	Crenulated, quartz-mica-fel chlorite schists and gneiss amphibolite layers.
14_a	C_m	Red and grey shales and sil grey and dark grey limeston petroliferous, red siltston kunkurs and much variegated sandstone. Rocky Brook For
14_b	C_m	Red, quartzose sandstone ar minor shales and siltstones Formation.
14_c	C_m	Basal conglomerates of gre calcite and hematite cemen and shales, red, grey and Windsor Group.
15	D (mainly)	Porphyritic biotite granit gneisses.
16	S(?)	Dominantly rhyolite and tr and pyroclastic rocks.
17	D and earlier	Granite, granodiorite, sye
18	S	Massive to slightly schis basic volcanic rocks; th fossiliferous limestone.
19	S and later	Silicic flow and pyroclas sandstone, conglomerate, and shale. Springdale Gr
20	Age and general description as for	
21	O	Basalt; minor pyroclastic flow rocks, basic sills. Formation.

1 See foot-notes on first page of table.

e A5.1, Continued[1]

3)	(4)	(5)
slate, greywacke, nerate, basic volcanic Taconic Klippen east. Humber Arm	(a) 8 (b) shale, sandstone, siltstone. (c) 2.73	
ite, shale, dolomite, e, conglomerate and base.	(a) 2 (b) schist (c) 2.71	
z-mica-feldspar- and gneisses; minor s.	(a) 4 (b) gneiss and schist (c) 2.75	
les and siltstones, thin, ey limestones, commonly ed siltstone with limey variegated; some red y Brook Formation.		6
andstone and conglomerate; siltstones. Humber Falls		6
ites of great variety with ntite cements, red siltstones , grey and khaki sandstones.		6
tite granite and hybrid	(a) 3 (b) granite and schist (c) 2.67	
lite and trachyte flow rocks.		
liorite, syenite.	(a) 1 (b) diorite (c) 2.83	20, 23
ghtly schistose silicic to rocks; thin beds of limestone.		
nd pyroclastic rocks; red glomerate, limy siltstone ringdale Group.	(a) 5 (b) altered volcanic, rhyolite, andesite, sandstone (c) 2.60	
tion as for sub-division 17.		23
pyroclastic rocks, silicic sic sills. Roberts Arm		24

table.

Table A5.1, Continued[1]

(1)	(2)	(3)	(4)	(5)
22	D and earlier	Gabbro, diorite, pyroxenite, quartz diorite, granodiorite, mafic syenite and related rocks.	(a) 2 (b) diorite & granite (c) 2.74	25, 27, 30, 32
23	D and earlier	Granite, granodiorite, syenite.	(a) 1 (b) granite (c) 2.60	17, 20
24	O	Basalt; minor pyroclastic rocks, silicic flow rocks, basic sills. Roberts Arm Formation.	(a) 1 (b) andesite (c) 2.67	21
25	D and earlier	Gabbro, diorite, pyroxenite, quartz diorite, granodiorite, mafic syenite and related rocks.	(a) 5 (b) siltstone, diorite, granite (c) 2.74	22, 27, 30, 32
26	O	Greywacke, conglomerate, basalt.	(a) 7 (b) diorite, sandstone, shale (c) 2.80	
27	D and earlier	Gabbro, diorite, pyroxenite, quartz diorite, granodiorite, mafic syenite and related rocks.		22, 25, 30, 32
28	O,S and earlier	Slate, greywacke, acidic to mafic volcanic rocks, quartzite, chert, limestone, and metamorphic equivalents		21
29	S	Sandstone, conglomerate, acidic to mafic volcanic rock, greywacke, shale, limestone. Botwood Group.	(a) 9 (b) sandstone, siltstone, shale, conglomerate, diorite (c) 2.72	
30	D and earlier	Diorite, quartz diorite, gabbro.		22, 25, 27, 32
31	O	Intermediate to mafic volcanic rocks, slate, greywacke, siltstone, chert, conglomerate, minor limestone. Gander Lake Group, middle & upper units.	(a) 4 (b) shale (c) 2.74	
32	O (?)	Diorite and gabbro		22,25, 27,30
33	O	Siltstone, quartzite, slate, greywacke, and metamorphic equivalents. Gander Lake Group, Lower Unit.	(a) 10 (b) shale, siltstone, schist, gneiss (c) 2.75	

[1] See foot-notes on first page of table.

Table A5.1, Continued[1]

(1)	(2)	(3)	(4)	(5)
11	€,O	Shale, sandstone, slate, greywacke, limestone, conglomerate, basic volcanic rocks. Possible Taconic Klippen transported from east. Humber Arm Group.	(a) 8 (b) shale, sandstone, siltstone. (c) 2.73	
12	€	Limestone, quartzite, shale, dolomite, slate, with arkose, conglomerate and basalt locally at base.	(a) 2 (b) schist (c) 2.71	
13	€ or earlier	Crenulated, quartz-mica-feldspar-chlorite schists and gneisses; minor amphibolite layers.	(a) 4 (b) gneiss and schist (c) 2.75	
14_a	C_m	Red and grey shales and siltstones, thin, grey and dark grey limestones, commonly petroliferous, red siltstone with limey kunkurs and much variegated; some red sandstone. Rocky Brook Formation.		6
14_b	C_m	Red, quartzose sandstone and conglomerate; minor shales and siltstones. Humber Falls Formation.		6
14_c	C_m	Basal conglomerates of great variety with calcite and hematite cements, red siltstones and shales, red, grey and khaki sandstones. Windsor Group.		6
15	D (mainly)	Porphyritic biotite granite and hybrid gneisses.	(a) 3 (b) granite and schist (c) 2.67	
16	S(?)	Dominantly rhyolite and trachyte flow and pyroclastic rocks.		
17	D and earlier	Granite, granodiorite, syenite.	(a) 1 (b) diorite (c) 2.83	20, 23
18	S	Massive to slightly schistose silicic to basic volcanic rocks; thin beds of fossiliferous limestone.		
19	S and later	Silicic flow and pyroclastic rocks; red sandstone, conglomerate, limy siltstone and shale. Springdale Group.	(a) 5 (b) altered volcanic, rhyolite, andesite, sandstone (c) 2.60	
20	Age and general description as for sub-division 17.			23
21	O	Basalt; minor pyroclastic rocks, silicic flow rocks, basic sills. Roberts Arm Formation.		24

[1] See foot-notes on first page of table.

Table A5.1, Contin

(1)	(2)	(3)
22	D and earlier	Gabbro, diorite, pyroxenite, qua diorite, granodiorite, mafic sye and related rocks.
23	D and earlier	Granite, granodiorite, syenite.
24	O	Basalt; minor pyroclastic rocks flow rocks, basic sills. Robert Formation.
25	D and earlier	Gabbro, diorite, pyroxenite, qua diorite, granodiorite, mafic sye and related rocks.
26	O	Greywacke, conglomerate, basalt.
27	D and earlier	Gabbro, diorite, pyroxenite, quar diorite, granodiorite, mafic syen and related rocks.
28	O,S and earlier	Slate, greywacke, acidic to mafic rocks, quartzite, chert, limeston metamorphic equivalents
29	S	Sandstone, conglomerate, acidic t volcanic rock, greywacke, shale, stone. Botwood Group.
30	D and earlier	Diorite, quartz diorite, gabbro.
31	O	Intermediate to mafic volcanic rc slate, greywacke, siltstone, cher conglomerate, minor limestone. (Lake Group, middle & upper units.
32	O (?)	Diorite and gabbro
33	O	Siltstone, quartzite, slate, gre and metamorphic equivalents. Ga Lake Group, Lower Unit.

[1] See foot-notes on first page of table.

l, Continued[1]

	(4)	(5)
enite, quartz mafic syenite	(a) 2 (b) diorite & granite (c) 2.74	25, 27, 30, 32
. syenite.	(a) 1 (b) granite (c) 2.60	17, 20
istic rocks, silicic ls. Roberts Arm	(a) 1 (b) andesite (c) 2.67	21
xenite, quartz , mafic syenite	(a) 5 (b) siltstone, diorite, granite (c) 2.74	22, 27, 30, 32
te, basalt.	(a) 7 (b) diorite, sandstone, shale (c) 2.80	
xenite, quartz , mafic syenite		22, 25, 30, 32
dic to mafic volcanic rt, limestone, and ts		21
te, acidic to mafic cke, shale, lime- .	(a) 9 (b) sandstone, siltstone, shale, conglomerate, diorite (c) 2.72	
te, gabbro.		22, 25, 27, 32
volcanic rocks, tstone, chert, imestone. Gander upper units.	(a) 4 (b) shale (c) 2.74	
		22,25, 27,30
slate, greywacke, lents. Gander .	(a) 10 (b) shale, siltstone, schist, gneiss (c) 2.75	

Table A5.1, Continued

(1)	(2)	(3)	(4)	(5)
34	D	Coarse grained porphyritic biotite granite. Ackley batholith.	(a) 1 (b) granite (c) 2.62	
35	Pε	Acidic to mafic volcanic rocks; slate, greywacke, conglomerate and metamorphic equivalents. Love Cove Group.	(a) 11 (c) 2.74 (b) basalt, andesite, rhyolite, granite, diorite, shale, siltstone, schist	
36	Pε	Siltstone, arkose, conglomerate, slate, acidic to intermediate volcanic rocks. Musgravetown Group.	(a) 9 (b) basalt, andesite, diorite, shale, sandstone (c) 2.80	
37	Pε	Green to black greywacke, cherty quartzite, slate; some sandstone and conglomerate. Connecting Point Group.	(a) 1 (b) composite shaly sandstone. (c) 2.65	

[1] See foot-notes on first page of table.

APPENDIX 6

ROCK SAMPLE DATA

A6.1 Sample density (dry) calculation.

A dry density of (2.74 ± 0.02) gm/cm^3 is obtained for rock 5, site 10, using

$$\rho_r = \frac{M_r \rho_w}{M_c - M_w - (M_c - M_r) \times \rho_w/\rho_c} \qquad (A6.1)$$

where ρ_r is the dry density, and

M_r (mass of uncoated rock) = (124.40 ± 0.20) gm

M_c (mass of coated rock) = (124.79 ± 0.20) gm

M_w (apparent mass of coated rock in distilled water) = (79.04 ± 0.20) gm

ρ_c (density of dry plastic coating) = (1.165 ± 0.004) gm/cm^3

ρ_w (density of distilled water at 4^{o}C) = 1.0000 gm/cm^3

The standard deviation of ± 0.20 gm, associated with each quoted mass, is based on a measurement check of 50 of these rock samples. It is assumed that, because the apparatus was not significantly disturbed between measurements of M_c and M_r, the standard deviation in $(M_c - M_r)$ does not exceed ± 0.10 gm. There is a small systematic discrepancy in ρ_r, not given above nor included in Table A6.1, due to the usage of water at a temperature of approximately 22^{o}C (density 0.998 gm/cm^3).

A6.2 Rock sample information.

This data is provided in Table A6.1. Table A3.1 gives the locations of the stations listed in column 3. Figures A5.2.1 to A5.2.6, with Table A5.1, contain the geologic subdivisions listed in column 4. Each sample at a site is given equal weight in the determination of the mean site density. Assistance in classifying these rocks was kindly provided by Dr. Harold Williams of Memorial University's Department of Geology.

Table A6.1 Rock sample data.

(1) Site	(2) Rock No.	(3) Located between stations or near station	(4) Located geologic subdivision[1]	(5) Rock density (g/cm^3)	(6) Mean site density (g/cm^3)	(7) Classification
1	80	10455	1	2.70 ± 0.03	2.73	Schist
	81			2.77 ± 0.03		Schist
2	11	10454 & 10455	1	2.87 ± 0.01	2.87	Schist
3	82	10451 & 10452	1	2.63 ± 0.10	2.71	Schist
	83			2.78 ± 0.05		Schist
4	8	10447 & 10448	1	2.79 ± 0.02	2.79	Schist
5	1	10445 & 10446	1	2.64 ± 0.04	2.64	Schist
6	66	10366	6	2.57 ± 0.01	2.57	Siltstone
7	7	10341 & 10342	7	2.57 ± 0.01	2.57	Sandstone
8	2	10233	10	2.73 ± 0.01	2.73	Grey limestone
9	21	10226 & 10227	11	2.63 ± 0.07	2.63	Shale
10	5	10224	11	2.74 ± 0.02	2.74	Shale
11	3	10221 & 10222	11	2.79 ± 0.05	2.79	Shale
12	23	10219 & 10220	11	2.77 ± 0.05	2.77	Shale
13	10	10217	11	2.74 ± 0.01	2.74	Siltstone
14	9	10208	10	2.73 ± 0.03	2.73	Limestone
15	6	10201	11	2.76 ± 0.02	2.76	Shale
16	22	10199 & 10200	10	2.72 ± 0.02	2.72	Limestone

[1]Refer Figures A5.2.1 - A5.2.6, with Table A5.1

... continued

Table A6.1, continued

(1)	(2)	(3)	(4)	(5)	(6)	(7)
17	25	10185 ± 10186	10	2.72 ± 0.02	2.72	Limestone
18	30	10060 & 9003	11	2.69 ± 0.03	2.69	Sandstone
19	17 18	10066	11	2.78 ± 0.05 2.70 ± 0.02	2.74	Shale Shale
20	28 29	10067 & 10109	10	2.79 ± 0.02 2.85 ± 0.02	2.82	Limestone Limestone
21	26	10068 & 10067	10	2.84 ± 0.01	2.84	Limestone
22	19	10069	12	2.67 ± 0.01	2.67	Schist
23	41 42	10078	12	2.74 ± 0.03 2.75 ± 0.01	2.75	Schist Schist
24	37 91	10081 & 10080	13	2.80 ± 0.01 2.79 ± 0.01	2.80	Gneiss Schist
25	39 40	9004	13	2.71 ± 0.01 2.77 ± 0.02	2.74	Schist Schist
26	32 33 34	10089 & 10079	13	2.81 ± 0.02 2.68 ± 0.01 2.84 ± 0.03	2.78	Schist Schist Schist
27	47	10095 & 10094	6	2.45 ± 0.03	2.45	Sandstone
28	12	10115	13	2.67 ± 0.02	2.67	Schist
29	138 139 140	10968	7	2.63 ± 0.02 2.58 ± 0.02 2.67 ± 0.01	2.63	Siltstone Siltstone Siltstone
30	124	10963	7	2.37 ± 0.01	2.37	Shale
31	143	10923 & 10959	7	2.68 ± 0.02	2.68	Schist
32	154	10921 & 10922	15	2.60 ± 0.02	2.60	Granite (Coarse grain)
33	130	10918 & 10919	15	2.70 ± 0.01	2.70	Schist

... continued

Table A6.1, continued

(1)	(2)	(3)	(4)	(5)	(6)	(7)
34	122	10915 & 10916	15	2.71 ± 0.03	2.71	Schist
35	111	10845 & 10846	17	2.83 ± 0.02	2.83	Diorite
36	118	10843	19	2.69 ± 0.01	2.69	Altered volcanic-fault rock
37	114	10835 & 10836	19	2.63 ± 0.03	2.63	Rhyolite
38	142	10827 & 10828	19	2.38 ± 0.03	2.38	Sandstone
39	128	10824 & 10825	19	2.64 ± 0.01	2.64	Sandstone
40	147	10817 & 10818	19	2.67 ± 0.02	2.67	Andesite
41	126	10780 & 10779	22	2.92 ± 0.04	2.92	Diorite
42	149	10781	22	2.56 ± 0.02	2.56	Granite (Medium grain)
43	141	10788 & 10787	23	2.60 ± 0.01	2.60	Granite (Fine grain)
44	148	10796 & 10795	24	2.67 ± 0.01	2.67	Andesite
45	125	10811	25	2.81 ± 0.01	2.81	Siltstone
46	15 16	10670	25	2.83 ± 0.01 2.64 ± 0.02	2.74	Quartz diorite Granite (Fine grain)
47	48 49 50	10669 & 10670	25	2.92 ± 0.02 2.74 ± 0.02 2.87 ± 0.02	2.84	Diorite Granite Diorite
48	51 52	10669	25	2.63 ± 0.02 2.51 ± 0.01	2.57	Granite (Medium grain) Granite (Medium grain)
49	57 58	10664 & 10665	25	2.65 ± 0.02 2.78 ± 0.02	2.72	Granite (Fine grain) Diorite
50	43 44 45	10663 & 10664	26	2.96 ± 0.02 2.84 ± 0.02 2.74 ± 0.02	2.85	Diorite Diorite Diorite

... continued

Table A6.1, continued

(1)	(2)	(3)	(4)	(5)	(6)	(7)
51	53	10661 & 10662	26	2.70 ± 0.02	2.78	Diorite
	54			2.73 ± 0.02		Diorite
	55			2.74 ± 0.02		Diorite
	56			2.97 ± 0.03		Diorite
52	14	10657	26	2.83 ± 0.02	2.83	Diorite
53	144	10759 & 10760	26	2.66 ± 0.01	2.66	Sandstone
	145			2.65 ± 0.01		Sandstone
54	136	10748 & 10749	26	2.77 ± 0.01	2.74	Silicious shale
	137			2.71 ± 0.01		Silicious shale
55	127	10744 & 10745	26	2.72 ± 0.04	2.72	Sandstone
56	153	10743	26	2.99 ± 0.03		Shale
57	13	10007	29	2.45 ± 0.02	2.45	Sandstone
59	20	10154 & 10155	29	2.78 ± 0.02	2.78	Siltstone
60	72	10486 & 10487	31	2.75 ± 0.01	2.75	Shale
61	4	10485 & 10486	31	2.75 ± 0.03	2.75	Shale
62	70	10481 & 10482	31	2.78 ± 0.02	2.78	Shale
63	75	10480 & 10481	31	2.68 ± 0.02	2.68	Shale
64	67	10562 & 10563	33	2.75 ± 0.02	2.75	Shale
66	63	10554 & 10555	33	2.77 ± 0.01	2.74	Shale
	64			2.70 ± 0.02		Shale with quartz
67	69	10545 & 10546	33	2.68 ± 0.01	2.68	Siltstone
68	89	10543 & 10544	33	2.80 ± 0.02	2.80	Siltstone
69	85	10539 & 10540	33	2.83 ± 0.01	2.76	Schist
	86			2.69 ± 0.02		Schist
70	84	10537 & 10538	33	2.80 ± 0.02	2.80	Schist

... continued

Table A6.1, continued

(1)	(2)	(3)	(4)	(5)	(6)	(7)
71	90 157	10533 & 10534	34	2.61 ± 0.01 2.63 ± 0.01	2.62	Granite (Medium to coarse grain)
72	65	10603	33	2.75 ± 0.02	2.75	Schist
73	87	10599 & 10600	33	2.72 ± 0.02	2.72	Schist
74	78	10597	33	2.68 ± 0.04	2.68	Schist
75	71 156	10577 & 10578	33	2.94 ± 0.02 2.69 ± 0.01	2.82	Gneiss with quartz Granite gneiss
76	76	10571 & 10572	35	2.76 ± 0.02	2.76	Diorite
77	106	11158	36	2.87 ± 0.01	2.87	Basalt
78	102	11152	35	2.83 ± 0.05	2.83	Basalt
79	98	11150	35	2.77 ± 0.03	2.77	Shale
80	103	11131	36	2.55 ± 0.02	2.55	Shale
81	104	11124	36	2.86 ± 0.02	2.86	Andesite
82	99	11118 & 11119	35	2.81 ± 0.02	2.81	Andesite
83	97	11117	35	2.72 ± 0.02	2.72	Rhyolite
84	105	11108	35	2.69 ± 0.01	2.69	Siltstone
85	133	11097	36	2.75 ± 0.02	2.75	Shale
86	112	11094	36	2.81 ± 0.03	2.81	Shale
87	131	11093	36	2.93 ± 0.04	2.93	Diorite
88	107 108 109	11083	36	2.76 ± 0.01 2.66 ± 0.01 2.77 ± 0.01	2.73	Sandstone Sandstone Shale
89	146	11078	36	2.95 ± 0.02	2.95	Andesite

... continued

Table A6.1, continued

(1)	(2)	(3)[1]	(4)	(5)	(6)	(7)
90	115	11075	35	2.63 ± 0.02	2.63	Granite (Medium grain)
91	129	11073	35	2.82 ± 0.06	2.82	Schist
92	135 151	11069	35	2.69 ± 0.02 2.70 ± 0.02	2.69	Diorite Andesite
93	110	11066	35	2.63 ± 0.01	2.63	Rhyolite
94	116 117	11061	35	2.68 ± 0.01 3.00 ± 0.02	2.84	Rhyolite Rhyolite
95	100 101	11057	35 36	2.85 ± 0.03 3.11 ± 0.06	2.98	Diorite Diorite
96	132	11002	36	2.78 ± 0.01	2.78	Basalt
97	150	11008	37	2.65 ± 0.03	2.65	Shale & sandstone
98	96 35 36	10031 & 11030	29	2.76 ± 0.01 2.83 ± 0.01 2.75 ± 0.03	2.78	Diorite Conglomerate (sandstone) Siltstone
99	59 92	10033 & 10022	29	2.81 ± 0.01 2.76 ± 0.04	2.79	Sandstone Conglomerate (pebbled)
100	61 94	10032	29	2.74 ± 0.02 2.74 ± 0.09	2.74	Conglomerate Conglomerate
101	95	10033	29	2.64 ± 0.02	2.64	Conglomerate
102	60	10022	29	2.75 ± 0.02	2.75	Sandstone
103	93	10024	29	2.76 ± 0.02	2.76	Sandstone
104	79	10499 & 10500	29	2.78 ± 0.04	2.78	Shale

[1]Sites 98 to 103 (inclusive) are along secondary highway from Notre Dame Junction to Lewisporte.

... continued

Table A6.1, continued

(1)	(2)	(3)[1]	(4)	(5)	(6)	(7)
105	113	11031		2.58 ± 0.0i	2.58	Diorite
106	152	11036		2.68 ± 0.02	2.68	Sandstone
107	134	11039		2.69 ± 0.02	2.69	Andesite
108	119	11045		2.98 ± 0.02	2.91	Andesite
	120			2.85 ± 0.01		Andesite
	121			2.90 ± 0.01		Andesite

[1]Sites 105 to 108 (inclusive) are along Trans-Canada highway between Come-by-Chance and Whitbourne.

APPENDIX 7

INTERPRETATION FORMULAE

A7.1 Polynomial expression for regional gravity.

This expression is given as a function of latitude, ϕ, and longitude, λ, to order N by

$$g_C(\phi,\lambda) = \sum_{i=1}^{N} \sum_{j=1}^{N-i} A_{ij} (\phi-\phi_o)^i (\lambda-\lambda_o)^j \qquad \text{(A7.1)}$$

where ϕ_o and λ_o represent a shift from the zero of latitude and longitude to local reference axes. The coefficients, A_{ij}, are determined, using multiple regression techniques, from a fit of this formula to the measured Bouguer anomaly values. This technique is discussed in detail by Simpson (1954), and has been used by Miller (1970) in connection with gravity regional-residual separation in eastern Notre Dame Bay (Section 1.2).

A7.2 Gravitational effect of a polygonal-shaped two-dimensional body.

The vertical component of gravity due to a two-dimensional body with elongation axis in a horizontal plane, and having polygonal-shaped cross-section, is given by an expression developed by Talwani, Worzel and Landisman (1959), and stated in the following form by Grant and West (1965):

$$g_o = 2G\,\Delta\rho \sum_{k=1}^{N} \frac{b_k}{1 + a_k^2} \left[\frac{1}{2} \ln\left(\frac{x_{k+1}^2 + z_{k+1}^2}{x_k^2 + z_k^2}\right) + a_k\left(\tan^{-1}\frac{x_{k+1}}{z_{k+1}} - \tan^{-1}\frac{x_k}{z_k}\right)\right] \qquad \text{(A7.2)}$$

where g_o is computed at the origin of a cartesian coordinate system constructed with +z vertically downwards and with the x-axis perpendicular to the elongation. Other symbols are: G, the universal gravitational constant; $\Delta\rho$, the density contrast; N, the number of sides; (x_k,z_k), (x_{k+1},z_{k+1}), the horizontal and vertical coordinates of the k^{th} and $(k+1)^{th}$ corner points, respectively; a_k and b_k, defined by

$$a_k = \frac{x_{k+1} - x_k}{z_{k+1} - z_k} \qquad \text{and} \qquad b_k = \frac{x_k z_{k+1} - x_{k+1} z_k}{z_{k+1} - z_k} \tag{A7.3}$$

The solution exhibits singularities for $(x_k,z_k) = (0,0)$, and where $z_k = z_{k+1}$. The former may be easily avoided in modelling, and the latter by-passed using the following expression, easily obtained from equation A7.2, for the condition that $z_k = z_{k+1}$

$$g_o = 2G\,\Delta\rho \sum_{k=1}^{N} z_k \left(\tan^{-1}\frac{x_k}{z_k} - \tan^{-1}\frac{x_{k+1}}{z_{k+1}}\right) \tag{A7.4}$$

A7.3 The gravitational attraction of a right rectangular prism.

The vertical component of gravity associated with a right rectangular prism is given by Nagy (1966) as follows:

$$g_o = G\,\Delta\rho \left|\left|\left| x \ln(y+r) + y \ln(x+r) - z \arcsin\frac{z^2 + y^2 + yr}{(y+r)(y^2+z^2)^{\frac{1}{2}}} \right|_{z_1}^{z_2} \right|_{y_1}^{y_2} \right|_{x_1}^{x_2} \tag{A7.5}$$

where x, y, and z are the axes of a cartesian coordinate system; (x_1,x_2), (y_1,y_2), and (z_1,z_2) represent limits of integration; G is the universal

gravitational constant; $\Delta\rho$ the density contrast; and $r = (x^2 + y^2 + z^2)^{\frac{1}{2}}$. The expression is valid only when the limits are substituted. When either the x, y, or both axes are crossed, the integration must be carried out for each quadrant separately, and the results added to give the required effect.

A7.4 Comparison of oblique and perpendicular horizontal line masses.

An infinite horizontal straight line mass in the cartesian co-ordinate system shown in figure A7.1 (with +z vertically downwards) intersects the x-z plane at the point $(0,0,z_L)$ and makes an angle γ with the y'-axis, where y' is drawn through this point parallel to the y-axis. The gravity effect at point P $(x_p,0,0)$ due to it is to be compared with that of an identical line mass along the y'-axis.

An expression giving the vertical component of gravity, g_ℓ, for an infinite horizontal line mass may be simply derived (e.g., see Garland, 1966), and stated in the form

$$g_\ell = 2G\,\Delta\rho_\ell\,\frac{z_L}{r^2} \qquad \text{(A7.6)}$$

where G is the universal gravitational constant; $\Delta\rho_\ell$ the (linear) density contrast; and r the distance along the perpendicular from the observation point, P, to the line mass, meeting it, for the oblique case shown in figure A7.1, at point (x_L,y_L,z_L). With r expressed in terms of z_L, x_p, and γ, equation A7.6 may be written

$$g_l = 2G\,\Delta\rho_l\,\frac{z_L}{z_L^2 + x_p^2\cos^2\gamma} \qquad \text{(A7.7)}$$

It follows from equation A7.7 that the gravitational effect of an identical perpendicular horizontal line mass ($\gamma = 0$) passing through the point $(0,0,z_L)$ is given by

$$g' = 2G\,\Delta\rho\,\frac{z_L}{z_L^2 + x_p^2} \qquad \text{(A7.8)}$$

and that the maximum value for both g and g' (where $x_p = 0$) is

$$g'_{max} = 2G\,\Delta\rho\,/\,z_L \qquad \text{(A7.9)}$$

A comparison of the oblique and perpendicular line mass gravity effects is given by the number F_1, defined as

$$F_1 = (g_\ell - g')\,/\,g'_{max} \qquad \text{(A7.10)}$$

Substitution of equations A7.7 to A7.9 into equation A7.10 yields after some rearranging of terms

$$F_1 = (\sin^2\gamma)\,/\,(1 + (x_p^2\,/\,3_L^2)\cos^2\gamma)\,(1 + z_L^2\,/\,x_p^2) \qquad \text{(A7.11)}$$

From figure A7.1 it can be seen that $x_p\,/\,z_L = \tan\beta$. Substitution of this into equation A7.11 gives

$$F_1 = \sin^2\gamma\,\sin^2\beta\,/\,(1 + \tan^2\beta\,\cos^2\gamma) \qquad \text{(A7.12)}$$

Figure A7.2 shows plots of F_1 versus β for various values of γ.

A7.5 Gravitational effect of a straight semi-infinite dipping line mass.

Figure A7.3 shows a semi-infinite straight line mass directed along the η-axis, which lies in the y-z plane of a cartesian coordinate system constructed with +z vertically downwards. The perpendicular, r, from the observation point P $(x_p,0,0)$ meets the line mass at $\eta = 0$. The line mass intersects the x-z plane at point $(0,0,z_L)$ and terminates at point I $(0,y_I,0)$, making an angle γ with the y-direction. The vertical component of gravitational attraction at P is given by

$$g_d = G\,\Delta\rho \int_{\eta} \frac{\cos\phi}{r^2 + \eta^2}\, d\eta \qquad \text{(A7.13)}$$

where

$$\cos\phi = (r\cos\alpha - \eta\sin\gamma) \,/\, (r^2 + \eta^2)^{\frac{1}{2}} \qquad \text{(A7.14)}$$

ϕ is angle between vertical and line joining P to the mass element at any point η; α is angle between r and vertical; and $\Delta\rho$ is linear mass density contrast, considered homogeneous.

Changing the variable from η to θ using $\eta = r\tan\theta$ and integrating from $\theta = -\frac{\pi}{2}$ to $\theta = \theta'$, where θ' is angle between r and $\overline{PI}$, yields

$$g_d = \frac{G\Delta\rho}{r}\,(\cos\alpha + \cos\alpha\,\sin\theta' + \sin\gamma\cos\theta') \qquad \text{(A7.15)}$$

which reduces to equation A7.6 for the horizontal case ($\gamma = 0$, $\theta' = \pi/2$).

To express g_d as a function of x_p, z_L, and γ, use is made of the following, simply obtained, relationships:

$$r = (x_p^2 + z_L^2\cos^2\gamma)^{\frac{1}{2}} \qquad \text{(A7.16)}$$

$$\cos \alpha = (z_L \cos^2 \gamma) / r \qquad \text{(A7.17)}$$

$$\cos \theta' = r / (x_p^2 + z_L^2 \cos^2 \gamma)^{\frac{1}{2}} \qquad \text{(A7.18)}$$

$$\sin \theta' = (1 - \cos^2 \theta')^{\frac{1}{2}} \qquad \text{(A7.19)}$$

The substitution of equations A7.16 to A7.19 into equation A7.15 yields

$$g_d = G \Delta\rho \frac{z_L \cos^2 \gamma}{(x_p^2 + z_L^2 \cos^2 \gamma)} \left[1 + \frac{z_L^2 + x_p^2 \tan^2 \gamma)^{\frac{1}{2}}}{z_L \cos \gamma} \right] \qquad \text{(A7.20)}$$

Substituting $\tan \beta = x_p / z_L$ gives

$$g_d = \frac{G \Delta\rho}{z_L} \frac{\cos^2 \gamma}{(\tan^2 \beta + \cos^2 \gamma)} \left[1 + \frac{(1 + \tan^2 \beta \tan^2 \gamma)^{\frac{1}{2}}}{\cos \gamma} \right] \qquad \text{(A7.21)}$$

The gravitational attraction of this dipping line mass may be compared with that of an infinite horizontal one of the same linear density, which intersects point $(0,0,z_L)$ perpendicular to x-z plane, using a quantity F_2, defined by

$$F_2 = (g_d - g') / g'_{max} \qquad \text{(A7.22)}$$

where g' and g'_{max} are given by equations A7.8 and A7.9, respectively. Substitution of these two and equation A7.21 into equation A7.22 yields

$$F_2 = \frac{\cos \gamma}{2(\tan^2 \beta + \cos^2 \gamma)} (\cos \gamma + (1 + \tan^2 \beta \tan^2 \gamma)^{\frac{1}{2}}) - \cos^2 \beta \qquad \text{(A7.23)}$$

Figure A7.4 shows plots of F_2 against β for various values of γ.

A7.6 Errors associated with a horizontal perpendicular representation of an oblique geologic structure.

The curves given in Figures A7.2 and A7.4 are directly applicable to the error determinations associated with the representation of an oblique two-dimensional cylinder, of circular cross-section, by a perpendicular one of identical cross-section and linear density. However, in practice, such an oblique body is represented by a two-dimensional perpendicular cylinder of elliptical cross-section.

This means that in order to make a valid comparison of the oblique line mass with its usual representation by means of a perpendicular model, the linear density of the oblique body has to be decreased by a factor of cos γ. Since curves incorporating this have not been here constructed, the cos γ factor has to be considered when using Figures A7.2 and A7.4.

For example, in the interpretation of the section between Notre Dame Junction and Traytown it will be noted that the majority of the mapped structures have departures of less than 15^{o} from perpendicularity. Figure A7.2 shows that a line mass with this obliqueness has a gravitational effect which is larger than than of a perpendicular line mass; the difference between them is roughly 2% of the maximum effect of the latter. However, because of the cos γ factor the oblique mass's effect is reduced by about 3½%, . From this an error of less than ±2% has been estimated.

It should be emphasized that this has been a discussion about line masses. For an accurate application to a real structure, F_1 and F_2 will have to be integrated over that body's volume.

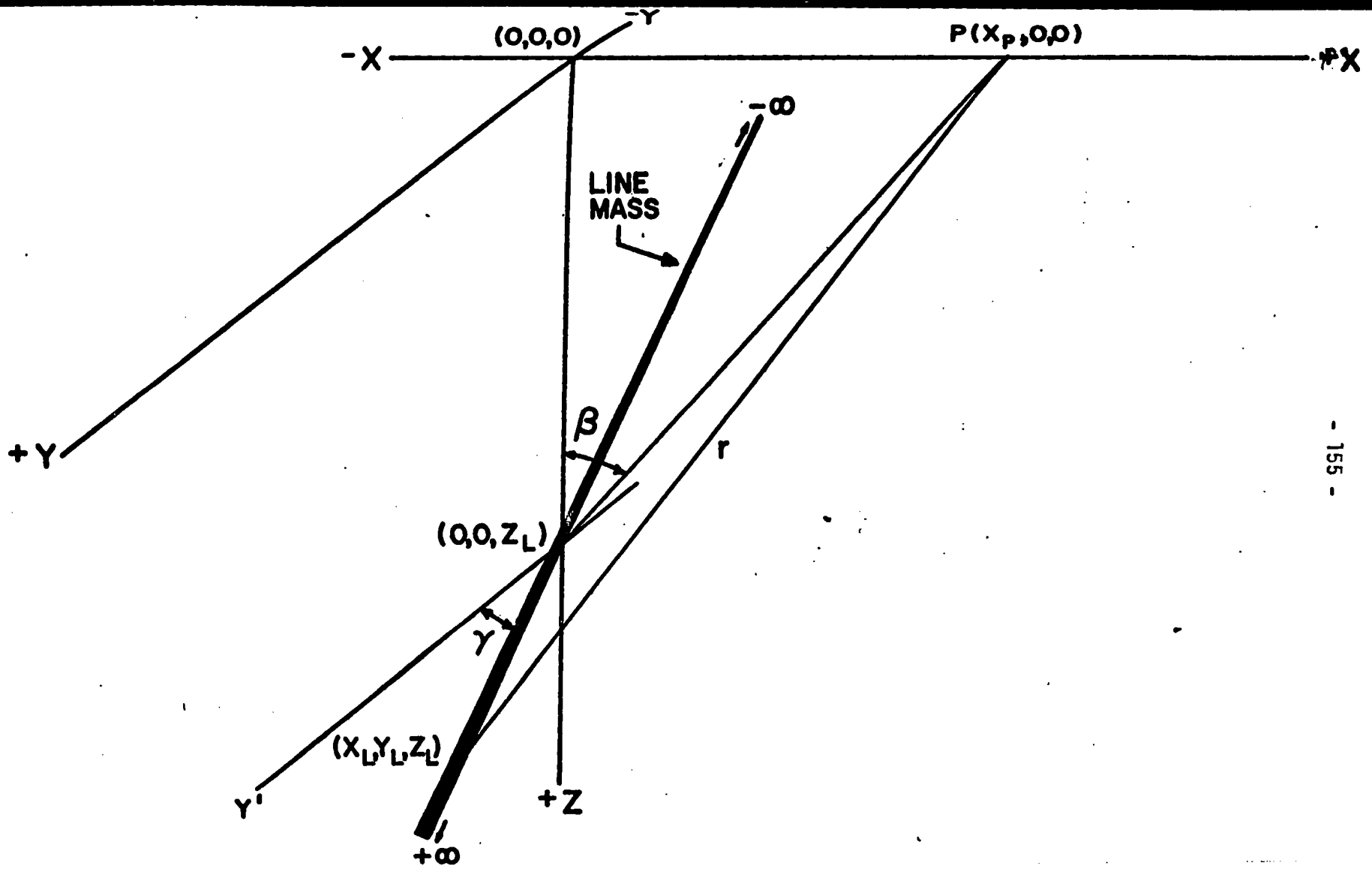

Figure A7.1 An infinite horizontal straight line mass is shown in a cartesian coordinate system intersecting the X-Z (vertical) plane at point $(0,0,Z_L)$, and making an angle γ with the Y'-axis (obtained by drawing a line through $(0,0,Z_L)$ parallel to the Y-axis). The line r is drawn from the observation point P on the X-axis perpendicular to the line mass, intersecting it at the point (X_L,Y_L,Z_L).

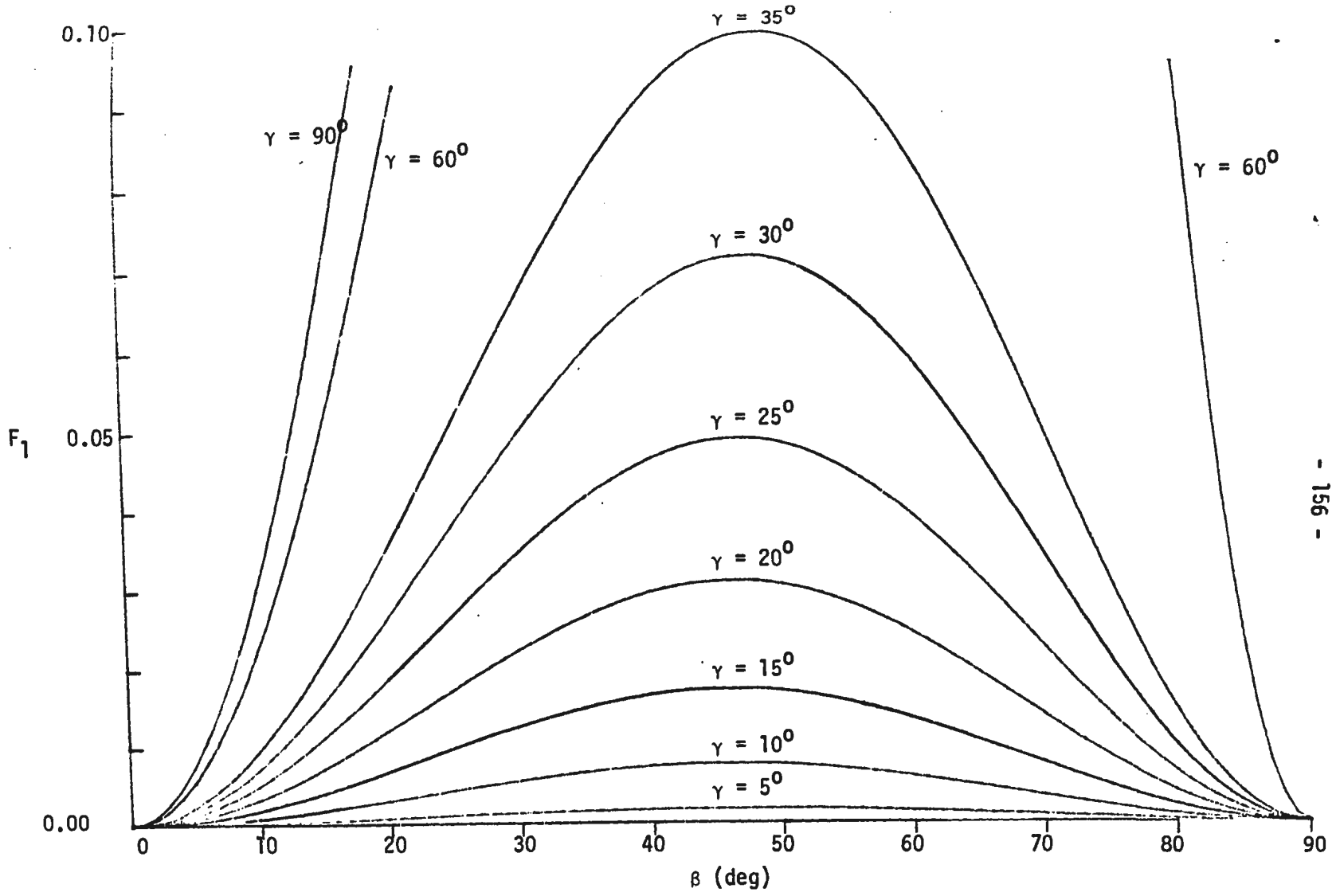

Figure A7.2 Comparisons of oblique and perpendicular horizontal line masses of same linear density. F_1 (defined by Equations A7.10 and A7.12) is plotted against β (the angle between the vertical and the normal drawn from the computation point to the perpendicular line mass) for various values of γ (the angle between the oblique and perpendicular masses). For application of these curves to model study error analysis, refer to Section A7.6.

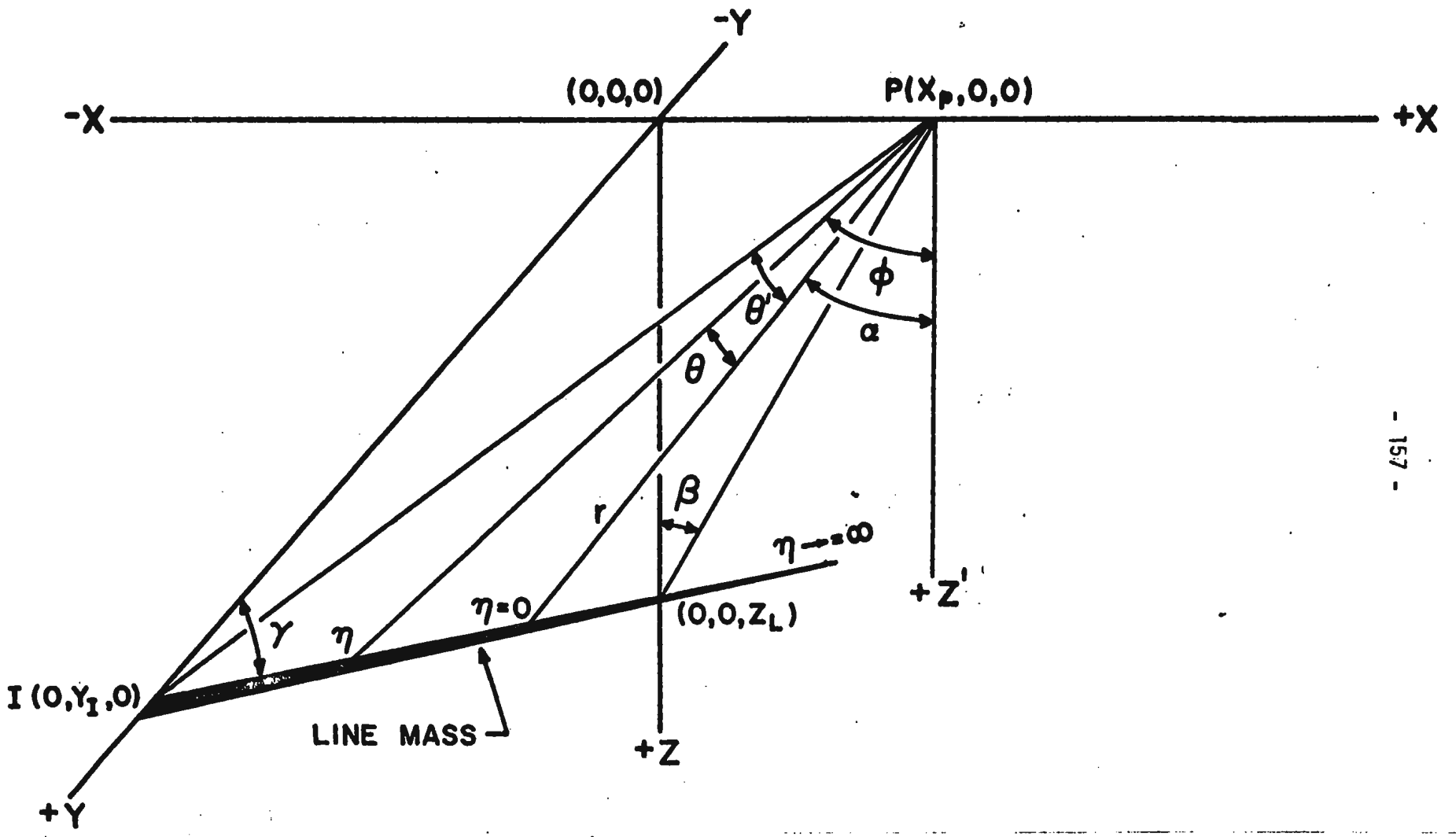

Figure A7.3 A semi-infinite straight line mass, lying in the Y-Z (vertical) plane of a cartesian coordinate system, dips at an angle γ below the Y-axis. The mass extends along a η-axis and terminates in the horizontal (X-Y) plane of the observation point, P. Symbols used in diagram are defined in section A7.5.

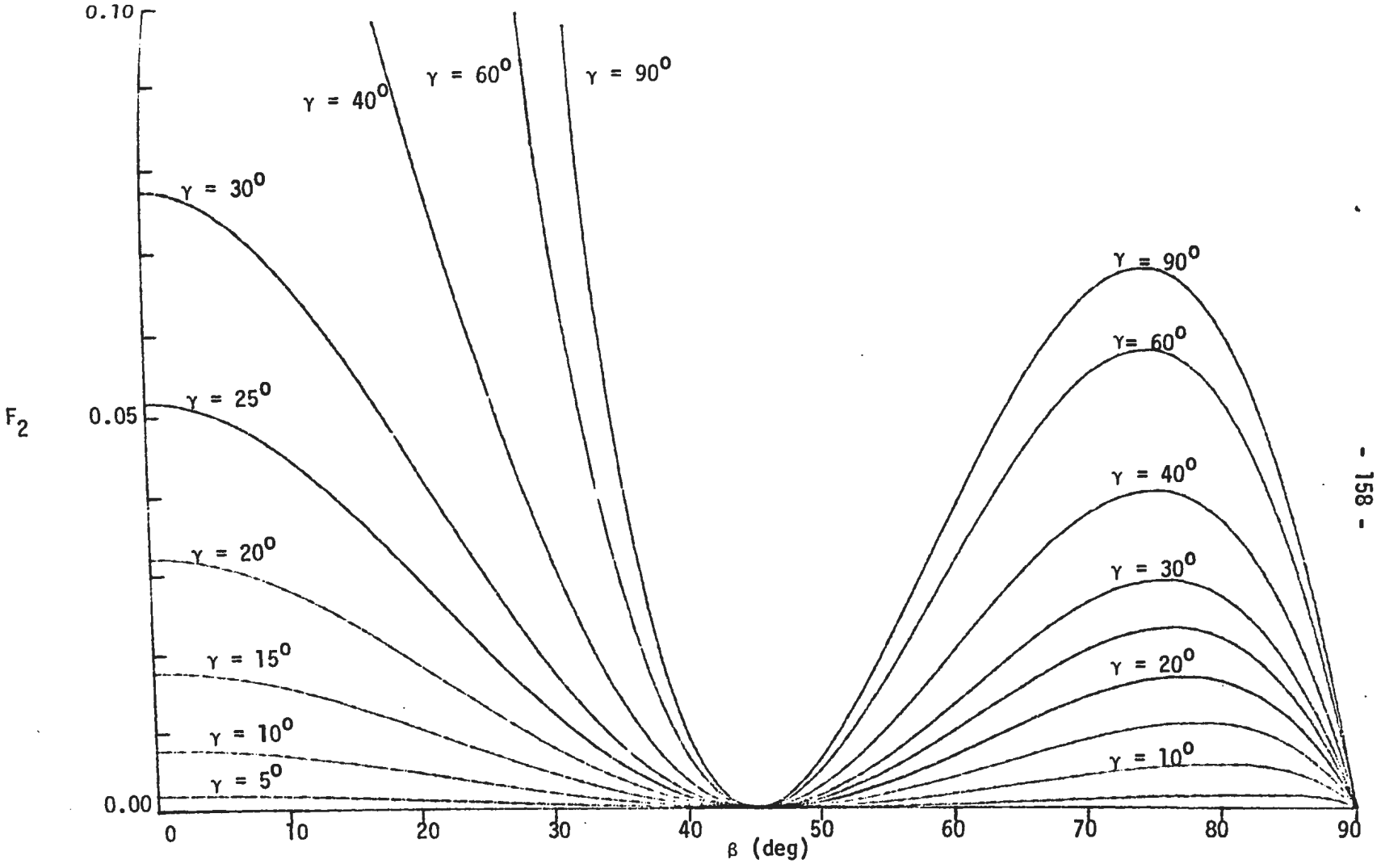

Figure A7.4 Comparisons of perpendicular and oblique line masses where both have same linear density and are contained in a vertical plane perpendicular to vertical plane of traverse. γ is angle between oblique mass and horizontal perpendicular one. F_2 (defined by Equations A7.22 and A7.23) is plotted against β (as defined in Figure A7.2) for various values of γ. For application of these curves to model study error analysis, refer to Section A7.6.

APPENDIX 8

END CORRECTIONS

A8.1 Introduction.

The computer program (Section 3.2) designed to calculate the gravitational effect of structural models also produced a plot of the observed and model anomaly profiles. Because it was not convenient to make conventional end corrections to these results, a technique for making such corrections at the "input" to the model program was devised. This method makes use of the computer program (designed and kindly provided by Dr. Dezso Nagy of the Dominion Observatory's Gravity Division) which gives the gravitational attraction of a right rectangular prism.

A8.2 End corrections for granitic and dioritic bodies near southeastern Gander Lake and Notre Dame Junction.

This "semi-infinite" granite body crossed the gravity traverse and abutted the Gander Lake group at an average distance of about 1 km from the profile (between M and N, figure 5.3.2). Initial two-dimensional model studies suggested its cross-sectional dimensions to be roughly 6 km (along traverse) by 3 km (depth). Dr. Nagy's program was then used to obtain the anomaly profile for such a semi-infinite rectangular prism, of density contrast -0.13 gm/cm^3, crossed at a distance of 1 km from its end. Next, profiles were determined for two dimensional (infinite) bodies of identical cross-section and for various density contrasts between -0.07 and -0.12 gm/cm^3.

A comparison of these profiles suggested that a two-dimensional body of density contrast -0.10 gm/cm^3 could adequately represent, in model studies, the semi-infinite granitic body. The error inherent in this representation is less than ±0.40 mgal.

Similarily, a density contrast of +0.03 gm/cm^3 was obtained for the two-dimensional body used to represent the semi-infinite bodies of diorite and Botwood group rocks (between K and L, figure 5.3.2).

A8.3 A general method for making end corrections.

It may be noted that the value of -0.10 gm/cm^3, obtained above, corresponds to the weighted mean of the density contrasts of the granite and Gander Lake group, where they have been given normalized weights of 0.75 and 0.25, respectively.

It is suggested that this weighting scheme can be applied to other bodies of similar cross-sectional shape, and terminated approximately 1 km from the traverse. It is recommended that this technique be investigated further with a view to tabulating these weights for various distances from the abutting surfaces, and for various cross-sectional shapes.

REFERENCES

Badgley, P.C. (1965) Structural and Tectonic Principles; Harper & Row, Publishers, New York, 521p.

Baird, D.M. (1960) Sandy Lake (west half), Newfoundland; Canada Geological Survey Map 47-1959.

Baird, D.M. and Cote, P.R. (1964) Lower Carboniferous Sedimentary Rocks in Southwestern Newfoundland and their Relations to Similar Strata in Western Cape Breton Island; Canadian Mining and Metallurgical Bulletin, 57, p.509.

Beers, Y. (1957) Introduction to the Theory of Error; Addison-Wesley Publishing Company, Inc., Reading, Massachusetts, 66p.

Bible, J.L. (1962) Terrain Correction Tables for Gravity; Geophysics 27, p. 715.

Clark, D. (1958) Plane and Geodetic Surveying, 5th Ed.; Constable and Co. Ltd.

Dainty, A.M., Keen, C.E., Keen, M.J., and Blanchard, J.E. (1966) Review of Geophysical Evidence on Crust and Upper-Mantle Structure on the Eastern Seaboard of Canada; from Geophysical Monograph No. 10, The Earth Beneath the Continents, J.S. Steinhart and T.J. Smith (Editors); American Geophysical Union, Washington, D.C.

Damrel, J.B. (1960) The Effect of Temperature and Time on the Scale Factor of the Worden Gravity Meter; Boll. Geofisica Teor. ed Appl. 2, p. 567.

Dobrin, M.B. (1960) Introduction to Geophysical Prospecting, 2nd Ed.; McGraw-Hill Book Company, Inc., Toronto, 446p.

Ewing, G.N., Dainty, A.M., Blanchard, J.E., and Keen, M.J. (1966) Seismic Studies on the Eastern Seaboard of Canada: The Appalachian System. I; Canadian Journal of Earth Sciences 3, p. 89.

Garland, G.D. (1965) The Earth's Shape and Gravity; Pergamon Press, New York, 183p.

Goodacre, A.K. (1964) Preliminary Results of Underwater Gravity Surveys in the Gulf of St. Lawrence, with map; Dom. Obs., Gravity Map Ser. No. 46.

Goodacre, A.K. and Nyland, E. (1966) Underwater Gravity Measurements in the Gulf of St. Lawrence; Royal Society of Canada, Sp. Pub. No. 9.

Grant, F.S. and West, G.F. (1965) Interpretation Theory in Applied Geophysics; McGraw-Hill Book Company, Toronto, 584p.

Jenness, S.E. (1958) Geology of the Gander River Ultrabasic Belt, Newfoundland; Newfoundland Geol. Survey Dept., No. 11, 58p.

---------- (1963) Terra Nova and Bonavista map-areas, Newfoundland; Canada Geological Survey Memoir 327, 184p.

Kay, M. (1969) Thrust Sheets and Gravity Slides of Western Newfoundland; p. 665 in North Atlantica - Geology and Continental Drift; Memoir 12, American Association of Petroleum Geologists, Tulsa, Okla.

Kissam, P. (1945) Precision Altimetry; reprint from "Surveying and Mapping", Vol. 5, No. 1, January, 1945.

Miller, H. (1970) A Gravity Survey of Eastern Notre Dame Bay, Newfoundland; Memorial University of Newfoundland (M.Sc. thesis).

Nagy, D. (1966) The Gravitational Attraction of a Right Rectangular Prism; Geophysics 31, p. 362.

Neale, E.R.W. and Nash, W.A. (1963) Sandy Lake (east half) Newfoundland; Canada Geological Survey Paper 62-28, 40p.

Nettleton, L.L. (1940) Geophysical Prospecting for Oil; McGraw-Hill, New York and London.

Riley, G.C. (1957) Red Indian Lake (west half), Newfoundland; Canada Geological Survey Map 8-1957.

---------- (1962) Stephenville Map Area, Newfoundland; Canada Geological Survey Memoir 323, 72p.

Rodgers, J. and Neale, E.R.W. (1963) Possible "Taconic" Klippen in Western Newfoundland; American Journal of Science 261, p. 713.

Roy, A. (1962) Ambiguity in Geophysical Interpretation; Geophysics 27, p. 90.

Sheridan, R.E. and Drake, C.L. (1968) Seaward Extension of the Canadian Appalachians; Canadian Journal of Earth Sciences 5, p. 337.

Simpson, S.M., (Jr.) (1954) Least Squares Polynomial Fitting to Gravitational Data and Density Plotting by Digital Computers; Geophysics 19, p. 255.

Talwani, M. and Ewing, M. (1960) Rapid Computation of Gravitational Attraction of Three-Dimensional Bodies of Arbitrary Shape; Geophysics 25, p. 203.

Talwani, M., Worzel, J.L., and Landisman, M. (1959) Rapid Gravity Computations for Two-Dimensional Bodies with Application to the Mendocino Submarine Fracture Zone; Journal of Geophysical Research 64, p. 49.

Topping, J. (1957) Errors of Observation and Their Treatment; The Institute of Physics, London, 119p.

Weaver, D.F. (1967) A Geological Interpretation of the Bouguer Anomaly Field of Newfoundland; Publication Dominion Observatory, Vol. 35, No. 5, p. 223.

---------- (1968) Preliminary Results of the Gravity Survey of the Island of Newfoundland with maps; Dominion Observatory Gravity Map Series 54 to 57, inclusive.

Williams, H. (1962) Botwood (west half) Map Area, Newfoundland; Canada Geological Survey Paper 62-9, 16p.

---------- (1964_a) The Appalachians in Northeastern Newfoundland - A Two-Sided Symmetrical System; American Journal of Science 262, p. 1137.

---------- (1964_b) Botwood, Newfoundland; Canada Geological Survey Map 60-1963.

---------- (1967) Island of Newfoundland; Canada Geological Survey Map 1231A.

---------- (1969) Pre-Carboniferous Development of Newfoundland Appalachians; p. 32 in North Atlantic - Geology and Continental Drift, Memoir 12, American Association of Petroleum Geologists, Tulta, Okla.

Williams, H., Kennedy, M.J., and Neale, E.R.W. (1970) The Hermitage Flexure, the Cabot Fault, and the Disappearance of the Newfoundland Central Mobile Belt; Geological Society of America Bulletin 81, p. 1563.